Quantum System Identification by Local Measurements

By

Akira Sone

B.E., Applied Physics, Keio University (2013)

SUBMITTED TO THE
DEPARTMENT OF NUCLEAR SCIENCE AND ENGINEERING

IN PARTIAL FULFILLMENT OF THE REQUIREMENTS FOR THE DEGREE OF
DOCTOR OF PHILOSOPHY IN QUANTUM ENGINEERING

AT THE
MASSACHUSETTS INSTITUTE OF TECHNOLOGY
JUNE, 2019

Signature of Author: _____

Akira Sone
Department of Nuclear Science and Engineering
May 10, 2019

Certified by: _____

Paola Cappellaro
Esther and Harold E. Edgerton Associate Professor of Nuclear Science and Engineering
Thesis supervisor

Certified by: _____

Ju Li
Battelle Energy Alliance Professor of Nuclear Science and Engineering
and Professor of Materials Science and Engineering
Thesis Reader

Accepted by: _____

Ju Li
Battelle Energy Alliance Professor of Nuclear Science and Engineering
and Professor of Materials Science and Engineering
Chair, Department Committee on Graduate Students

Quantum System Identification by Local Measurements

by

Akira Sone

Submitted to the Department of Nuclear Science and Engineering
on May 10, 2019, in partial fulfillment of the
requirements for the degree of
Doctor of Philosophy in Quantum Engineering

Abstract

Quantum information processing, including quantum computation, quantum communication, and quantum metrology, is expected to be the next-generation information technology capable of outperforming classical devices. The physical platform for quantum information devices requires many-body quantum systems with many interacting qubits (two-level systems), and several experimental systems have been actively studied in recent years for realizing such scalable quantum information processors. Reliable quantum information processing essentially requires robust initialization of the quantum system, robust control protocols and precise measurement. As these indispensable tasks strongly depend on the physical properties and dynamics of the quantum system, the precise characterization of the experimental system, namely quantum system identification, is a crucial prerequisite.

In a closed quantum system, the Hamiltonian includes the information about the properties of the system, such as the number of qubits, single-body energy of qubits, topology of qubit network graph and coupling types between qubits. For thermal equilibrium state, the temperature also becomes an important parameter characterizing the thermal properties of the system. Quantum system identification aims at extracting these elements from measurements of the system dynamics or state. However, performing measurement over the whole many-qubit system is typically a demanding task in the laboratory. Furthermore, given the lack of knowledge about the system, one cannot control or measure the system with high accuracy before characterizing it. Thanks to recent advances in quantum metrology with a single qubit sensor, a well-characterized qubit system can play the role of a quantum probe, which is coherently coupled to the target system, thus enabling practical schemes to identify the target many-body quantum system indirectly through system-probe correlations. More broadly, this quantum probe strategy is an example of system identification performed via local measurements.

This thesis focuses on the role of quantum correlations in quantum system identification assisted by local measurements in two different regimes: (1) dynamical and (2) equilibrium regime.

In the dynamical regime, we introduce the mathematical concept of quantum sys-

tem identifiability with respect to Hamiltonian parameter identification and Hilbert space dimension identification. Exploiting the linearity of the dynamics, we employ linear system realization theory, algebraic geometry and graph-theory to analyze the identifiability of an unknown Hamiltonian or the dimensions of the Hilbert space of the target many-body quantum system. Based on the formalism, we propose practical algorithms for both identifiability problems. We further find that propagation of correlations between the quantum probe and the whole system is a necessary condition to fully identify the parameters and dimensions of the target system through local measurements on the quantum probe.

In the equilibrium regime, the thesis discusses the problem of estimating either the temperature or Hamiltonian parameters, which can in general be extracted by characterizing the thermal equilibrium state. We discuss a general local measurement scheme, which we call “greedy local measurement scheme", where one performs sequential optimal measurement on a complete set of subsystems. We introduce a practical measure of nonclassical correlations, called discord for local metrology, to measure the nonclassical correlations induced by local optimal measurements. By comparing the greedy local measurement scheme and global measurement scheme, we explicitly demonstrate that in the high-temperature limit discord for local metrology quantifies the ultimate precision limit loss in local metrology. Conversely, this shows that nonclassical correlations could contribute to sensitivity enhancement in parameter estimation even at thermal equilibrium.

These results can be expected to contribute to the characterization of near-term quantum information processors, such as Noisy Intermediate-Scale Quantum (NISQ) devices, and to find applications in quantum sensing, e.g. in room-temperature nanoscale magnetic resonance sensing of nuclear spins in molecules or imaging of biological complex systems.

Thesis Supervisor: Paola Cappellaro, Ph.D.
Title: Esther and Harold Edgerton Associate Professor of Nuclear Science and Engineering

This thesis is dedicated to my grandfather, Dianying Zhao.

Acknowledgments

This thesis would not be possible without supports from many people. First and foremost, I would like to express my gratitude to my academic supervisor Prof. Paola Cappellaro for providing me freedom to pursue my interests and helping me challenge many interesting problems in quantum control, quantum metrology, and quantum information. Paola always encouraged me to connect my interests with state-of-the-art science and technology to find possible applications of the theory developed to various fields. This really stimulated me, and broadened my horizons. Besides the research, Paola provided me the opportunity of teaching nuclear physics and quantum feedback control in her classes. This really enabled me to improve my skills in teaching undergraduate and graduate classes and to find the beauty of teaching. I owe my confidence and happiness in research and teaching to Paola.

I am deeply grateful to Prof. Ju Li for his helpful discussions in committee meeting. Ju always helped me improve my research by sharing his insightful ideas in condensed matter physics. I always learn a lot of things about condensed matter physics from him. Especially, his analysis or way of thinking inspired me to look at problems in different ways.

My heartfelt appreciation goes to Prof. Mingda Li. Mingda is my idol. His enthusiasm in teaching and research indeed inspired me, and he became a man that I really want to be. I was very impressed by his kindness with his students and his devotion to research. When he introduced dislons to me, I really enjoyed his presentation, which was very easy for me to capture the big picture about dislons and its importance in material science. His way of teaching and discussing research inspired me a lot. Besides the research, we sometime talked about life, and he also gave me helpful advice about my future career plan.

I am also deeply grateful to Prof. Bilge Yildiz. I discussed my research with Bilge, and she usually asked very important questions about the possible applications of the theory developed in my research. This really helped me consider more about the practicability of my research and also broaden my horizons.

Special thanks go to Masashi Hirose, who is a former Ph.D. student at Cappellaro's group and my great "Senpai" from Keio University. I can safely say that without Masashi, it would not be possible for me to complete my Ph.D. study. Masashi meant a lot to me. Since I came to Cambridge, Masashi had supported me in every place. He helped me overcome many challenges in my life in Cambridge especially in the periods of qualify exams. I will never forget what he has done for me, and I will help others as Masashi helped me.

I would like to thank to my collaborators Prof. Daoyi Dong, Dr. Yuanlong Wang, and Dr. Hidehiro Yonezawa from University of New South Wales and Prof. Ian Petersen from Australian National University for their helpful discussions and collaborations in Hamiltonian identification problem. Special thanks go to Quntao Zhuang, who is not only my great collaborator but also my great friend like my brother. We did not only enjoy talking about physics with each other but also enjoy hiking, surfing, and singing in karaoke together.

I am grateful to all current members in QEG: Dianne, Dominika, Mo, David, Changhao, Yixiang, Pai, Calvin, Genyue and Chao. I am also grateful to the previous members in QEG: Ken, Scott, Kasturi, Alex, Ashok, Luca, Ulf, Joe, Clarice, Elica and Nicole. Thank you all for your support.

I would like to thank my friends from all around the world, who really have made my life fruitful and become a big part of my family in Cambridge, especially Qingyang, Cong, Zhuoxuan, Lun, Youzhi, Dixia, Yulin, Hui, Xiangming, Jiawei, Qichen, Bo, Yongbin, Chuteng, Zheng, Benjamin, Pranam, Jude, and Tadayuki, Kosuke, Jeehyun and the members in JAM basketball team. I am also very grateful to my friends working on quantum information science for fruitful discussions especially, Zi-Wen, Ryuji, Donggyu, Can, Elton, and Zhicheng. Thank you all for your generosity, friendship, and brotherhood. I would love to offer my gratitude to MIT Christian Fellowship, MIT Catholic Community, MIT Christian Faculty community, especially Bill, Jorgen, Zach, Whijae, Jing, and Pastor Lee. I am also very grateful to St. Cecilia Parish especially Fr. John and Mark. Thank you so much for your prayers and spiritual supporting during my Ph.D. life.

I would like to thank to Dr. Benjamin Yadin, Dr. Kavan Modi, Prof. Anna Sanpe, Prof. Shuichi Adachi, Prof. Naoki Yamamoto, Prof. Junko-Ishi Hayase, and Prof. Kohei M. Itoh, Dr. Mohan Sarovar and Prof. Madalin Guta for helpful advice and discussions in my research. I also would like to thank to Prof. Charles Shadle for improving my music composition, which really helped me compose many pieces of music to make my life fruitful.

Here, I would love to offer my special thanks to my great students in the class 22.11 (2015) and class 22.02 (2018). Please let me list up all of your names in order to show my respect to all of you because you all really helped me discover my values. For class 22.11 (2015), I would like to thank to Norman, Scott, Yifeng, Minh, Alicia, Guillaume, Anil, Sterling, Briana, Artyom, Shikhar, Stephen, Hin, Samuel, Florian, Paolo, Jill, Pablo, Andrew, Juan, Jonathan, Malik, Jiayue, Robert, and Chris. For class 22.02 (2018), I would like to thank to Chris, Jared, Sara, Charles, Vivek, Monica, Adam, Lucas, Benjamin, Amelia, Nicholas, Jarod, and Jingyi. Thank you very much for your generosity and support to make the recitation and office hours exciting. I also would love to also thank to two of my smart UROP student, Rob and Xiaoyang for your collaboration in the project of practical algorithm for Hamiltonian identifiability. It was my great honor to be able to present at APS March Meeting at Boston in 2019. I would like to thank to NSF, U.S Army Research Office, Thomas G. Stockham Jr. Fellowship, Funai Oversea Scholarship for the funding support.

Finally, I would like to offer my deep gratitude to my families. I would like to thank to my father Kenryo and my mother Riri for their great support from Japan. I would like to thank to my beloved wife, Wenjun, for her love and dedication to create a beautiful family together. Wenjun has supported and encouraged me in the toughest periods in my Ph.D. life. I would love to thank to my uncle Xiaobin for encouraging me to overcome many difficulties. Finally, I would love to thank to my grandfather Dianying Zhao, who is also my first physics teacher, for inspiring me and leading me to this journey to pursue the beauty of physics. He told me that whenever we encounter difficulties in our research, let us be joyful and grateful because we are at the frontier of science. With this spirit, my journey never ends.

Contents

List of Figures

Chapter 1

Introduction

1.1 Quantum system identification

Quantum information processing (QIP) is a next-generation information technology, which is expected to process a huge volume of data with the less computational complexity (quantum computer) than the conventional computer, simulate characteristic behaviors and dynamics of the quantum matters more accurately (quantum simulator), realize an ultrafast and energy-saving communication protocols with high security (quantum communication and quantum cryptography), or realize precision sensing techniques in the nanoscale (quantum metrology) [116]. Particularly, recent research development in atomic, molecule, and optical physics and condensed matter physics has not only led to breakthroughs in understanding characteristic behaviors and properties of quantum matters, but also paved a path to robustly engineering the system for the realization of QIP.

In QIP, the basic unit of quantum information is called qubit, which is the binary bit in quantum information, and it can be realized by a two-level system, such as spin-1/2 particle or polarization of photons. The QIP devices are composed of qubits, and they process information through their interactions. In order to build up a reliable QIP devices, seven conditions are essentially required to meet [43]:

1. Well-characterized many-qubit systems

2. Robust initialization of the target system to a simple fiducial state

3. Robust controls by universal set of quantum gates

4. Precise system-dependent measurement

5. Long coherence time

   (Two more conditions for quantum communications)

6. Interconversion of stationary and flying qubits

7. Transmission of intact qubits between specific locations.

The first five conditions are for quantum computation, quantum simulation, and quantum metrology, and the last two conditions are for quantum communications. The characterization of many-qubit systems is the most important task as the prerequisite for QIP because the initialization, controls, and measurements are all dependent on the physical properties and the dynamics of the system. Practically, prior information about the system is always limited; therefore, it is required to extract missing information about the system. This task is called quantum system identification, which is the prerequisite for any technology in QIP [24].

The dynamics of a closed quantum system is determined by its Hamiltonian, which contains all the elements on which the properties of the system are dependent. Therefore, identifying the Hamiltonian is a central task for all QIP technologies. Let us consider an interacting many-qubit systems. The Hamiltonian can be usually characterized by the number of qubits, which gets the dimension of its Hilbert space, by single-particle energies and coupling strengths, and by the interaction model, which includes the topology of the qubit network (See Fig. 1-1). For a closed quantum systems, quantum system identification means the identification of its Hamiltonian through a set of measurements. Identifying Zeeman energy shifts [161, 107, 150] yields information on the spin species. By identifying the interaction Hamiltonian, we can obtain information on (1) the system graph [81], the coupling type, and the relative positions from the coupling strengths [22, 42, 161, 150]. Identifying only the first two

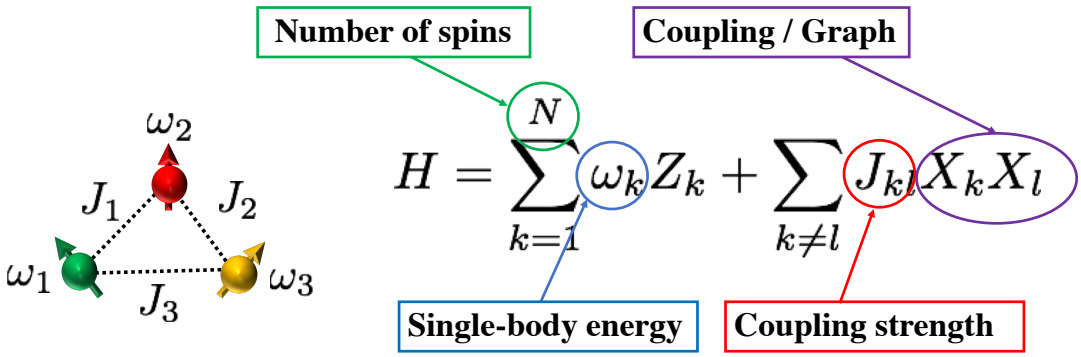

Figure 1-1: Hamiltonian for many-qubit system. Hamiltonian contains the information characterizing the system, such as the dimension of its Hilbert space, single-body energy, the graph topology, couplings and coupling strengths.

pieces of information (graph and couplings) enables writing a general model for the many-qubit system (See Sec. 2.3.1) [140]. Then, to further specify the system, one needs to identify not only the Hamiltonian parameters (See Sec. 2.4) [161, 107, 150, 162, 22, 42, 139], but also the number of qubits in the system (See Sec. 2.3) [140].

Furthermore, temperature T also plays an important role in determining the thermodynamic properties of the system, such as magnetization or heat capacity. In QIP, for example, for quantum annealers [78, 44], which is an optimization algorithm to find global minimum of a given objective function from the set of possible solutions, the temperature determines the performance of the algorithm and recent research pointed out the fundamental limitation of the quantum annealers at fixed finite temperature with rigorous analysis on the behavior of the temperature scaling for the quantum annealers to be a good optimizers [4]. Since the study of thermodynamics extends to the nanoscale, temperature estimation also requires a fully quantum treatment [17, 18, 109, 33, 126, 76, 103, 155, 34, 122, 120, 66]. Therefore, estimating the temperature at the nanoscale, namely quantum thermometry, is also an important task.

Quantum system identification techniques can be expected to contribute to the development in precision metrology. Quantum metrology [53, 54, 40] utilizes quantum resources such as entanglement and coherence to improve the precision of measure-

ments beyond classical limits. Particularly, recent progress in quantum metrology assisted by single quantum probe has demonstrated the ability to achieve precise estimation of a few unknown parameters [102, 14]. These advances now open experimental opportunities for multiple parameter estimation, while offering the advantage of nanoscale probing and coherent coupling of complex quantum systems. The possible applications range from clock synchronization [52], to quantum illumination [93, 144, 166], superdense measurement of quadratures [51, 141, 9] and range velocity [165], distributed sensing [50, 124, 167], point separation sensing [113, 97, 146, 83], magnetic field sensing [11, 145], tructural determination of a complex molecule [3, 2, 95], biosensing [32, 10, 85] and studying magnetism at the nanoscale [147, 154]. These techniques require an accurate and efficient methods to characterize the system, and the parameter estimation techniques provided through quantum system identification are expected to provide a powerful tools for realizing these metrology techniques.

1.2 Local measurements for quantum system identification

Various methods have been developed for quantum system identification, especially for Hamiltonian parameter estimation, including quantum process tomography [23, 22, 42, 150], Bayesian analysis [56, 129, 132], compressive sensing [134, 100, 8], and eigensystem realization algorithm [161, 162, 69]. Not only many of these techniques are quite complex, but they also often assume complete access to the system to be identified: full controllability and observability via the coupling of the target quantum system with a classical apparatus. Recently, the Noisy Intermediate-Scale Quantum (NISQ) device [123], composed of ten to fifty qubits, is expected to be available in the near future. However, fully addressing the system is still a demanding task. Therefore, for both near future and long future, we need to consider performing quantum system identification of total system by local measurements on its subsystems, which are well characterized.

In the dynamical regime (Chap. 2), we consider a practical scheme, in which we perform quantum system identification using coupling of the target system with a *quantum probe* [23, 22, 42, 161, 162, 138, 137]. Because recent progress in estimating a few parameters of a single small quantum system, we consider a model in which a single quantum probe, which is a well-characterized quantum system, is coherently coupled to the target system, and the Hamiltonian of the target system is estimated through the set of measurement outcomes of the probe at each time step (See Fig. 1-2).

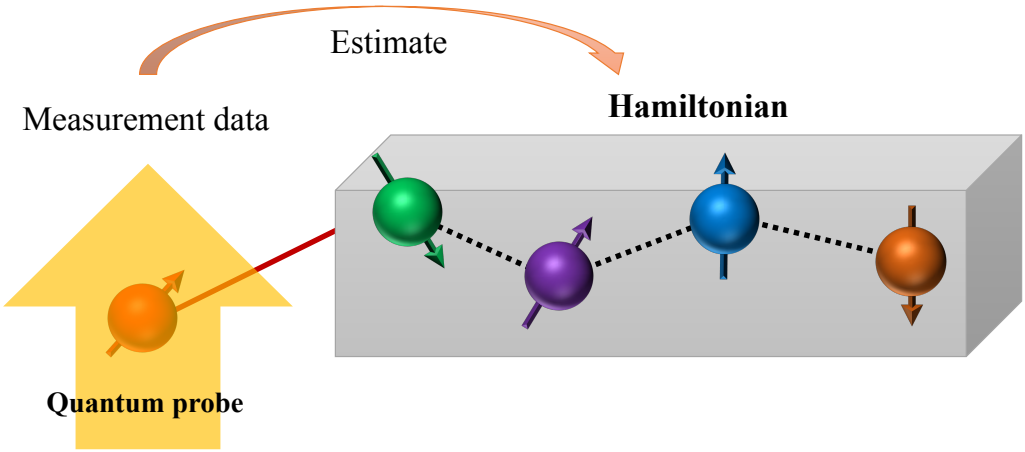

Figure 1-2: Quantum system identification assisted by a single-probe measurement. A single quantum probe is coherently coupled to the target system, and its Hamiltonian is estimated from the set of measurement results obtained by the local measurements on the quantum probe.

In the equilibrium regime (Chap. 3), we consider more general scheme, in which we consider a sequential measurements on the subsystems of the target systems. In particular, we consider the case where each subsystem is measured sequentially with a local optimal measurement in a sense that the estimation variance takes the minimum for estimating a parameter characterizing the system, and (classical) feedforward from the previous measurement result [96, 111, 139, 140]. We call this scheme a "greedy" local measurement scheme [139, 140], and this scheme still remains practical and belongs to the class of local operations and classical communication (LOCC) [115]. A practical LOCC protocol is the *greedy* local scheme, where we sequentially measure each subsystem with a local optimal measurement (see Fig. 1-3).

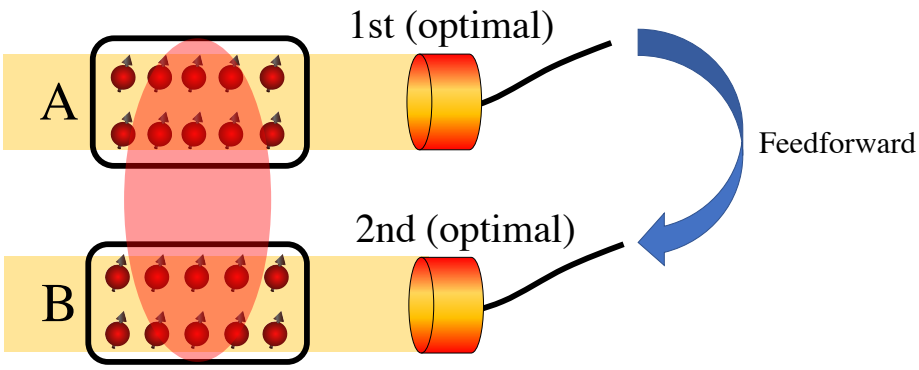

Figure 1-3: Greedy local measurement scheme. We first optimally measure a subsystem A and then optimally measure the other subsystem B based on the measurement result of A.

1.3 Overview of the Thesis

In Chapter. 2, the concept of identifiability of Hilbert space and Hamiltonian parameters of a many-body quantum system assisted by a single-probe measurement in the dynamical regime is studied. After reviewing linear system realization theory and eigensystem realization algorithm, the identifiability of the Hilbert space dimension estimation and Hamiltonian parameters are studied by employing linear system realization theory and algebraic geometry approach. Furthermore, the necessary condition for the system to be identifiable is provided in the context of correlations. In Chapter. 3, after reviewing the ultimate precision limit in estimation, which is quantified by quantum Fisher information and quantum discord, a new measure of nonclassical correlations which is revealed by the local optimal measurements, called discord for local metrology, is introduced, and the role of discord for local metrology in Hamiltonian parameter estimation or thermometry is described. In Chapter. 4, we will conclude the thesis, and propose the future direction of the research on quantum system identification problem.

Chapter 2

Quantum system identification in dynamical regime

This chapter discusses the identifiability of Hilbert space dimension and Hamiltonian parameters of a target many-body quantum system through the measurement on a single quantum probe coupled to the target system.

This chapter is structured as followings. In Sec. 2.2, we review the linear system realization theory for classical systems following Refs [80, 79, 130] and the eigensystem realization algorithm for parameter estimation introduced by Zhang and Sarovar in [161, 162], which is derived from classical linear system realization theory. Based on linear system realization theory approach to closed quantum system, we will introduce the concept of interaction model, which describes the connectivity between every two spins, and discuss the identifiability of the dimension of a finite-dimensional Hilbert space describing an interacting qubit system [137] in Sec. 2.3. Then, in Sec. 2.4, we will discuss the identifiability of Hamiltonian parameters [138] by the employing eigensystem realization algorithm approach to Hamiltonian parameter estimation [161, 162] and Gröbner basis [36, 37, 21, 47, 12]. I further provide the necessary experimental resources, such as the lower bound in number of sampling points and upper bound in total evolution time required to identify all the parameters. Focusing on the Hamiltonians of spin-chain model with nearest-neighbor interaction, we classify the Hamiltonians based on their identifiability, and provide an explanation about

the necessary condition for the system to be identified based on the concept of correlation propagations. We also propose a possibility of engineering a non-identifiable Hamiltonian to be an identifiable Hamiltonian with the control protocols assisted by periodic driving. In Sec. 2.6, we conclude the chapter, and point out several possible future directions along this research.

2.1 Introduction

The dimension of the Hilbert space (or system dimension) is indeed an important information for any quantum device. The performance of quantum protocols, such as the computational complexity of quantum algorithms [116] or quantum process tomography [150], is strictly dependent on the dimension. In addition, the dimension also determines what experimental resources, such as the number of sampling points and the total time evolution, are needed to characterize the rest of the Hamiltonian parameters [139]. These dimension-dependent quantities are important for practical applications of quantum engineering. Therefore, dimension estimation is a significant task in quantum system identification.

Because the dynamics of closed quantum system is linear, we can employ the tools developed in classical linear system theory to approach the identification problem. Classical linear system identification has been a widely studied subject for the past decades [92]. A popular system identification method for the linear time-invariant (LTI) systems is the eigensystem realization algorithm (ERA) [80]. ERA has been applied in several fields to study classical systems, from structural engineering [28] to aerospace engineering [112]. The first applications of ERA to quantum system identification both for close and open systems were given by Zhang and Sarvoar [161, 162], and a robust estimation was experimentally demonstrated for a closed quantum system [69]. A key step of the algorithm is the singular value decomposition of a Hankel matrix, whose elements are the measurement data at equally spaced sampling times. In the noiseless case, the rank of the Hankel matrix is equivalent to the model order, which is the degree of the characteristic polynomial of the irreducible

transfer function describing the system dynamics in the Laplace space [7]. This can be interpreted as the minimum number of independent state variables required to fully describe the dynamics of the system.

In a general many-body interacting system, the state variables are the observables, including the observable to be directly measured and the operators generated from the dynamics, which can be *indirectly* observed and controlled. Then, the key insight into dimension estimation is that the number of generated correlations will strongly depend on the system dimension. We can thus expect that the dimension will be a function of the model order, which is revealed by realization theory and experimental measurements.

For the identifiability of Hamiltonian parameters, we employ ERA to analyze the required experimental resources to achieve Hamiltonian identification. To achieve this, we propose a systematic algorithm to test Hamiltonian identifiability by employing the idea of Gröbner basis, which is an essential concept in the commutative algebra and algebraic geometry [37, 36, 47, 12]. In particular, we use these techniques to explore what Hamiltonian models can be identified when restricting our access to a single quantum probe. Furthermore, we provide a lower bound in the number of sampling points required to fully identify the Hamiltonian, which sets an upper bound for the total evolution time and thus the total measurement time.

2.2 State-space representation for closed quantum system dynamics

In this section, we review the state-space representation approach to analyze closed quantum system dynamics, which was introduced by Zhang and Sarovar in [161, 162], classical linear system realization theory [80, 79, 130], and the eigensystem realization algorithm (ERA) approach [80] to Hamiltonian parameter estimation developed in [161, 162].

2.2.1 Accessible set

The Hamiltonian H is generally parameterized by

$$H = \sum_{k=1}^{M} \theta_k S_k, \tag{2.1}$$

where $\{\theta_k\}_{k=1}^{M} \in \mathbb{R} \setminus \{0\}$ and $\{S_k\}_{k=1}^{M}$ are Hermitian operators. For an interaction N qubit system, $\{iS_k\}_{k=1}^{M}$ are independent elements of a Lie algebra in $\mathfrak{su}(2^N)$. Let us define a set

$$G_0 = \{O_1, O_2, \cdots, O_l \mid iO_i \in \mathfrak{su}(2^N)\},$$

which we call *observable set* of operators that we can directly measure on our quantum probe, and let these operators satisfy the following condition

$$[O_i, H] \neq 0 \ (i = 1, 2, \cdots, l).$$

Next, let Γ be the set of operators constructing the Hamiltonian:

$$\Gamma = \{S_k \mid iS_k \in \mathfrak{su}(2^N), k = 1, 2, \cdots, M\}.$$

Each operator to be measured evolves under the Heisenberg's equation of motion

$$\frac{d}{dt} O_i = i[H, O_i]. \tag{2.2}$$

The commutator generates a set of new operators $\{O_{i,1}, O_{i,2}, \cdots, O_{i,m}\}$, where $O_{i,p}$ denotes the $p-$th new operator generated from the commutator between the operator O_i and Hamiltonian H. As these operators also evolve in time, the commutator between $\{O_{i,p}\}_{p=1}^{m}$ and the Hamiltonian generates new operators again. The, intuitively, the dynamics is fully generated by repeated commutators. In order to mathematically

describe this process, we define an iterative procedure

$$G_j \equiv G_{j-1} \cup [\![G_{j-1}, \Gamma]\!], \tag{2.3}$$

where

$$[\![G_{j-1}, \Gamma]\!] \equiv \{O_i | \mathrm{tr}(O_i^\dagger [g, \gamma]) \neq 0,\ g \in G_{j-1}, \gamma \in \Gamma\}.$$

Because of the finite dimensionality of $\mathfrak{su}(2^N)$, the iterative procedure in Eq. (2.3) will saturate, and we can obtain a saturated set of operators G, which is called *accessible set* [161, 162]. Therefore, G includes all the operators generated from G_0 from the dynamics, and some of these generated operators represent the correlations between the target system and the quantum probe. In the following, we write $|G|$ as the number of elements in the accessible set G.

Example: Accessible set of 3-qubit exchange Hamiltonian

Let us provide an example for 3-qubit exchange interaction Hamiltonian:

$$H = \frac{J_1}{2}(X_1X_2 + Y_1Y_2) + \frac{J_2}{2}(X_2X_3 + Y_2Y_3), \tag{2.4}$$

where X_k, Y_k, Z_k are the each components of Pauli matrices acting on k-th qubit:

$$X = \begin{pmatrix} 0 & 1 \\ 1 & 0 \end{pmatrix}, Y = \begin{pmatrix} 0 & -i \\ i & 0 \end{pmatrix}, Z = \begin{pmatrix} 1 & 0 \\ 0 & -1 \end{pmatrix}.$$

For N-qubit system, X_k, Y_k and Z_k are precisely

$$\begin{aligned} X_k &\equiv \mathbb{1}_1 \otimes \mathbb{1}_2 \cdots \mathbb{1}_{k-1} \otimes X \otimes \mathbb{1}_{k+1} \otimes \mathbb{1}_N \\ Y_k &\equiv \mathbb{1}_1 \otimes \mathbb{1}_2 \cdots \mathbb{1}_{k-1} \otimes Y \otimes \mathbb{1}_{k+1} \otimes \mathbb{1}_N \\ Z_k &\equiv \mathbb{1}_1 \otimes \mathbb{1}_2 \cdots \mathbb{1}_{k-1} \otimes Z \otimes \mathbb{1}_{k+1} \otimes \mathbb{1}_N, \end{aligned}$$

where $\mathbb{1}$ is the 2×2 identity matrix. Pauli matrices satisfy the following commutation relations:

$$[X_k, Y_l] = 2i\delta_{kl} Z_k, \ [Y_k, Z_l] = 2i\delta_{kl} X_k, \ [Z_k, X_l] = 2i\delta_{kl} Y_k.$$

In 3-qubit exchange Hamiltonian, the operator set Γ is given as

$$\Gamma = \{X_1X_2 + Y_1Y_2, X_2X_3 + Y_2Y_3\}.$$

Suppose that we are going to measure X_1, then the observable set becomes

$$G_0 = \{X_1\}.$$

First, let us calculate $G_1 = G_0 \cup [\![G_0, \Gamma]\!]$. Here,

$$[\![G_0, \Gamma]\!] = \Big\{[X_1, X_1X_2 + Y_1Y_2], [X_1, X_2X_3 + Y_2Y_3]\Big\} = \{Z_1Y_2\},$$

which means that Z_1Y_2 is the new generated operator evolving with X_1 due to the dynamics. Here, we only care about the operator but not the coefficients. Therefore,

$$G_1 = G_0 \cup [\![G_0, \Gamma]\!] = \{X_1\} \cup \{Z_1Y_2\} = \{X_1, Z_1Y_2\}.$$

Then, we also need to calculate $G_2 = G_1 \cup [\![G_1, \Gamma]\!]$. Here,

$$\begin{aligned}[\![G_1, \Gamma]\!] &= \Big\{[X_1, X_1X_2 + Y_1Y_2], [X_1, X_2X_3 + Y_2Y_3], [Z_1Y_2, X_1X_2 + Y_1Y_2], [Z_1Y_2, X_2X_3 + Y_2Y_3]\Big\} \\ &= \{Z_1Y_2, X_1, Z_1Z_2X_3\}.\end{aligned}$$

Here, as we can see we can again obtain a new operator $Z_1Z_2X_3$, which are evolving with X_1 and Z_1Y_2. Therefore,

$$G_2 = G_1 \cup [\![G_1, \Gamma]\!] = \{X_1, Z_1Y_2\} \cup \{Z_1Y_2, X_1, Z_1Z_2X_3\} = \{X_1, Z_1Y_2, Z_1Z_2X_3\}.$$

Then, we calculate $G_3 = G_2 \cup [\![G_2, \Gamma]\!]$. Here,

$$\begin{aligned}[\![G_2, \Gamma]\!] = \Big\{ & [X_1, X_1X_2 + Y_1Y_2], [X_1, X_2X_3 + Y_2Y_3], \\ & [Z_1Y_2, X_1X_2 + Y_1Y_2], [Z_1Y_2, X_2X_3 + Y_2Y_3], \\ & [Z_1Z_2X_3, X_1X_2 + Y_1Y_2], [Z_1Z_2X_3, X_2X_3 + Y_2Y_3] \Big\} \\ = & \{Z_1Y_2, X_1, Z_1Z_2X_3\}.\end{aligned}$$

and

$$G_3 = G_2 = \{X_1, Z_1Y_2, Z_1Z_2X_3\}.$$

Therefore, G_2 is the accessible set G, i.e.

$$G = \{X_1, Z_1Y_2, Z_1Z_2X_3\}, \tag{2.5}$$

and these operators are evolving together through the dynamics.

2.2.2 State-space representation

In the following, without loss of generality, we will typically consider only observable O_1 on the first spin, which is the quantum probe, i.e. $G_0 = \{O_1\}$. From the iterative procedure in Eq. (2.3), Eq. (2.2) can be written as

$$\frac{d}{dt}O_i = i[H, O_i] = \sum_{l=1}^{|G|} \Big(\sum_{k=1}^{M} \theta_k V_{kml} \Big) O_l, \tag{2.6}$$

where

$$V_{kml} = \mathrm{Tr}\big[i[S_m, O_k] O_l \big] \in \mathbb{R}.$$

Let ρ_0 be the initial state of the joint system of the target and quantum probe, so that the expectation value of O_1 is given by $x_1(t) \equiv \langle O_1(t) \rangle = \mathrm{Tr}[\rho_0 O_1(t)]$. Then, the expectation values of the elements in the accessible set G form a state vector

(coherent vector) $\mathbf{x}(t) = (x_1(t), x_2(t), \cdots, x_{|G|}(t))^T \in \mathbb{R}^{|G|}$. Then, from Eq. (2.6), we have

$$\frac{d}{dt}x_i(t) = \sum_{l=1}^{|G|}\Big(\sum_{k=1}^{M}\theta_k V_{mkl}\Big)x_l(t),$$

so that in matrix form, we have

$$\frac{d\mathbf{x}(t)}{dt} = \tilde{\mathbf{A}}\mathbf{x}(t),$$

where $\tilde{\mathbf{A}} \in \mathbb{R}^{|G|\times|G|}$ is a skew-symmetric matrix, which contains the parameters $\{\theta_k\}_{k=1}^{M}$ in its off-diagonal elements. Note that $\tilde{\mathbf{A}}$ does not necessarily have to contain all the parameters but when the dynamics correlates all the spins with the quantum probe, $\tilde{\mathbf{A}}$ contains all the parameters. This is actually the necessary condition for the system to be identified [138], which will be explained in detail in Sec, 2.4.

Let $y(t) \in \mathbb{R}$ be the output data obtained by the output matrix $\mathbf{C} \in \mathbb{R}^{1\times|G|}$. Then, we can obtain the following state-space representation

$$\begin{aligned}\frac{d\mathbf{x}(t)}{dt} &= \tilde{\mathbf{A}}\mathbf{x}(t)\\ y(t) &= \mathbf{C}\mathbf{x}(t).\end{aligned} \tag{2.7}$$

This is called classical linear time-independent (LTI) system [80, 79, 130], and this shows that the quantum evolution in closed quantum system can be reduced into equivalent classical LTI system. Furthermore, it is useful to define the corresponding time-discrete representation

$$\begin{aligned}\mathbf{x}(j+1) &= \mathbf{A}\mathbf{x}(j)\\ y(j) &= \mathbf{C}\mathbf{x}(j),\end{aligned} \tag{2.8}$$

where $\mathbf{x}(j) \equiv \mathbf{x}(j\Delta t), y(j) \equiv y(j\Delta t)$ and $\mathbf{A} \equiv e^{\tilde{\mathbf{A}}\Delta t}$. Eq. 2.8 is useful in practical settings because the measurement results are usually acquired at the discrete-time steps. Note that since any matrix exponential is a nonsingular matrix, the rank of $\mathbf{A}$

is always

$$\text{rank}(\mathbf{A}) = \text{rank}(e^{\tilde{\mathbf{A}}\Delta t}) = \dim(\mathbf{x}(t)) = |G|.$$

Example: State-space representation of 3-qubit exchange Hamiltonian

Let us construct state-space representation of 3-qubit exchange Hamiltonian in Eq. (2.4). Now, from Eq. (2.5), we know that the accessible set is

$$G = \{X_1, Z_1Y_2, Z_1Z_2X_3\}.$$

When we generate G, we did not care about the coefficients from the commutators between the generated time-varying operators and Hamiltonian. Now, we need to take into account the coefficients. Let us calculate $[\![G, H]\!]$, then we can find

$$\begin{aligned}
[X_1, H] &= \Big[X_1, \frac{J_1}{2}(X_1X_2 + Y_1Y_2) + \frac{J_2}{2}(X_2X_3 + Y_2Y_3)\Big] = \frac{J_1}{2}[X_1, Y_1Y_2] \\
&= iJ_1 \cdot Z_1Y_2 \\
[Z_1Y_2, H] &= \Big[Z_1Y_2, \frac{J_1}{2}(X_1X_2 + Y_1Y_2) + \frac{J_2}{2}(X_2X_3 + Y_2Y_3)\Big] \\
&= \frac{J_1}{2}[Z_1Y_2, Y_1Y_2] + \frac{J_2}{2}[Z_1Y_2, X_2X_3] = -iJ_1 \cdot X_1 - iJ_2 \cdot Z_1Z_2X_3 \\
[Z_1Z_2X_3, H] &= \Big[Z_1Z_2X_3, \frac{J_1}{2}(X_1X_2 + Y_1Y_2) + \frac{J_2}{2}(X_2X_3 + Y_2Y_3)\Big] \\
&= \frac{J_2}{2}[Z_1Z_2X_3, X_2X_3] = iJ_2 \cdot Z_1Y_2
\end{aligned}$$

Therefore,

$$\begin{aligned}
\frac{d}{dt}X_1 &= -i[X_1, H] = J_1 \cdot Z_1Y_2 \\
\frac{d}{dt}Z_1Y_2 &= -i[Z_1Y_2, H] = -J_1 \cdot X_1 - J_2 \cdot Z_1Z_2X_3 \\
\frac{d}{dt}Z_1Z_2X_3 &= -i[Z_1Z_2X_3, H] = J_2 \cdot Z_1Y_2.
\end{aligned}$$

Therefore, we have

$$\frac{d}{dt}\begin{pmatrix} X_1 \\ Z_1Y_2 \\ Z_1Z_2X_3 \end{pmatrix} = \begin{pmatrix} 0 & J_1 & 0 \\ -J_1 & 0 & -J_2 \\ 0 & J_2 & 0 \end{pmatrix}\begin{pmatrix} X_1 \\ Z_1Y_2 \\ Z_1Z_2X_3 \end{pmatrix}.$$

Let ρ_0 be the initial state. Then, we have

$$\begin{aligned} x_1(t) &= \mathrm{Tr}[\rho_0 X_1(t)] \\ x_2(t) &= \mathrm{Tr}[\rho_0 Z_1Y_2(t)] \\ x_3(t) &= \mathrm{Tr}[\rho_0 Z_1Z_2X_3(t)]. \end{aligned}$$

If we choose the initial state to be

$$\rho(0) = \frac{1}{2}\begin{pmatrix} 1 & 1 \\ 1 & 1 \end{pmatrix} \otimes \frac{\mathbb{1}}{2} \otimes \frac{\mathbb{1}}{2},$$

then, the initial coherent vector becomes

$$\begin{aligned} x_1(0) &= \mathrm{Tr}[\rho_0 X_1(0)] = 1 \\ x_2(0) &= \mathrm{Tr}[\rho_0 Z_1Y_2(0)] = 0 \\ x_3(0) &= \mathrm{Tr}[\rho_0 Z_1Z_2X_3(0)] = 0. \end{aligned}$$

Then, we can construct a coherent vector

$$\mathbf{x}(t) = \begin{pmatrix} x_1(t) & x_2(t) & x_3(t) \end{pmatrix}^T$$

with

$$\mathbf{x}_0 = \begin{pmatrix} 1 & 0 & 0 \end{pmatrix}^T.$$

Since we want to measure X_1, then we choose

$$\mathbf{C} = \begin{pmatrix} 1 & 0 & 0 \end{pmatrix}$$

so that we can obtain

$$y(t) = \mathbf{C}\mathbf{x}(t) = \begin{pmatrix} 1 & 0 & 0 \end{pmatrix} \begin{pmatrix} x_1(t) \\ x_2(t) \\ x_3(t) \end{pmatrix} = x_1(t).$$

Therefore, we can obtain

$$\begin{aligned} \frac{d\mathbf{x}(t)}{dt} &= \tilde{\mathbf{A}}\mathbf{x}(t) \\ y(t) &= \mathbf{C}\mathbf{x}(t), \end{aligned} \tag{2.9}$$

where

$$\tilde{\mathbf{A}} = \begin{pmatrix} 0 & J_1 & 0 \\ -J_1 & 0 & -J_2 \\ 0 & J_2 & 0 \end{pmatrix}.$$

Furthermore, we can find that

$$|G| = \text{rank}(e^{\tilde{\mathbf{A}}\Delta t}) = 3.$$

2.2.3 Linear system realization theory

Let us consider a classical LTI system in Eq. 2.7. By performing a Laplace transformation, the irreducible transfer function $\Xi(s)$ is given by

$$\Xi(s) = \mathbf{C}(s\mathbf{I} - \tilde{\mathbf{A}})^{-1}\mathbf{x}_0 = \frac{P(s)}{Q(s)},$$

which describes the dynamics of the LTI system of Eq. (2.7) in Laplace space. Since the irreducible transfer function depends on $\tilde{\mathbf{A}}$, $\mathbf{C}$, and the initial state $\mathbf{x}_0$, $[\tilde{\mathbf{A}}, \mathbf{C}, \mathbf{x}_0]$ is called *realization* of the irreducible transfer function $\Xi(s)$ (or the LTI system). $\mathbf{I}$ is $n \times n$ identity matrix and the system initial state must be chosen such that $\mathbf{x}_0 \neq \mathbf{0}$. $P(s)$ and $Q(s)$ are polynomials in the Laplace variable s. In particular, $Q(s)$ is called the characteristic polynomial of $\Xi(s)$. The degree of $Q(s)$ is called *model order* [7], which is defined as

$$n = \deg(Q(s)). \tag{2.10}$$

The model order n can be interpreted as the minimum number of independent state variables required to fully describe the dynamics of the system. From Eq. (2.8), if we define $\mathbf{H}_{r,s}$ as the following Hankel matrix

$$\mathbf{H}_{r,s} = \begin{pmatrix} y(0) & y(1) & \cdots & y(s-1) \\ y(1) & y(2) & \cdots & y(s) \\ \vdots & \vdots & \ddots & \vdots \\ y(r-1) & y(r) & \cdots & y(r+s-2) \end{pmatrix} = \begin{pmatrix} \mathbf{C}\mathbf{x}_0 & \mathbf{C}\mathbf{A}\mathbf{x}_0 & \cdots & \mathbf{C}\mathbf{A}^{s-1}\mathbf{x}_0 \\ \mathbf{C}\mathbf{A}\mathbf{x}_0 & \mathbf{C}\mathbf{A}^2\mathbf{x}_0 & \cdots & \mathbf{C}\mathbf{A}^{s}\mathbf{x}_0 \\ \vdots & \vdots & \ddots & \vdots \\ \mathbf{C}\mathbf{A}^{r-1}\mathbf{x}_0 & \mathbf{C}\mathbf{A}^{r}\mathbf{x}_0 & \cdots & \mathbf{C}\mathbf{A}^{r+s-2}\mathbf{x}_0 \end{pmatrix},$$

and $\mathbf{H}_{r,s}$ can be decomposed into

$$\mathbf{H}_{r,s} = \begin{pmatrix} \mathbf{C} \\ \mathbf{C}\mathbf{A} \\ \vdots \\ \mathbf{C}\mathbf{A}^{r-1} \end{pmatrix} \begin{pmatrix} \mathbf{x}_0 & \mathbf{A}\mathbf{x}_0 & \cdots & \mathbf{A}^{s-1}\mathbf{x}_0 \end{pmatrix} = \mathbf{M}_O(r)\mathbf{M}_C(s), \tag{2.11}$$

where $\mathbf{M}_O(r) \in \mathbb{R}^{r \times |G|}$ is called *observability matrix* defined as

$$\mathbf{M}_O(r) = \begin{pmatrix} \mathbf{C} \\ \mathbf{C}\mathbf{A} \\ \cdots \\ \mathbf{C}\mathbf{A}^{r-1} \end{pmatrix}$$

and $\mathbf{M}_C(s) \in \mathbb{R}^{|G| \times s}$ is called *controllability matrix* defined as

$$\mathbf{M}_C(s) = \begin{pmatrix} \mathbf{x}_0 & \mathbf{A}\mathbf{x}_0 & \cdots & \mathbf{A}^{s-1}\mathbf{x}_0 \end{pmatrix}. \tag{2.12}$$

When a LTI system with $\dim(\mathbf{x}(t)) = |G|$ is minimal, namely both controllable and observable, we have [80, 79, 130]:

$$\mathrm{rank}(\mathbf{M}_C(s)) = \mathrm{rank}(\mathbf{M}_O(r)) = |G|, \tag{2.13}$$

where $r, s \geq |G|$. Therefore, from Sylvester inequality [68], we have

$$\mathrm{rank}(\mathbf{M}_C(s)) + \mathrm{rank}(\mathbf{M}_O(r)) - |G| \leq \mathrm{rank}(\mathbf{H}_{r,s}) \leq \min\{\mathrm{rank}(\mathbf{M}_C(s)), \mathrm{rank}(\mathbf{M}_O(r))\},$$

which yields

$$\mathrm{rank}(\mathbf{H}_{r,s}) = |G|.$$

Furthermore, the rank of the Hankel matrix $\mathbf{H}_{r,s}$ is equivalent to model order [79]:

$$\mathrm{rank}(\mathbf{H}_{r,s}) = n,$$

where $r, s \geq n$. Therefore, when the system is minimal, we must have $|G| = n$ [137].

Example: Transfer function of 3-qubit exchange Hamiltonian

Here, let us discuss the transfer function of 3-qubit exchange Hamiltonian in Eq. (2.4). From Eq. (**??**), the transfer function is given as

$$\Xi(s) = \begin{pmatrix} 1 & 0 & 0 \end{pmatrix} \left[s \begin{pmatrix} 1 & 0 & 0 \\ 0 & 1 & 0 \\ 0 & 0 & 1 \end{pmatrix} - \begin{pmatrix} 0 & J_1 & 0 \\ -J_1 & 0 & -J_2 \\ 0 & J_2 & 0 \end{pmatrix} \right]^{-1} \begin{pmatrix} 1 \\ 0 \\ 0 \end{pmatrix},$$

which yields

$$\Xi(s) = \frac{s^2 + J_2^2}{s^3 + (J_1^2 + J_2^2)s}. \tag{2.14}$$

As we can see that

$$|G| = \deg\Big(s^3 + s^3 + (J_1^2 + J_2^2)s\Big) = 3,$$

which is the model order of the system.

Controllability and Observability

Here, let us prove Eq. (2.13) by following Refs. [80, 79, 130]. Here, let us consider the following general discrete-time LTI system

$$\begin{aligned} \mathbf{x}(k+1) &= \mathbf{A}\mathbf{x}(k) + \mathbf{B}\mathbf{u}(k),\ \mathbf{x}(0) = \mathbf{0} \\ \mathbf{y}(k) &= \mathbf{C}\mathbf{x}(k), \end{aligned} \tag{2.15}$$

where $\mathbf{A} \in \mathbb{R}^{n\times n}$, $\mathbf{x}(k) \in \mathbb{R}^n$, $\mathbf{C} \in \mathbb{R}^{m\times n}$, $\mathbf{B} \in \mathbb{R}^{n\times r}$, $\mathbf{y}(k) \in \mathbb{R}^m$, and $\mathbf{u}(k) \in \mathbb{R}^r$. Here, $\mathbf{u}(k)$ is the input vector, which actually corresponds to the control in classical control theory and generally $\mathbf{u}(k)$ can take any types of functions. Note that here $\mathbf{x}(0)$ could be different from $\mathbf{x}_0$, which is the initial state which we discussed above. The solution for $\mathbf{x}(k)$ is then given by

$$\mathbf{x}(k) = \mathbf{A}^k\mathbf{x}(0) + \sum_{j=1}^{k-1} \mathbf{A}^j\mathbf{B}\mathbf{u}(k-j-1), \tag{2.16}$$

and in this case the controllability matrix and observability matrix are given by

$$\mathbf{M}_C(s) = \begin{pmatrix} \mathbf{B} & \mathbf{AB} & \cdots & \mathbf{A}^{s-1}\mathbf{B} \end{pmatrix},$$

and

$$\mathbf{M}_O(r) = \begin{pmatrix} \mathbf{C} \\ \mathbf{CA} \\ \cdots \\ \mathbf{CA}^{r-1} \end{pmatrix}$$

where $s, r \geq n$.

The definition of the controllability is

Definition 1 (Controllability)**.** *The LTI system Eq. (2.15) is controllable if there exits a control sequence* $\{\mathbf{u}(j)\}$ *such that* $\mathbf{x}(0)$ *can be transferred into an arbitrary state* $\mathbf{x}_p$ *at time* p*, i.e.* $\mathbf{x}_p = \mathbf{x}(p)$.

Then, we obtain the following theorem:

Theorem 1. *The LTI system Eq. (2.15) is controllable if and only if*

1. *Controllability grammian*

$$\mathbf{W}_C(k) = \sum_{j=0}^{k} (\mathbf{A}^j\mathbf{B})(\mathbf{A}^j\mathbf{B})^T \in \mathbb{R}^{n\times n}$$

   is non-singular:

$$det\Big(\mathbf{W}_C(k)\Big) \neq 0.$$

2. *Controllability matrix* $\mathbf{M}_C(n)$ *has full rank:*

$$rank(\mathbf{M}_C(n)) = rank(\mathbf{A}) = n.$$

and (1) and (2) are equivalent.

Proof. Let us prove Theorem. 1.

1. $\det(\mathbf{W}_C(k)) \neq 0 \Longrightarrow$ The LTI system Eq. (2.15):

   Let $\mathbf{W}_C(k)$ be non-singular, i.e. $\det(\mathbf{W}_C(k)) \neq 0$. From Eq. (2.16), for an arbitrary $\mathbf{x}_p$, if we choose

   $$\mathbf{u}(p-j-1) = -\mathbf{B}^T(\mathbf{A}^j)^T\mathbf{W}_C^{-1}(p)(\mathbf{A}^p\mathbf{x}(0) - \mathbf{x}_p),$$

   then, we can obtain

   $$\mathbf{x}(p) = \mathbf{A}^p\mathbf{x}(0) - \sum_{j=0}^{p-1}\mathbf{A}^j\mathbf{B}\mathbf{B}^T(\mathbf{A}^j)^T\mathbf{W}_C^{-1}(p)(\mathbf{A}^p\mathbf{x}(0) - \mathbf{x}_p).$$

   Since the controllability grammian is defined as

   $$\mathbf{W}_C(p) = \sum_{j=0}^{p-1}\mathbf{A}^j\mathbf{B}\mathbf{B}^T(\mathbf{A}^j)^T,$$

   we can obtain

   $$\mathbf{x}_p = \mathbf{A}^p\mathbf{x}(0) - \mathbf{W}_C(p)\mathbf{W}_C^{-1}(p)(\mathbf{A}^p\mathbf{x}(0) - \mathbf{x}_p) = \mathbf{x}_p.$$

   Therefore, there exists a classical control sequence $\{\mathbf{u}(p-j-1)\}_{j=0}^{p-1}$, which can transfer $\mathbf{x}(0)$ to an arbitrary state $\mathbf{x}_p$ at time p. From the Def. 1, the LTI system is controllable.

2. The LTI system Eq. (2.15) is controllable $\Longrightarrow \det(\mathbf{W}_C(k)) \neq 0$:

   Let us fix k. If $\mathbf{W}_C(k) = 0$, then there must exist a non-zero vector $\mathbf{a}$ such that

   $$\mathbf{W}_C(k)\mathbf{a} = \mathbf{0}.$$

   Therefore, we have

   $$\mathbf{a}^T\mathbf{W}_C(k)\mathbf{a} = \sum_{j=0}^{k-1}\mathbf{a}^T\mathbf{A}^j\mathbf{B}\mathbf{B}^T(\mathbf{A}^j)^T\mathbf{a} = \sum_{j=0}^{k}\left(\mathbf{B}^T(\mathbf{A}^j)^T\mathbf{a}\right)^T\left(\mathbf{B}^T(\mathbf{A}^j)^T\mathbf{a}\right),$$

which yields:

$$\mathbf{a}^T \mathbf{W}_C(k)\mathbf{a} = \sum_{j=0}^{k-1} \left\| \mathbf{B}^T (\mathbf{A}^j)^T \mathbf{a} \right\|^2 = 0.$$

However, if the LTI system Eq. (2.15) is controllable, there exists control $\mathbf{u}(k-j-1)$ which transfers an initial state $\mathbf{x}_0 = \mathbf{a}$ to $\mathbf{0}$. Therefore, we can write

$$\mathbf{0} = \mathbf{A}^k \mathbf{a} + \sum_{j=0}^{k-1} \mathbf{A}^j \mathbf{B}\mathbf{u}(k-j-1).$$

Therefore,

$$\mathbf{0} = \mathbf{a}^T \mathbf{A}^k \mathbf{a} + \sum_{j=0}^{k-1} \mathbf{a}^T \mathbf{A}^j \mathbf{B}\mathbf{u}(k-j-1).$$

Since $\mathbf{B}^T (\mathbf{A}^j)^T \mathbf{a} = \mathbf{0} \iff \mathbf{a}^T \mathbf{A}^j \mathbf{B} = \mathbf{0}^T$, we have

$$\mathbf{a}^T \mathbf{A}^j \mathbf{a} = \mathbf{0}. \tag{2.17}$$

For arbitrary non-zero $\mathbf{A}$, Eq. (2.17) holds if and only if $\mathbf{a} = \mathbf{0}$, which contradicts our assumption that $\mathbf{a} \neq \mathbf{0}$. Therefore, by contradiction, $\det(\mathbf{W}_C(k)) \neq 0$. Therefore, we can obtain

$$\text{LTI system is controllable} \iff \det\Big(\mathbf{W}_C(k)\Big) \neq 0.$$

3. $\det(W_C(k)) \neq 0 \Longrightarrow \text{rank}(\mathbf{M}_C(n)) = \text{rank}(\mathbf{A}) = n$:

   If $\mathbf{M}_C(n)$ does not have full rank, i.e. $\text{rank}(\mathbf{M}_C(n)) \leq n-1$, then, there exists a non-zero vector $\mathbf{a}$ such that

$$\mathbf{a}^T \mathbf{M}_C(n) = \mathbf{a}^T \begin{pmatrix} \mathbf{B} & \mathbf{AB} & \cdots & \mathbf{A}^{n-1}\mathbf{B} \end{pmatrix} = \mathbf{0},$$

which yields

$$\mathbf{a}^T\mathbf{A}^j\mathbf{B} = \mathbf{0},\ j = 0, 1, 2, \cdots, n-1.$$

Therefore,

$$\sum_{j=0}^{k-1} \mathbf{a}^T\mathbf{A}^j\mathbf{B}\mathbf{B}^T(\mathbf{A}^j)^T\mathbf{a} = \mathbf{a}^T\mathbf{W}_C(k)\mathbf{a} = 0,$$

which indicates that $\mathbf{W}_C(k)$ is singular

$$\det\Big(\mathbf{W}_C(k)\Big) = 0.$$

Therefore, we have

$$\text{rank}(\mathbf{M}_C(n)) \leq n-1 \Longrightarrow \det\Big(\mathbf{W}_C(k)\Big) = 0.$$

By taking the contraposition, we have

$$\det\Big(\mathbf{W}_C(k)\Big) \neq 0 \Longrightarrow \text{rank}(\mathbf{M}_C(n)) = n.$$

4. $\text{rank}(\mathbf{M}_C(n)) = \text{rank}(\mathbf{A}) = n \Longrightarrow \det(\mathbf{W}_C(k)) \neq 0$:

   If $\det(\mathbf{W}_C(k)) = 0$, then there exists a non-zero vector $\mathbf{a}$ such that

$$\mathbf{W}_C(k)\mathbf{a} = 0,$$

which yields

$$\mathbf{a}^T\mathbf{A}^j\mathbf{B} = \mathbf{0}.$$

Therefore,

$$\mathbf{a}^T\mathbf{M}_C(n) = \mathbf{a}^T\begin{pmatrix}\mathbf{B} & \mathbf{AB} & \cdots & \mathbf{A}^{n-1}\mathbf{B}\end{pmatrix} = \mathbf{0}.$$

Therefore,

$$\mathrm{rank}(\mathbf{M}_C(n)) \leq n-1,$$

and we obtain

$$\det\Big(\mathbf{W}_C(k)\Big) = 0 \Longrightarrow \mathrm{rank}(\mathbf{M}_C(n)) \leq n-1.$$

By taking the contraposition, we have

$$\mathrm{rank}(\mathbf{M}_C(n)) = n \Longrightarrow \det\Big(\mathbf{W}_C(k)\Big) \neq 0.$$

Therefore, we can obtain

$$\det\Big(\mathbf{W}_C(k)\Big) \neq 0 \Longleftrightarrow \mathrm{rank}(\mathbf{M}_C(n)) = n.$$

From these results, we can finally obtain the following equivalence:

The LTI system Eq. (2.15) is controllable $\Longleftrightarrow \det\Big(\mathbf{W}_C(k)\Big) \neq 0 \Longleftrightarrow \mathrm{rank}(\mathbf{M}_C(n)) = n,$

which proves Theorem 1. □

Note that the proof for Theorem. 1 is a general approach. In order to match the discussion for the case

$$\begin{aligned} \mathbf{x}(k+1) &= \mathbf{A}\mathbf{x}(k) \\ y(k) &= \mathbf{C}\mathbf{x}(k), \end{aligned} \tag{2.18}$$

we can take the following setting:

$$\mathbf{u}(k) = \begin{cases} 1 \ (k=0) \\ 0 \ (k=1) \end{cases}$$

and

$$\mathbf{x}(0) = \mathbf{0}$$

so that if we define $\mathbf{B} = \mathbf{x}_0$ then we have

$$\begin{aligned}
\mathbf{x}(0) &= \mathbf{0} \\
\mathbf{x}(1) &= \mathbf{B} = \mathbf{x}_0 \\
\mathbf{x}(2) &= \mathbf{AB} = \mathbf{A}\mathbf{x}_0 \\
&\vdots \\
\mathbf{x}(s-2) &= \mathbf{A}^{s-1}\mathbf{B} = \mathbf{A}^{s-1}\mathbf{x}_0 \\
\mathbf{x}(s-1) &= A^s\mathbf{B} = \mathbf{A}^s\mathbf{0}
\end{aligned}$$

Then, the controllability matrix can be written as

$$\mathbf{M}_C(s) = \begin{pmatrix} \mathbf{x}_0 & \mathbf{A}\mathbf{x}_0 & \cdots & \mathbf{A}^{s-1}\mathbf{x}_0 \end{pmatrix},$$

which is equivalent to Eq. (2.12); therefore, the whole proof also works for the system described by Eq. (2.18), which is the case for the dynamics of closed quantum systems.

The definition of the observability is

Definition 2 (Observability)**.** *The LTI system Eq. (2.15) is observable if there exits a time p and initial state $\mathbf{x}_0$ can be determined uniquely from measurement results $\{\mathbf{y}(j)\}$.*

Then, we can obtain the following theorem:

Theorem 2. *The LTI system Eq. (2.15) is observable if and only if*

1. *Observability grammian*

$$\mathbf{W}_O(k) = \sum_{j=0}^{k} (\mathbf{C}\mathbf{A}^j)^T (\mathbf{C}\mathbf{A}^j) \in \mathbb{R}^{n\times n}$$

is non-singular:

$$det\Big(\mathbf{W}_O(k)\Big) \neq 0.$$

2. *Controllability matrix* $\mathbf{M}_O(n)$ *has full rank:*

$$rank(\mathbf{M}_O(n)) = rank(\mathbf{A}) = n.$$

and (1) and (2) are equivalent.

Proof. 1. $\det(\mathbf{W}_O(k)) \neq 0 \Longrightarrow$ The LTI system Eq. (2.15) is observable:

Let $\mathbf{W}_O(k)$ be non-singular, i.e. $\det(\mathbf{W}_O(k)) \neq 0$. Since at time j, we have

$$\mathbf{y}(j) = \mathbf{C}\mathbf{A}^j\mathbf{x}(0).$$

Multiplying $(\mathbf{C}\mathbf{A}^p)^T$ from left to $\mathbf{y}$, we have

$$\sum_{j=0}^{k-1}(\mathbf{C}\mathbf{A}^j)^T\mathbf{y}(j) = \sum_{j=0}^{k-1}(\mathbf{C}\mathbf{A}^j)^T(\mathbf{C}\mathbf{A}^j)\mathbf{x}(0) = \mathbf{W}_O(k)\mathbf{x}(0).$$

Therefore, $\mathbf{x}(0)$ can be uniquely determined by

$$\mathbf{x}(0) = \mathbf{W}_O^{-1}(k)\sum_{j=0}^{k-1}(\mathbf{C}\mathbf{A}^j)^T\mathbf{y}(j)$$

from the measurement results $\{\mathbf{y}(j)\}_{j=0}^{k-1}$.

2. The LTI system Eq. (2.15) is observable $\Longrightarrow \det(\mathbf{W}_O(k)) \neq 0$:

If $\det(\mathbf{W}_O(k)) = 0$, there must exist a non-zero vector $\mathbf{a}$ such that

$$\mathbf{W}_O(k)\mathbf{a} = \mathbf{0}$$

and

$$\mathbf{a}^T\mathbf{W}_O(k)\mathbf{a} = \sum_{j=0}^{k-1}(\mathbf{C}\mathbf{A}^j\mathbf{a})^T(\mathbf{C}\mathbf{A}^j\mathbf{a}),$$

which yields

$$\mathbf{a}^T\mathbf{W}_O(k)\mathbf{a} = \sum_{j=0}^{k-1}\left\|\mathbf{C}\mathbf{A}^j\mathbf{a}\right\|^2 = 0.$$

Therefore,

$$\mathbf{C}\mathbf{A}^j\mathbf{a} = \mathbf{0},$$

which shows that $\mathbf{y}(j) = \mathbf{C}\mathbf{A}^j\mathbf{a} = 0\ \forall j$; therefore, the LTI system of Eq. (2.18) is unobservable. Therefore,

$$\det(\mathbf{W}_O(k)) = 0 \Longrightarrow \text{the LTI system of Eq. (2.18) is unobservable.}$$

Taking the counterposition, we have

$$\text{the LTI system of Eq. (2.18) is observable.} \Longrightarrow \det(\mathbf{W}_O(k)) \neq 0.$$

This proves

$$\text{the LTI system of Eq. (2.18) is observable.} \Longleftrightarrow \det(\mathbf{W}_O(k)) \neq 0.$$

3. $\text{rank}(\mathbf{M}_O(n)) = \text{rank}(\mathbf{A}) = n \Longrightarrow \det(\mathbf{W}_O(k)) \neq 0$:
   If $\det(\mathbf{W}_O(k)) = 0$, then there exists a non-zero vector $\mathbf{a}$ such taht

$$\mathbf{C}\mathbf{A}^j\mathbf{a} = \mathbf{0}.$$

Therefore, we have

$$\mathbf{M}_O(n)\mathbf{a} = \begin{pmatrix} \mathbf{C} \\ \mathbf{CA} \\ \vdots \\ \mathbf{CA}^{n-1} \end{pmatrix} \mathbf{a} = \mathbf{0}.$$

Therefore,

$$\text{rank}(\mathbf{M}_O(n)) \leq n-1,$$

which leads to

$$\det(\mathbf{W}_O(k)) = 0 \Longrightarrow \text{rank}(\mathbf{M}_O(k)) \leq n-1.$$

By taking the contraposition, we have

$$\text{rank}(\mathbf{M}_O(k)) = n \Longrightarrow \det(\mathbf{W}_O(k)) \neq 0.$$

4. $\det(\mathbf{W}_O(k)) \neq 0 \Longrightarrow \text{rank}(\mathbf{M}_O(n)) = \text{rank}(\mathbf{A}) = n$:

   If $\text{rank}(\mathbf{M}_O(n)) \leq n-1$, there must exists a non-zero vector $\mathbf{a}$ such that

$$\mathbf{M}_O(n)\mathbf{a} = \begin{pmatrix} \mathbf{C} \\ \mathbf{CA} \\ \vdots \\ \mathbf{CA}^{n-1} \end{pmatrix} \mathbf{a} = \mathbf{0}$$

   so that

$$\mathbf{a}^T\mathbf{W}_O(n)\mathbf{a} = \sum_{j=0}^{k-1} (\mathbf{CA}^j\mathbf{a})^T(\mathbf{CA}^j\mathbf{a}) = 0,$$

which indicates that

$$\det(\mathbf{W}_O(n)) = 0.$$

By taking the counterposition, we have

$$\det(\mathbf{W}_O(n)) \neq 0 \Longrightarrow \mathrm{rank}(\mathbf{M}_O(n)) = n.$$

Therefore, we can obtain

$$\det(\mathbf{W}_O(k)) \neq 0 \Longleftrightarrow \mathrm{rank}(\mathbf{M}_O(n)) = \mathrm{rank}(\mathbf{A}) = n.$$

From these discussions, we can arrive at

The LTI system Eq. (2.15) is observable $\Longleftrightarrow \det(\mathbf{W}_O(k)) \neq 0 \Longleftrightarrow \mathrm{rank}(\mathbf{M}_O(n)) = \mathrm{rank}(\mathbf{A}) = n,$

which proves Theorem. 2. □

From Theorem. 1 and Theorem. 2, we can obtain Eq. (2.13) for $s, r \geq n$.

2.2.4 Eigensystem realization algorithm (ERA)

Here, we introduce the eigensystem realization algorithm (ERA), which is a well developed system identification method for classical systems [80], and it is widely used from structural engineering [28] to aerospace engineering [112]. In the context of quantum system identification, Zhang and Savorar employed this method for Hamiltonian parameter estimation [161, 162], and a robust estimation was experimentally demonstrated for a closed quantum system [69].

The central idea of ERA is to provide a new realization $[\tilde{\mathbf{A}}_{\mathrm{e}}, \mathbf{C}_{\mathrm{e}}, \mathbf{x}_{0,\mathrm{e}}]$ from the sampling points $\{y(j)\}$. In order to solve this problem, we consider the singular value

decomposition (SVD) of Hankel matrix $\mathbf{H}_{r,s}$. The SVD of $\mathbf{H}_{r,s}$ yields

$$\mathbf{H}_{r,s} = \mathbf{U}\begin{pmatrix}\mathbf{\Sigma} & \mathbf{O}\\ \mathbf{O} & \mathbf{O}\end{pmatrix}\mathbf{V}^T = \begin{pmatrix}\mathbf{U}_1 & \mathbf{U}_2\end{pmatrix}\begin{pmatrix}\mathbf{\Sigma} & \mathbf{O}\\ \mathbf{O} & \mathbf{O}\end{pmatrix}\begin{pmatrix}\mathbf{V}_1^T\\ \mathbf{V}_2^T\end{pmatrix},$$

where $\mathbf{U}$ and $\mathbf{V}$ are unitary matrices (i.e. $\mathbf{U}\mathbf{U}^T = \mathbf{U}^T\mathbf{U} = \mathbf{I}$ and $\mathbf{V}\mathbf{V}^T = \mathbf{V}^T\mathbf{V} = \mathbf{I}$), and $\mathbf{\Sigma}$ is the singular value matrix. Since $n = \text{rank}(\mathbf{H}_{r,s})$, there are n nonzero singular values of $\mathbf{H}_{r,s}$ so that $\mathbf{\Sigma}$ is a $n \times n$ diagonal matrix containing the nonzero singular values. Then, from Eq. (2.11), we can write

$$\mathbf{M}_O(r) = \mathbf{U}_1\mathbf{\Sigma}^{1/2}$$
$$\mathbf{M}_C(s) = \mathbf{\Sigma}^{1/2}\mathbf{V}_1^T.$$

Next, let us consider the following shifted Hankel matrix $\bar{\mathbf{H}}_{r,s}$:

$$\bar{\mathbf{H}}_{r,s} = \begin{pmatrix} y(1) & y(2) & \cdots & y(s)\\ y(2) & y(3) & \cdots & y(s+1)\\ \vdots & \vdots & \ddots & \vdots\\ y(r) & y(r+1) & \cdots & y(r+s-1)\end{pmatrix} = \begin{pmatrix} \mathbf{C}\mathbf{A}\mathbf{x}_0 & \mathbf{C}\mathbf{A}^2\mathbf{x}_0 & \cdots & \mathbf{C}\mathbf{A}^s\mathbf{x}_0\\ \mathbf{C}\mathbf{A}^2\mathbf{x}_0 & \mathbf{C}\mathbf{A}^3\mathbf{x}_0 & \cdots & \mathbf{C}\mathbf{A}^{s+1}\mathbf{x}_0\\ \vdots & \vdots & \ddots & \vdots\\ \mathbf{C}\mathbf{A}^r\mathbf{x}_0 & \mathbf{C}\mathbf{A}^{r+1}\mathbf{x}_0 & \cdots & \mathbf{C}\mathbf{A}^{r+s-1}\mathbf{x}_0\end{pmatrix}, \tag{2.19}$$

which can be written as

$$\bar{\mathbf{H}}_{r,s} = \begin{pmatrix}\mathbf{C}\\ \mathbf{C}\mathbf{A}\\ \vdots\\ \mathbf{C}\mathbf{A}^{r-1}\end{pmatrix}\mathbf{A}\begin{pmatrix}\mathbf{x}_0 & \mathbf{A}\mathbf{x}_0 & \cdots & \mathbf{A}^{s-1}\mathbf{x}_0\end{pmatrix} = \mathbf{M}_O(r)\mathbf{A}\mathbf{M}_C(s),$$

which yields

$$\mathbf{A} = \mathbf{M}_O^{-1}(r)\bar{\mathbf{H}}_{r,s}\mathbf{M}_C^{-1}(s) = \mathbf{\Sigma}^{-1/2}\mathbf{U}_1^T\bar{\mathbf{H}}_{r,s}\mathbf{V}_1\mathbf{\Sigma}^{-1/2},$$

so that

$$\tilde{\mathbf{A}} = \frac{1}{\Delta t} \ln[\mathbf{\Sigma}^{-1/2}\mathbf{U}_1^T \bar{\mathbf{H}}_{r,s} \mathbf{V}_1 \mathbf{\Sigma}^{-1/2}].$$

As we can see, we can obtain a new realization deriving from our measurement result as

$$\begin{aligned} \tilde{\mathbf{A}}_e &= \frac{1}{\Delta t} \ln[\mathbf{\Sigma}^{-1/2}\mathbf{U}_1^T \bar{\mathbf{H}}_{r,s} \mathbf{V}_1 \mathbf{\Sigma}^{-1/2}] \\ \mathbf{C}_e &= [\mathbf{M}_C(s)]_{\text{first row}} = [\mathbf{\Sigma}^{1/2}\mathbf{V}_1^T]_{\text{first row}} \\ \mathbf{x}_{0,e} &= [\mathbf{M}_O(r)]_{\text{first column}} = [\mathbf{U}_1\mathbf{\Sigma}^{1/2}]_{\text{first column}}. \end{aligned} \tag{2.20}$$

Then, we can obtain the corresponding transfer function as

$$\Xi_e(s) = \mathbf{C}_e(s\mathbf{I} - \tilde{\mathbf{A}}_e)^{-1}\mathbf{x}_{0,e}.$$

In principle, since the original irreducible transfer function $\Xi(s)$ and the transfer function derived from the new realization $\Xi_e(s)$ describe same dynamics, we must have

$$\Xi(s) = \Xi_e(s). \tag{2.21}$$

Note that the coefficients of Laplace variable s in $\Xi(s)$ are polynomials in $\theta_1, \theta_2, \cdots, \theta_M$ because they are derived from the theoretical model, and the coefficients of Laplace variable s in $\Xi_e(s)$ are just numbers coming from the measurement results. Since Eq. (2.21) holds for any s, we can obtain a system of polynomial equations:

$$\begin{aligned} f_1(\theta_1, \theta_2, \cdots, \theta_M) &= 0 \\ f_2(\theta_1, \theta_2, \cdots, \theta_M) &= 0 \\ &\vdots \\ f_p(\theta_1, \theta_2, \cdots, \theta_M) &= 0 \end{aligned} \tag{2.22}$$

and $\{\theta_1, \theta_2, \cdots, \theta_M\}$ can be found by solving this system of polynomial equations.

Example: Eigensystem realization algorithm for 3-qubit exchange Hamiltonian

Here, let us show the example for the eigensystem realization algorithm for 3-qubit exchange Hamiltonian in Eq. (2.4). Through eigensystem realization algorithm, we can find that the transfer function with new realization has the form

$$\Xi_e(s) = \frac{s^2 + a_3 s + b_2}{s^3 + a_1 s^2 + b_1 s + a_2},$$

where

$$b_1, b_2 \gg a_1, a_2, a_3,$$

which is coming from the numeric error of the algorithm. From Eq. (2.14), we can obtain the following system of polynomial equations

$$\begin{aligned} J_2^2 &= b_2 \\ J_1^2 + J_2^2 &= b_1, \end{aligned} \tag{2.23}$$

where $b_1 \geq b_2 \geq 0$.

2.3 Hilbert space dimension identifiability

In this section, we will discuss the identifiability of Hilbert space dimension assisted by single-probe measurements. The dimension of the Hilbert space (or system dimension) is indeed an important information for any quantum device. The performance of quantum protocols, such as the computational complexity of quantum algorithms [116] or quantum process tomography [150], is strictly dependent on the dimension. In addition, in our recent work [138], we demonstrated that the dimension also determines what experimental resources, such as the number of sampling points and the total time evolution, are needed to characterize the rest of the Hamiltonian parameters. These dimension-dependent quantities are important for practical appli-

cations of quantum engineering. Therefore, dimension estimation is a significant task in quantum system identification.

The estimation of the Hilbert space dimension was first addressed by Brunner [20] as the concept of dimension witness, which is a test giving a bound on the Hilbert space dimension which can reproduce the measurement data [20, 151, 149, 153, 48, 19, 60, 16, 136, 39, 65, 1, 27], in which measuring all correlations generated in the system is essentially required, without any prior knowledge on the target system.

Here, we assume instead that the interaction model, which will be defined more precisely in Def. 3, is given as prior information. Although graph structure and coupling types are known in this scenario, the exact Hamiltonian is still unknown. This is because we cannot measure all the correlations if the exact dimension of the target system is unknown. Then, we employed an more practical scenario, in which the target system cannot be directly addressed but interacting with a well-characterized single quantum probe. By employing the concept of model order in linear system realization theory in Sec. 2.2.3, we demonstrated that the Hilbert space dimension can be *exactly* identified if all the spins in the target system are correlated with the quantum probe [137].

2.3.1 Interaction model

Generally, an interacting many-body system can be represented by a graph $\mathcal{G} = (V(\mathcal{G}), E(\mathcal{G}))$, where $V(\mathcal{G})$ denotes the set of vertices representing particles and $E(\mathcal{G})$ denotes the set of edges representing the connectivity between every pair of particles [31]. In the following, we define $|V(\mathcal{G})|$ as the number of vertices, and $|E(\mathcal{G})|$ as the number of edges in the graph $\mathcal{G}$. Adding and deleting vertices and edges are called primary operations on the graph $\mathcal{G}$ [58]. Although edges generally describe the interactions between two particles, here we keep the network topology separated from the actual coupling strength, with the graph only encoding information on the former. Therefore, we only consider an unweighted and undirected graph.

Without loss of generality, we focus on many-qubit system. The graph of the many-qubit system can be characterized by taking the following rules on edges:

Rule 1: The single- energy term can be described by a *self-loop*, which joins a single vertex to itself.

Rule 2: The qubit-qubit interaction term can be described by a *proper edge*, which joins two distinct vertices.

Taking into account these rules, an interacting qubit system can be described by the adjacency matrix $\mathbf{Adj}(\mathcal{G})$:

$$[\mathbf{Adj}(\mathcal{G})]_{ij} = \begin{cases} 1, \text{ a vertex } v_i \text{ has self-loop, i.e. } i = j. \\ 1, \text{ vertices } v_i \text{ and } v_j \text{ are adjacent.} \\ 0, \text{ otherwise} \end{cases},$$

which shows the graph structure of the system.

Let us consider a sequence of graphs $\{\mathcal{G}_k\}_{k\geq 1}$, in which the rule that each corresponding adjacency matrix satisfies is fixed. Since the construction of the adjacency matrix depends on the elementary operations, fixing a rule means that a sequence of graphs $\{\mathcal{G}_k\}_{k\geq 1}$ is constructed from a given initial graph $\mathcal{G}_0$ by repeating a succession of fixed elementary operations. In graph theory, $\{\mathcal{G}_k\}_{k\geq 0}$ is called recursively constructible family of graphs [117]. For example, consider the one-dimensional Ising model without transverse fields, i.e. no self-loops: $H = \sum_{k=1}^{N-1} \frac{J_k}{2} Z_k Z_{k+1}$, where Z_k is the z-component of Pauli's matrices acting on k-th spin. The fixed elementary operation, here, is to add one vertex and proper edge from the right side which joins neighboring vertices. If we label each spin by $1, 2, 3, \cdots$ from the left side, the initial graph $\mathcal{G}_0$ is the first spin, and the corresponding adjacency matrices for the sequence of graphs $\{\mathcal{G}_1, \mathcal{G}_2, \mathcal{G}_3, \cdots\}$ satisfy:

$$[\mathbf{Adj}(\{\mathcal{G}_{k\geq 1}\})]_{i,j} = \begin{cases} 1, \text{ when } i = j \pm 1 \\ 0, \text{ otherwise.} \end{cases}$$

With the conditions that the graphs must be connected, undirected and unweighted, an interaction model can be defined as the following [137]:

Definition 3 (Interaction model)**.** *An interaction model $\mathcal{M}$ is defined by a coupling type and a recursively constructible family of connected graphs $\{\mathcal{G}_k\}_{k\geq 0}$, which are undirected and unweighted.*

Note that elementary operations can be defined in any spatial dimensions; therefore this definition is valid generally even for higher spatial dimensions.

2.3.2 Noiseless dimension estimation

General theory

Let us consider an interacting N-qubit Hamiltonian described by Eq. (2.1) and denote its Hilbert space as $\mathcal{H}$. Given a closed quantum system, the minimality of the corresponding classical LTI system is based on the choice of the basis. Let this N-qubit be represented by using an orthonormal operator basis $B = \{iO_i\}_{i=1}^{j} \subset \mathfrak{su}(2^N)$, for which the corresponding classical LTI system is both controllable and observable, namely $|G| = n$. Here O_i are tensor products of Pauli matrices and identity matrix. Let us choose the observable set

$$G_0 = \{\Pi_l |\ i\Pi_l \in B, [\Pi_l, H] \neq 0, l = 1, 2, \cdots, L\}.$$

Here, we restrict $\{\Pi_l\}_{l=1}^{L}$ to be observables on the quantum probe. Given a fixed basis, the three quantities G_0, $\mathcal{M}$, and the initial state of the joint system ρ_0 uniquely determine the dynamics of the system and thus the accessible set, we introduce the following space, which we call *system space*,

$$\mathcal{S} = [G_0, \mathcal{M}, \rho_0].$$

Then, we can obtain the following theorem [137]:

Theorem 3. *Given a system space $\mathcal{S} = [G_0, \mathcal{M}, \rho_0]$ expressed in a basis yielding a minimal realization of the equivalent classical LTI system, and whose quantum dynamics generates correlation between the observed quantum probe and the rest of*

the qubits, the dimension of the Hilbert space $\mathcal{H}$ is given by:

$$dim(\mathcal{H}) = 2^{f_{\mathcal{S}}(n)},$$

where n is the model order of the system and $f_{\mathcal{S}}$ is a strictly increasing function uniquely determined by the system space $\mathcal{S}$.

Proof. For a given graph $\mathcal{G}$, through the iterative procedure Eq. (2.3), we can obtain the corresponding accessible set $G(\mathcal{G})$, which emphasizes the fact that the accessible set is dependent on the structure of the graph $\mathcal{G}$. Note that given a basis B, $G(\mathcal{G})$ will be uniquely determined with fixed observable set G_0 and operator set of Hamiltonian Γ; therefore, $|G(\mathcal{G})|$ is also uniquely determined. Therefore, given an interaction model $\mathcal{M}$, if the dynamics correlates all the qubits with the quantum probe, an increase in graph size $\mathcal{G}_k$ will lead to an increase in $|G(\mathcal{G})|$. Then, for a fixed basis B and observable set G_0, a succession of elementary operations on graph $\mathcal{G}$ can generate a recursively constructible family of graphs $\{\mathcal{G}_k\}_{k\geq 0}$. Therefore, the increase in the vertices $|V(\mathcal{G}_k)|$ leads to an increase in $\{|G(\mathcal{G})|\}_{k\geq 0}$ so that $|G(\mathcal{G})|$ is a strictly increasing function of the number of qubits N in the system:

$$\frac{d}{dN}|G(\mathcal{G})| > 0.$$

Since the system space $\mathcal{S} = [G_0, \mathcal{M}, \rho_0]$ yields the minimal state-space representation, we have $|G| = n$, where n is the model order so that

$$\frac{d}{dN}n > 0.$$

Therefor, there exists a strictly increasing function $f_{\mathcal{S}} : n \to N$ such that

$$N = f_{\mathcal{S}}(n).$$

Since the dimension of N-body qubit system is given as

$$\dim(\mathcal{H}) = 2^N,$$

so that we can obtain $\dim(\mathcal{H}) = 2^{f_{\mathcal{S}}(n)}$. □

This can be simply illustrated in Fig. 2-1. Suppose that we want to estimate

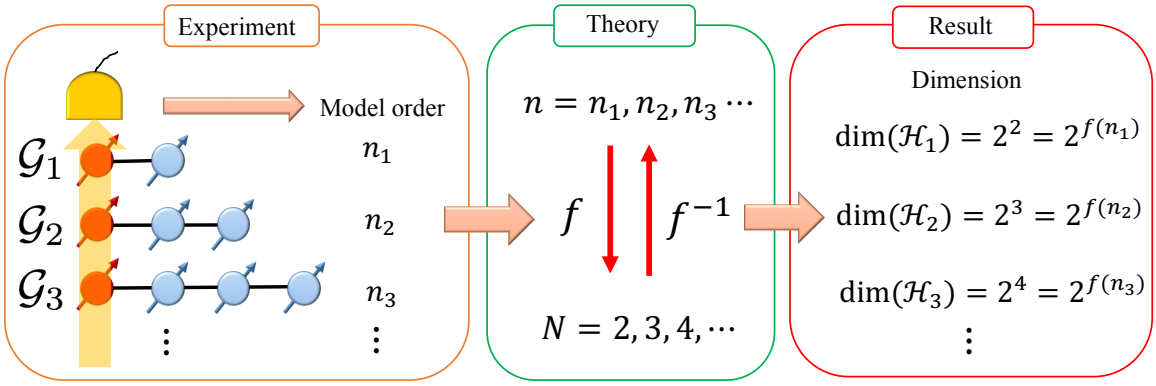

Figure 2-1: Dimension estimation conceptual scheme. We first derive the function $f_{\mathcal{S}}$ such that $N = f_{\mathcal{S}}(n)$. Through the measurement, we can determine the model order n, yielding the system dimension as $\dim(\mathcal{H}) = 2^N = 2^{f_{\mathcal{S}}(n)}$.

the dimension by measuring only the first spin (quantum probe). We first have to obtain the relation $N = f_{\mathcal{S}}(n)$, and find the model order n to obtain the dimension $\dim(\mathcal{H}) = 2^{f_{\mathcal{S}}(n)}$.

Algorithm for noiseless dimension estimation

Since the model order n is always equivalent to the rank of the Hankel matrix $\mathbf{H}_{r,s}$, defined in Sec. 2.2.3

$$n = \mathrm{rank}(\mathbf{H}_{r,s}),$$

we can estimate the dimension of the Hilbert space $\dim(\mathcal{H})$ via the following procedure:

Step 1: From the prior information about the interaction model $\mathcal{M}$ and selecting a

basis B that gives a minimal realization, we theoretically obtain a recurrence relation between the model order n and the quantum system dimension, yielding the function $f_{\mathcal{S}}(n)$.

Step 2: We repeatedly prepare the initial state of the probe so that $\mathbf{x}(0) \neq \mathbf{0}$, and measure the probe at equally spaced sampling points, obtaining the outcomes $y(j) = y(j\Delta t)$. (see Sec. 2.3.3 for details on how to choose the sampling time Δt from the sampling theorem [135]).

Step 3: We construct a sequence of square Hankel matrix $\{\mathbf{H}_{2,2}, \mathbf{H}_{3,3}, \cdots, \mathbf{H}_{k,k}, \cdots\}$, and calculate their determinant. In the absence of noise, the dimension of the total system is given by the minimum n such that the Hankel matrix determinant is zero:

$$\min_n \det(\mathbf{H}_{n+1,n+1}) = 0.$$

In the presence of noise, we can simply construct a large enough Hankel matrix and determine the corresponding n by finding a singular value λ_n such that $\lambda_n \gg \lambda_{n+1}$. (For details, see Sec. 2.3.3).

Examples of Noiseless Dimension Estimation

Let us consider an interacting qubit chain system with nearest-neighbor couplings. Let us denote $\mathcal{H}$ the Hilbert space of the total system and $\dim(\mathcal{H})$ the dimension of the Hilbert space, including the quantum probe. For N qubit system, we have

$$\dim(\mathcal{H}) = 2^N.$$

The initial state of the quantum probe is the eigenstate of the observable to be measured so that $\mathbf{x}_0 \neq \mathbf{0}$. Reflecting a practical scenario, where the rest of spins are inaccessible and cannot be initialized, we assume that the rest of spins are in the maximally mixed state $(\mathbb{1}/2)^{\otimes(N-1)}$, where $\mathbb{1}$ is the 2×2 identity matrix. This scenario is particularly pertinent when a system at room temperature is considered: a

paradigmatic example is the nitrogen-vacancy spin, which can be used as a quantum probe to determine the Hamiltonian of other electronic and nuclear spins at room-temperature NMR system [143, 2].

Let us consider the nearest-neighbor coupling with transverse fields:

$$H = \sum_{k=1}^{N} \frac{\Omega_k}{2} S_k^{\gamma} + \sum_{k=1}^{N-1} \Big(\frac{A_k}{2} S_k^{\alpha} S_{k+1}^{\alpha} + \frac{B_k}{2} S_k^{\beta} S_{k+1}^{\beta} + \frac{C_k}{2} S_k^{\gamma} S_{k+1}^{\gamma} \Big),$$

where $\{iS_k^{\alpha}, iS_k^{\beta}, iS_k^{\gamma}\} \in \mathfrak{su}(2)$ are the general spin-1/2 operators acting on k-th qubit. Suppose that our quantum probe is the first spin, and

$$[S_k^{\alpha}, S_l^{\beta}] = 2i\delta_{kl}\epsilon_{\alpha\beta\gamma} S_k^{\gamma}, \tag{2.24}$$

where $\epsilon_{\alpha\beta\gamma}$ is the Levi-Civita symbol defined as

$$\epsilon_{\alpha\beta\gamma} = \begin{cases} +1 & (\alpha,\beta,\gamma) = (x,y,z), (y,z,x) \text{ or } (z,x,y) \\ -1 & (\alpha,\beta,\gamma) = (z,y,z), (x,z,y) \text{ or } (y,x,z) \\ 0 & \alpha = \beta, \text{ or } \beta = \gamma, \text{ or } \gamma = \alpha. \end{cases}$$

Here, as an example, we will show the detailed steps to obtain $\dim(\mathcal{H})$ by considering the following case [137]: $A_k \neq 0, B_k = C_k = 0$ and $(S_k^{\alpha}, S_k^{\beta}, S_k^{\gamma}) = (X_k, Y_k, Z_k)$, where X_k, Y_k, Z_k are the Pauli's matrices satisfying

$$[X_k, Y_k] = 2iZ_k, \ [Y_k, Z_k] = 2iX_k, \ [Z_k, X_k] = 2iY_k.$$

Therefore, let us consider the following Hamiltonian

$$H = \sum_{k=1}^{N} \frac{\Omega_k}{2} Z_k + \sum_{k=1}^{N-1} \frac{A_k}{2} X_k X_{k+1}.$$

The operator set for this model is

$$\Gamma = \{Z_1, Z_2, \cdots, Z_M, X_1X_2, X_2X_3, \cdots, X_{M-1}X_M\}.$$

Let us choose the observable set as

$$G_0 = \{X_1\}.$$

The interaction model is described by the sequence of graphs satisfying the following adjacency matrices

$$[\mathrm{Adj}(\{\mathcal{G}_{k\geq 1}\})]_{i,j} = \begin{cases} 1 \text{ when } i = j \pm 1 \text{ and } i = j \\ 0, \text{ otherwise} \end{cases}.$$

with the coupling type of nearest-neighboring Ising coupling with single-qubit energies. In order to make sure that $\langle X_1(0)\rangle \neq 0$, we can choose the following initial state

$$\rho_0 = \frac{\mathbb{1} + X_1}{2} \otimes \left(\frac{\mathbb{1}}{2}\right)^{\otimes(N-1)} = \frac{1}{2}\begin{pmatrix} 1 & 1 \\ 1 & 1 \end{pmatrix} \otimes \frac{1}{2^{N-1}}\begin{pmatrix} 1 & 0 \\ 0 & 1 \end{pmatrix}^{\otimes(n-1)}. \tag{2.25}$$

For any finite dimensions of the Hilbert space, we can perform the iterative procedure in Eq. (2.3). Then, we obtain

$$G_1 = G_0 \cup [\![G_0,\ \Gamma]\!] = \{X_1,\ Y_1\}.$$

Since Y_1 does not commute with the Hamiltonian, the commutator $[Y_1, H]$ yield further contributions under the operation

$$[\![Y_1,\ \Gamma]\!] = \{X_1, Z_1X_2\}.$$

Thus, we obtain

$$G_2 = \{X_1, Y_1, Z_1X_2\}.$$

In a similar way, we also have

$$G_3 = G_2 \cup [\![G_2,\ \Gamma]\!] = \{X_1, Y_1, Z_1X_2, Z_1Y_2\}.$$

Then, we can finally obtain the following accessible set for N qubit $G^{(N)}$

$$G^{(N)} = \{X_1, Y_1, Z_1X_2, Z_1Y_2, ..., Z_1 \cdots Z_{N-1}X_N, Z_1 \cdots Z_{N-1}Y_N\} \tag{2.26}$$

as it can be proved by induction:

1. $N = 2$: By the iterative procedure in Eq. (2.3), the accessible set can be explicitly found to be:

   $$G^{(2)} = \{X_1, Y_1, Z_1X_2,\ Z_1Y_2\},$$

   which satisfies Eq. (2.3.2).

2. $N = w + 1$ $(\forall w \in \mathbb{N})$: Let us assume that for w qubits we obtained

   $$G^{(w)} = \{X_1, Y_1, Z_1X_2, Z_1Y_2, ..., Z_1 \cdots Z_{w-1}X_w, Z_1 \cdots Z_{w-1}Y_w\}.$$

Then, for $N = w + 1$, the Hamiltonian operator set is:

$$\Gamma^{(w+1)} = \Gamma^{(w)} \cup \{Z_{w+1}, X_wX_{w+1}\}$$

and by the iterative procedure in Eq. (2.3) we obtain:

$$G^{(w+1)} = G^{(w)} \cup \{Z_1 \cdots Z_wX_{w+1},\ Z \cdots Z_wY_{w+1}\},$$

which yields:

$$G^{(w+1)} = \{X_1, Y_1, Z_1X_2, Z_1Y_2, ..., Z_1 \cdots Z_{w-1}X_w, Z_1 \cdots Z_{w-1}Y_w, Z_1 \cdots Z_wX_{w+1}, Z_1 \cdots Z_wY_{w+1}\}.$$

This demonstrates that Eq. (2.3.2) also holds for $N = w + 1$. Therefore, we can conclude that for the Ising model with transverse field, Eq. (2.3.2) holds, yielding

$$|G^{(N)}| = 2N.$$

By constructing a state-space representation, the system matrix $\tilde{\mathbf{A}}$ becomes a $2N \times 2N$ skew-symmetric matrix with the only nonzero elements $\tilde{\mathbf{A}}_{2k,2k-1} = \Omega_k$ and $\tilde{\mathbf{A}}_{2k+1,2k} = J_k$. Since we want to measure $G_0 = \{S_1^x\}$, the output matrix is $\mathbf{C} = \begin{pmatrix} 1 & 0 & \cdots & 0 \end{pmatrix}$. Given the initial state, the initial coherent vector is $\mathbf{x}(0) = (1,\ 0,\ \cdots,\ 0)^T$, and $(\tilde{\mathbf{A}}, \mathbf{C}, \mathbf{x}(0))$ generates an irreducible transfer function $T(s) = \mathbf{C}(s\mathbf{I} - \tilde{\mathbf{A}})^{-1}\mathbf{x}(0) = P(s)/Q(s)$, where $\deg(Q(s)) = 2N$. Recall that the model order is the number of poles of the irreducible transfer function; therefore, given an irreducible transfer function $T(s) = P(s)/Q(s)$, we have always $n = \deg(Q(s))$. When the system is minimal, we also have $\deg(Q(s)) = |G|$. In this way, we can check observability and controllability of the system by finding the degree of the transfer function's characteristic polynomial. For the Ising model with transverse field, since $|G| = \deg(Q(s)) = 2N$, the system is minimal, and the model order is $n = 2N$. Therefore, the dimension of the Hilbert space is given by

$$\dim(\mathcal{H}) = 2^N = 2^{n/2}.$$

In the same way, we can obtain the following results.

Nearest-neighbor couplings with transverse field

We will summarize the results for nearest-neighbor couplings with transverse field [137]:

$$H = \sum_{k=1}^{N} \frac{\Omega_k}{2} S_k^\gamma + \sum_{k=1}^{N-1} \left(\frac{A_k}{2} S_k^\alpha S_{k+1}^\alpha + \frac{B_k}{2} S_k^\beta S_{k+1}^\beta + \frac{C_k}{2} S_k^\gamma S_{k+1}^\gamma \right),\ \Omega_k \neq 0.$$

1. Ising model:

   As we have seen above, when $(A_k \neq 0, B_k = C_k = 0)$, by choosing $G_0 = \{S_1^\alpha\}$ or $G_0 = \{S_1^\beta\}$, the systems are minimal and we can obtain $n = 2N$ so that

$$\dim(\mathcal{H}) = 2^N = 2^{n/2}. \tag{2.27}$$

2. Exchange model:

   When $(A_k \neq 0, B_k \neq 0, C_k = 0)$, by choosing $G_0 = \{S_1^\alpha\}$ or $G_0 = \{S_1^\beta\}$, the systems are minimal and we can obtain $n = 2N$ so that

$$\dim(\mathcal{H}) = 2^N = 2^{n/2}.$$

3. Heisenberg's model:

   When $(A_k \neq 0, B_k \neq 0, C_k \neq 0)$, by choosing $G_0 = \{S_1^\alpha\}$ or $G_0 = \{S_1^\beta\}$, the systems are minimal and we can obtain $n = n^{2N-1}$ so that

$$\dim(\mathcal{H}) = 2^N = \sqrt{2n}.$$

Nearest-neighbor couplings without transverse field

We will summarize the results for nearest-neighbor couplings without transverse field [137]:

$$H = \sum_{k=1}^{N-1} \Big(\frac{A_k}{2} S_k^\alpha S_{k+1}^\alpha + \frac{B_k}{2} S_k^\beta S_{k+1}^\beta + \frac{C_k}{2} S_k^\gamma S_{k+1}^\gamma \Big).$$

1. Ising model:

   When $(A_k =\neq 0, B_k = C_k = 0)$, we can obtain $n = 2$. In this case, the iteration procedure Eq. (2.3) saturates very quickly, and accessible set only contains the correlation operator of the quantum probe and the spin next to the probe. This is an example of the case that only some spins become correlated with quantum probe so that Theorem. 5 does not hold. In this case, we need to

apply transverse field to generate global correlations between the system and quantum probe so that the dimension of the Hilbert space can be obtain as Eq. (2.27).

2. Exchange model:

   When $(A_k \neq 0, B_k \neq 0, C_k = 0)$, by choosing $G_0 = \{S_1^\alpha\}$ or $G_0 = \{S_1^\beta\}$, the systems are minimal and we can obtain $n = N$ so that

$$\dim(\mathcal{H}) = 2^N = 2^n. \tag{2.28}$$

3. Heisenberg's model:

   When $(A_k \neq 0, B_k \neq 0, C_k \neq 0)$, we can choose either $G_0 = \{S_1^\alpha\}, \{S_1^\beta\}$ or $\{S_1^\gamma\}$ for our observable to measure. For this choice, the system is minimal. By induction, we can obtain the following relation:

$$n = \begin{cases} 4^{N-1} - 1 & (N : \text{odd}) \\ 4^{N-1} & (N : \text{even}) \end{cases}.$$

   Therefore, the dimension of the total system for each case is given by:

$$\dim(\mathcal{H}) = \begin{cases} 2\sqrt{n+1} & (N : \text{odd}) \\ 2\sqrt{n} & (N : \text{even}) \end{cases}. \tag{2.29}$$

Example of dimension estimation without controllability or observability

Here, we show an example to show that $\frac{dn}{dN} > 0$ cannot ensure that the system is minimal [137]. This can be understood as the following. Although the operators describing full correlations between the rest of qubits and the quantum probe can be generated, the choice of the initial state and measurement observables can also change the controllability and observability of the system. A good example is the

following Hamiltonian:

$$H = \sum_{k=1}^{N-1} \Big(\frac{J_k}{2} S_k^z S_{k+1}^z + \frac{L_k}{2} S_k^z S_{k+1}^x \Big).$$

Let us choose the observable set $G_0 = \{X_1\}$ or $G_0 = \{Y_1\}$, which actually yield same model order. Here, let us take $G_0 = \{X_1\}$. From the iterative procedure in Eq. (2.3), we can obtain:

$$G^{(N)} = \{X_1, Y_1 Z_2, Y_1 X_2, ..., Y_1 \cdots Y_{N-1} Z_N, Y_1 \cdots Y_{N-1} X_N\},$$

which actually contains all the generated operators describing the correlations of all qubits with a single quantum probe. Here, we can find

$$|G^{(N)}| = 2N - 1.$$

By constructing a state-space representation, $\tilde{\mathbf{A}}$ becomes a $(2N-1) \times (2N-1)$ skew-symmetric matrix with the only nonzero elements $\tilde{\mathbf{A}}_{2k,2k-1} = J_k$ and $\tilde{\mathbf{A}}_{2k+1,2k-1} = L_k$. In order to make sure $\mathbf{x}_0 \neq \mathbf{0}$, we can take the initial state in Eq. (2.25). Then, we can find that the irreducible transfer function $T(s) = P(s)/Q(s)$ has the property of $\deg(Q(s)) = 2N - 2$, which means that the model order is

$$n = |G^{(N)}| - 1 = 2N - 2,$$

and

$$\frac{dn}{dN} > 0$$

so that n is an increasing function of N. In this case, the system dimension becomes:

$$\dim(\mathcal{H}) = 2^{\frac{N+1}{2}}.$$

However, we have $n \neq |G|$. This means that the system is not minimal. This shows that there exist systems either not controllable or observable, even if we can directly generate the operators describing the correlation between all the qubits and a single quantum probe. In this particular case, since

$$\text{rank}(M_O(r)) = \text{rank}(M_C(s)) = |G^{(N)}| - 1 < |G^{(N)}|,$$

the system is both not controllable and not observable. This means that there is an extra operator generated, which is not needed to be counted in order to describe the dynamics of the system, and the system can be reduced to the one with the effective size. Therefore, controllability and observability strictly depends on the choice of the observable set G_0 and the initial state ρ_0.

2.3.3 Noisy dimension estimation

In practical scenarios, we have to take into account the effect of noise on the detector. The measurement outcomes at each sampling time can be written as $y(j)+\zeta(j)$, where $z(j)$ is the noise, which usually leads the experimental Hankel matrix, of dimension $r \times r$, to have full rank, i.e $\text{rank}(\mathbf{H}_{r,r}) = r$. Therefore, extracting the model order n seems to be impossible in the noisy case. However, this can be resolved by looking at the singular values of the noisy Hankel matrix, at least for weak enough noise, to find the "true" rank of the ideal Hankel matrix [137].

Let $\mathbf{H}_{r,r}$ be the $r \times r$ Hankel matrix obtained from noisy experimental data. Let the true model order be $n < r$. If the noise is weak, the experimental Hankel matrix is close enough to the ideal one, so that we can expect that its singular values $\{\lambda_k\}_{k=1}^{r}$ in decreasing order would be $\lambda_1 \geq \lambda_2 \geq \cdots \lambda_n \gg \lambda_{n+1} \geq \cdots \lambda_r > 0$. Although $\{\lambda_l\}_{l=n+1}^{r}$ are non-zero due to the noise, they should still be small because the noise is comparatively small. Then, by constructing a sequence of singular value ratios, $\{\lambda_k/\lambda_{k+1}\}_{k=1}^{r-1}$, we can expect to be able to determine the most probable model order n by finding a sharp peak at λ_n/λ_{n+1}.

We investigated the robustness of this method by simulating the exchange model

without transverse field:

$$H = \sum_{k=1}^{N-1} (X_k X_{k+1} + Y_k Y_{k+1}) \tag{2.30}$$

for $N = 4, 5, 6$ qubits. As we have seen in Sec. 2.3.2, the model order for this Hamiltonian is

$$n = N.$$

Here, we consider the case of estimating the model order by measuring only X_1. From the sampling theorem [135], the sampling time Δt can be chose as $\Delta t = \pi/\omega_{\max}$, where $\omega_{\max}$ is the largest eigenvalue of the Hamiltonian. Here, note that in principle, $\omega_{\max}$ is unknown, but an upper bound can be determined by assuming a maximum system dimension, a maximum parameter strength and all the coupling strengths to take this maximum value [137].

An added noise $\zeta(j)$ is characterized by a normal distribution with variance $10^{-7} - 10^{-4}$, which corresponds to $35 - 20$ [dB].We plot the median of the ratios between the singular values $\{\lambda_k/\lambda_{k+1}\}_{k=1}^{15}$ over 500 random Hamiltonian realizations as a function of the possible model order k. We choose the sampling time Δt by assuming that the number of qubits N could be at most 10 and all the coupling strengths take the possible maximum number 100 (this assumptions set $\omega_{\max}$). For each Hamiltonian, we construct 100×100 Hankel matrices $\mathbf{H}_{100,100}$ and estimate $\{\lambda_k/\lambda_{k+1}\}$ 100 times to evaluate the average. Then, we determine the true model order n by finding the largest sharp peak at λ_n/λ_{n+1}. The results of these simulations are shown in Figs. 2-2-2-4 [137].

From these results, we can conclude that when the Signal-to-Noise Ratio (SNR) is large enough, the largest sharp peak tends to occur at the true model order. Furthermore, the weaker the noise is, the sharper the peak is at the true model order. However, when N increases, the peak becomes less sharp, which means that the dimension estimation of the Hilbert space requires very large SNR. From Figs. 2-2- 2-4,

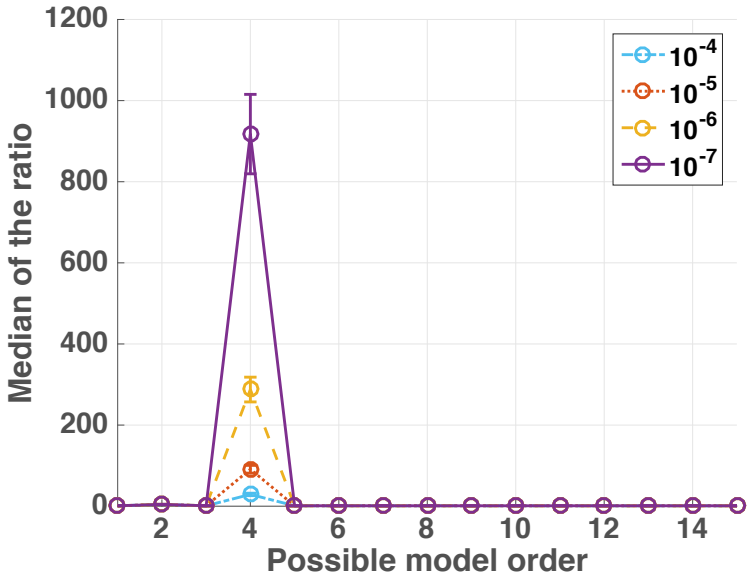

Figure 2-2: $N = 4$: Actual model order is $n = 4$. Solid line with circles: $\sigma^2 = 10^{-7}$; dashed line with circles: variance $\sigma^2 = 10^{-6}$; dotted line: variance $\sigma^2 = 10^{-5}$; dashed-dotted line: variance $\sigma^2 = 10^{-4}$. The error bars are the median of the standard deviation of the singular value ratio over 500 random Hamiltonian realizations. The final sharp peak occurs at $k = 4$, and from $k = 5$ the ratios are almost the same. The final peak becomes sharper as the variance of the noise becomes smaller.

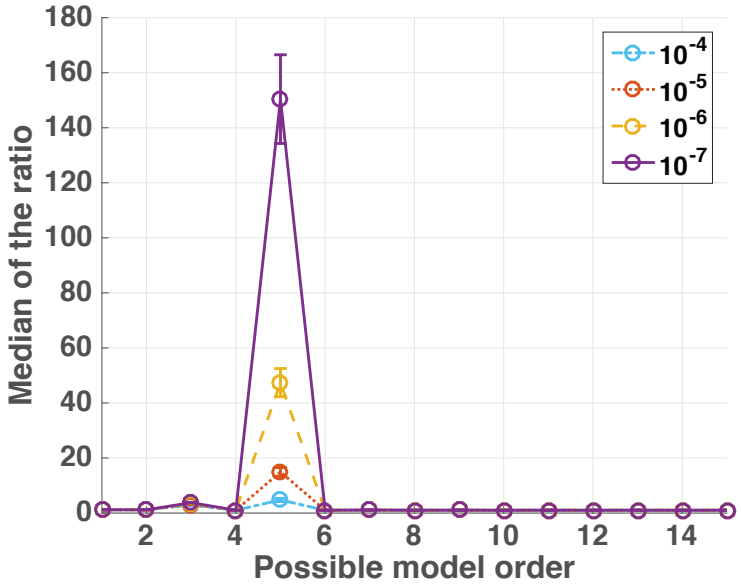

Figure 2-3: $N = 5$: Actual model order is $n = 5$. Simulation details are the same as in Fig. 2-2. The final sharp peak occurs at $k = 5$, and from $k = 6$ the ratios are almost same. The final peak becomes sharper as the variance of the noise becomes smaller.

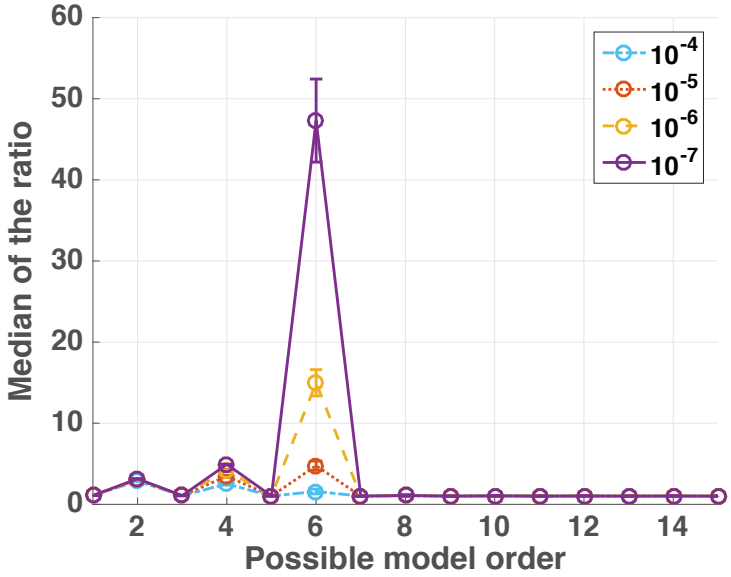

Figure 2-4: $N = 6$: Actual model order is $n = 6$. Simulation details are the same as in Fig. 2-2. We can see that when SNR $\geq$ 25dB the final peak occurs at $k = 6$, and we can see the flatting part from $k = 7$. The final peak becomes much sharper as the variance of the noise becomes smaller.

it can be expected that from $N = 7$, at least SNR $\geq$ 35dB is required, which is demanding to realize in the current laboratory conditions. Therefore, we conclude that this method can be useful only for a few-body interacting qubit system. Furthermore, this method is model-sensitive, which means that the the function $f_{\mathcal{S}} : n \to N$ is strictly sensitive to the interaction model $\mathcal{M}$. Therefore, it is needed to use modified function for the suspected model to find the dimension. For instance, if we allow noise on the exchange model in Eq. (2.30), e.g. $C_k \ll 1$, we can no longer use Eq. (2.28) but we need to use Eq. (2.29).

2.4 Hamiltonian parameter identifiability

In this section, we will discuss the identifiability of Hamiltonian parameter [138] by employing the eigensystem realization algorithm approach to Hamiltonian parameter estimation [161, 162] in Sec. 2.2 and the Gröbner basis [36, 37, 21, 47, 12].

The concept of identifiability has been studied in several different contexts [24, 25,

59]. Guţă and Yamamoto [59] employed a transfer function approach to systematically study system identifiability of the linear quantum systems with continuous variables. Their result applies to continuous-variable quantum systems in *infinite-dimensional* Hilbert space, such as a quantum optomechanical system [75, 157] or atomic ensembles confined in an optical cavity [88]. However, here we are interested in interacting many-qubit systems that can be described by discrete, *finite-dimensional* Hilbert spaces. Given the fact that the algebraic structure of the spin operators is different, we reformulate the conditions for identifiability of many-qubit Hamiltonians.

We also derive the lower bound in number of sampling points, and upper bound in total evolution time required to identify all the parameters. Focusing on the Hamiltonians of qubit-chain model with nearest-neighbor interaction, we classify the Hamiltonians based on their identifiability determined by Gröbner basis, and explain the propagation of the global correlations between the system and quantum probe is the necessary condition for the Hamiltonian of the total system to be identified, and propose a control protocol to engineer the non-identifiable Hamiltonian into identifiable Hamiltonian with periodic driving fields on time average.

2.4.1 Basic theory of Gröbner basis

Recall that by employing eigensystem realization algorithm, we can obtain two transfer functions: one is from theoretical model with coefficients of the Laplace variable s being the polynomials of the parameters and the other one is from our experimental data with coefficients of the Laplace variable s being just the numbers so that we can obtain Eq. (2.21) and thus the system of polynomial equations Eq. (2.22). Therefore, the identifiability of the Hamiltonian parameters can be interpreted as the solvability of the system of polynomial equations.

Gröbner basis is an essential concept in the commutative algebra, algebraic geometry, and computational algebra [36, 37, 21, 47, 12], and it is employed to solve the system of polynomial equations. Here, we use Gröbner basis techniques to explore what Hamiltonain models can be identified when restricting our access to a single quantum probe. Before discussing the application of Gröbner basis for Hamiltonian

identification, we summarize important mathematical concepts of Gröbner basis by following [36, 37, 21, 47, 12].

Gröbner basis is first introduced by Buchberger in [21], which is a systematic method to solve a system of multivariate polynomial equations and determining its solvability over the complex field $\mathbb{C}$.

Monomial, polynomial, and monomial ordering

In order to discuss Gröbner basis, we need to review the concept of monomial, polynomial and monomial ordering. Let $\mathbb{Z}_{\geq 0}$ be the set of all nonnegative integers. A monomial in $\theta_1, \cdots, \theta_M$ is the product $\theta_1^{\alpha_1} \cdots \theta_M^{\alpha_M}$, where $\alpha_1, \cdots, \alpha_M \in \mathbb{Z}_{\geq 0}$. For simplicity, let us introduce the vectors $\theta = (\theta_1, \cdots, \theta_M) \in k^M$ and $\alpha = (\alpha_1, \cdots, \alpha_M) \in \mathbb{Z}_{\geq 0}^M$. Then, we write monomials as $z^\alpha \equiv \theta_1^{\alpha_1} \cdots \theta_M^{\alpha_M}$ and the monomial degree is

$$|\alpha| = \sum_{k=1}^{M} \alpha_k. \tag{2.31}$$

A polynomial $f \in k[\theta_1, \cdots, \theta_M]$ is a finite linear combination of the monomials with coefficients in a field k:

$$f = \sum_{\alpha} c_\alpha \theta^\alpha, \quad c_\alpha \in k. \tag{2.32}$$

Monomial ordering is an important ingredient in all algorithms developed in commutative algebra. Let us introduce the so-called Lexicographic order (lex). Suppose that we have $\alpha = (\alpha_1, \cdots, \alpha_M) \in \mathbb{Z}_{\geq 0}^M$ and $\beta = (\beta_1, \cdots, \beta_M) \in \mathbb{Z}_{\geq 0}^M$. If the leftmost nonzero entry of $\alpha - \beta \in \mathbb{Z}^M$ is positive, we write $\alpha \succ_{lex} \beta$ or $z^\alpha \succ_{lex} z^\beta$. For each variable $\theta_1, \cdots, \theta_M$, the variables are ordered in the following way according to the lex ordering: $\theta_1 \succ_{lex} z_2 \succ_{lex} \cdots \succ_{lex} \theta_M$. By fixing the monomial ordering $\succ$, we can define the following terms:

1. The **multidegree** of a polynomial f is : $\text{multideg}(f) = \max(\alpha \in \mathbb{Z}_{\geq 0}^M | c_{\alpha \neq 0})$ with respect to $\succ$.

2. The **leading coefficient** of a polynomial f is: $\text{LC}(f) = c_{\text{multideg}(f)} \in k$.

3. The **leading monomial** of f is $\mathrm{LM}(f) = x^{\mathrm{multideg}(f)}$.

4. The **leading term** is $\mathrm{LT}(f) = \mathrm{LC}(f) \cdot \mathrm{LM}(f)$.

Ideals and affine variety

Let $k[\theta_1, \cdots, \theta_M]$ be a commutative ring. A subset $I \subseteq k[\theta_1, \cdots, \theta_M]$ is called an ideal if it satisfies the following conditions:

1. $0 \in I$.

2. If $f, g \in I$, then $f + g \in I$.

3. If $f \in I$ and $h \in k$, then $hf \in I$.

We are in particular interested in *polynomial ideals*. We denote the set of all polynomials in $\theta_1, \cdots, \theta_M$ with coefficients on a field k by $k[\theta_1, \cdots, \theta_M]$. Then, a subset $\mathcal{I} = \langle f_1, \cdots, f_p \rangle \subseteq k[\theta_1, \ldots, \theta_M]$ such that:

$$\mathcal{I} = \langle f_1, \cdots, f_p \rangle = \Big\{ \sum_{k=1}^{p} h_k f_k \Big| h_1, \cdots, h_p \in k[\theta_1, \cdots, \theta_M] \Big\} \tag{2.33}$$

is an ideal of $k[\theta_1, \cdots, \theta_M]$. We call $\mathcal{I}$ a *polynomial ideal* generated by $f_1, \cdots, f_p$, and $f_1, \cdots, f_p$ are called the bases of the polynomial ideal $\mathcal{I}$.

The radical of $\mathcal{I}$ is defined by:

$$\sqrt{\mathcal{I}} = \{ f \in k[\theta_1, \cdots, \theta_M] | f^r \in \mathcal{I} \text{ for some integer } r \geq 1 \}, \tag{2.34}$$

and we always have $\mathcal{I} \subseteq \sqrt{\mathcal{I}}$. Particularly, when $\mathcal{I} = \sqrt{\mathcal{I}}$, $\mathcal{I}$ is called a radical ideal.

Let $\mathbf{V}(f_1, \cdots, f_p)$ be the set of solutions of a system of polynomial equations, i.e.

$$\mathbf{V}(f_1, ..., f_p) = \{ (a_1, ..., a_n) \in k^n \mid f_l(a_1, ..., a_n) = 0,\ l = 1, 2, \cdots, p \}. \tag{2.35}$$

$\mathbf{V}(f_1, \cdots, f_p)$ is called the *affine variety* defined by $f_1, \cdots, f_p$. If $\{f_1, \cdots, f_p\}$ and $\{g_1, \cdots, g_t\}$ generate same polynomial ideal $\mathcal{I}$, then $\mathbf{V}(f_1, \cdots, f_p) = \mathbf{V}(g_1, \cdots, g_t)$.

Any polynomial ideal $\mathcal{I}$ always satisfies:

$$\mathbf{V}(\sqrt{\mathcal{I}}) = \mathbf{V}(\mathcal{I}), \tag{2.36}$$

and, particularly, if k is an algebraically closed field $\mathbb{C}$, the affine variety and the radical ideal are in one-to-one correspondence.

Definition of Gröbner basis

For a polynomial ideal $\mathcal{I} \in k[\theta_1, \cdots, \theta_M] \setminus \{0\}$, fixing a monomial order $\succ$, we define the leading term of the ideal, $\mathrm{LT}(\mathcal{I}) = \{\mathrm{LT}(f) | \exists f \in \mathcal{I} \setminus \{0\}\}$, and we write the monomial ideal generated by the elements of $\mathrm{LT}(\mathcal{I})$ as $\langle \mathrm{LT}(\mathcal{I}) \rangle$. If $\mathcal{I} = \langle f_1, \cdots, f_p \rangle$, we always have $\mathrm{LT}(f_k) \in \mathrm{LT}(\mathcal{I}) \subseteq \langle \mathrm{LT}(\mathcal{I}) \rangle$.

From the Hilbert Basis Theorem [36], every polynomial ideal $\mathcal{I} \setminus \{0\}$ has a finite generating set $\mathscr{G}(\mathcal{I}) = \{g_1, \cdots, g_t\}$, which satisfies $\langle \mathrm{LT}(\mathcal{I}) \rangle = \langle \mathrm{LT}(g_1), \cdots, \mathrm{LT}(g_t) \rangle$. $\mathscr{G}(\mathcal{I})$ is called a *Gröbner basis* for the polynomial ideal $\mathcal{I}$. Therefore, the Hilbert Basis Theorem suggests that every polynomial ideal has a corresponding Gröbner basis. By adding the following restrictions:

1. every polynomial g_j is monic. i.e. $\mathrm{LC}(g_j) = 1$;

2. for every set of two distict polynomial g_j and g_i, $\mathrm{LM}(g_j)$ is not divisible by $\mathrm{LM}(g_i)$ for any $i \neq j$,

we can obtain a unique minimal basis. The Gröbner basis with these restrictions is called *reduced Gröbner basis*, which is denoted by $\mathscr{G}_{\mathrm{red}}(\mathcal{I})$.

Buchberger's algorithm for constructing the Gröbner basis

The Gröbner basis can be constructed by the Buchberger's algorithm [21, 36, 37, 21, 47, 12]. Let $S(f_i, f_j)$ be the S-polynomial of the pair (f_i, f_j), which is defined as:

$$S_{i,j} = \frac{\mathrm{LCM}[\mathrm{LM}(f_i), \mathrm{LM}(f_j)]}{\mathrm{LM}(f_i)} f_i - \frac{\mathrm{LCM}[\mathrm{LM}(f_i), \mathrm{LM}(f_j)]}{\mathrm{LM}(f_j)} f_j, \tag{2.37}$$

where $\mathrm{LCM}[\mathrm{LM}(f_i), \mathrm{LM}(f_j)]$ denotes the least common multiple of $\mathrm{LM}(f_i)$ and $\mathrm{LM}(f_j)$. Let $\mathrm{rem}(S_{i,j}, G)$ be the remainder of dividing $S_{i,j}$ by all elements in G. Let us consider the ideal $\mathcal{I} \subset \mathbb{C}[\theta_1, \cdots, \theta_M]$ generated by $f_1, \cdots, f_p$. In the following, the Buchberger's algorithm introduced in [37] is shown:

INPUT: $F = \{f_1, \cdots, f_p\}$

OUTPUT: The Gröbner basis $\mathscr{G}(\mathcal{I}) = \{g_1, \cdots, g_t\}$ for the ideal $\mathcal{I}$.

$G := F$

repeat

  $G' := G$

  for all $\{f_i, f_j\}, we \neq j$ in G' **do**

    $R := \mathrm{rem}(S_{i,j}, G')$

    if $R \neq 0$ **then**

      $G := G \cup \{\mathrm{rem}(S_{i,j}, G')\}$

    end if

  end for

until $G = G'$

RETURN G

Construction of radicals of zero-dimensional ideal

Let us consider the following system of polynomial equations in Eq. (2.22):

$$\begin{aligned} f_1(\theta_1, \cdots, \theta_M) &= 0 \\ f_2(\theta_1, \cdots, \theta_M) &= 0 \\ &\vdots \\ f_p(\theta_1, \cdots, \theta_M) &= 0 \end{aligned} \tag{2.38}$$

and $f_1, \cdots, f_p \in \mathbb{C}[\theta_1, \cdots, \theta_M]$. Suppose that Eq. (2.38) has a finite set of solutions. Then, the polynomial ideal $\mathcal{I}$ generated by $f_1, \cdots, f_n$ is called zero-dimensional ideal. Here, let us introduce the procedure to construct the radical $\sqrt{\mathcal{I}}$. By Buchberger's algorithm and the definition of the reduced Gröbner basis, we can obtain the following

reduced Gröbner basis:

$$\begin{aligned}\mathscr{G}_{\text{red}}(\mathcal{I}) = \{&g_1(\theta_1),\\ &g_{2,1}(\theta_1,\theta_2),\cdots,g_{2,v_2}(\theta_1,\theta_2),\\ &\vdots\\ &g_{M,1}(\theta_1,\cdots,\theta_M),\cdots,g_{M,v_M}(\theta_1,\cdots,z_M)\}.\end{aligned} \tag{2.39}$$

and $\mathscr{G}_{\text{red}}(\mathcal{I})$ generates the same ideal. Let h_j be an unique monic generator of the elimination ideal $\mathcal{I}\cap\mathbb{C}[\theta_j]$. Then, we can choose h_j such that $h_j\in\mathscr{G}(\mathcal{I})\cap\mathbb{C}[\theta_j]$ by the Elimination Theorem [37], which states that if we define $\mathcal{I}_l$ the l-th elimination ideal as

$$\mathcal{I}_l = \mathcal{I}\cap k[\theta_{l+1},\ldots,\theta_M],$$

fixing the lex order $\theta_1\succ_{lex}\theta_2\succ_{lex}\cdots\succ_{lex}\theta_M$, for every l, the Gröbner basis for the l-th elimination ideal is written by:

$$\mathscr{G}_l = \mathscr{G}\cap k[\theta_{l+1},\cdots,\theta_M], \tag{2.40}$$

where $\mathscr{G}_l$ is the Gröbner basis for $\mathcal{I}$.

Let $\varphi_j(\theta_j)$ be $\varphi_j = h_j/\gcd(h_j,\partial_{\theta_j}h_j)$, the radical of the zero-dimensional ideal $\mathcal{I}$ is given by:

$$\sqrt{\mathcal{I}} = \mathcal{I} + \langle\varphi_1,\cdots,\varphi_n\rangle. \tag{2.41}$$

(See e.g., [12] for the proof). In particular, by Seidenberg's Lemma [12], when $\varphi_j = 1$, $\mathcal{I}$ is a radical zero-dimensional ideal, and the Gröbner basis for the radical zero-dimensional ideal has a special shape, as described by the Shape lemma [36], such that:

$$\mathscr{G} = \{\theta_1^\alpha + q_1(\theta_1),\cdots,\theta_{n-1}+q_{n-1}(\theta_1),\theta_M+q_n(\theta_1)\}, \tag{2.42}$$

where $\alpha\in\mathbb{N}$ and $q_j(\theta_1)$ are the univariate polynomials in θ_1 with degree $\deg(q_j)<\alpha$.

Solvability and Gröbner basis

The reduced Gröbner basis is useful since the corresponding system of polynomial equations:

$$g_1(\theta_1, \cdots, \theta_M) = \cdots = g_t(\theta_1, \cdots, \theta_M) = 0$$

has the same zeros as the original system of polynomial equations in Eq. (2.38), and usually has a simpler form.

The solvability of the system of polynomial equations over $\mathbb{C}$ depends on the shape of the Gröbner basis as follows:

1. **No solution** [37]: When Eq. (2.38) is not solvable, Buchberger's algorithm yields $\mathscr{G}_{\text{red}}(\mathcal{I}) = \{1\}$.

2. **Finite set of solutions** [36, 47]: When Eq. (2.38) has finite solvability (a finite number of solutions), $\mathcal{I}$ is called zero-dimensional ideal. With lexicographic order, $\mathscr{G}_{\text{red}}(\mathcal{I})$ has the shape:

$$\begin{aligned}\mathscr{G}_{\text{red}}(\mathcal{I}) = \{&g_1(\theta_1),\\ &g_{2,1}(\theta_1, \theta_2), \cdots, g_{2,v_2}(\theta_1, \theta_2),\\ &\vdots\\ &g_{M,1}(\theta_1, \cdots, \theta_M), \cdots, g_{M,v_M}(\theta_1, \cdots, \theta_M)\}.\end{aligned}$$

   This allows all the values of the parameters to be similarly obtained recursively. In particular, when $\mathcal{I}$ is a radical zero-dimensional ideal, the Gröbner basis has a particular shape (Shape lemma):

$$\mathscr{G}_{\text{red}}(\mathcal{I}) = \{\theta_1^\alpha + q_1(\theta_1), \theta_2 + q_2(\theta_1), \cdots, \theta_M + q_M(\theta_1)\},$$

   where $q_j(\theta_1)$ is an univariate polynomial in θ_1 with the condition that $\alpha > \deg(q_j)$ for $\alpha \in \mathbb{N}$. From Sturm theorem [36], we can obtain the number of distinct real zeros of $\theta_1^\alpha + q_1(\theta_1) = 0$ and hence the number of real solutions of

the original system of polynomial equations.

3. **Only one solution** [47]: When Eq. (2.38) has only one solution, the radical of the zero-dimensional ideal is the maximal ideal, which has the form of $\langle \theta_1 - a_1, \cdots, \theta_M - a_M \rangle$. Therefore, the Gröbner basis for $\sqrt{\mathcal{I}}$ has the form

$$\mathscr{G}_{\text{red}}(\sqrt{\mathcal{I}}) = \{\theta_1 - a_1, \cdots, \theta_M - a_M\}.$$

Example: Reduced Gröbner basis for 3-qubit exchange Hamiltonian

From Eq. (2.23), the ideal is

$$\mathcal{I} = \{f_1(J_1, J_2), f_2(J_1, J_2)\} = \{J_1^2 + J_2^2 - b_1, J_2^2 - b_2\}$$

Then, Buchberger's algorithm, which in this case is just the Gaussian elimination for linear systems with respect to J_1^2 and J_2^2, yields

$$\mathscr{G}_{\text{red}} = \{J_1^2 - (b_1 - b_2), J_2^2 - b_2\},$$

which shows that for $|J_1|$ and $|J_2|$, there is only one set of solution.

$$\{\ |J_1|, |J_2|\ \} = \{\sqrt{b_1 - b_2}, b_2\}$$

Comments on efficiency of Gröbner basis

The computation of Gröbner basis takes tremendously large complexity [37]. Let F be a set of polynomials $\{f_1, \cdots, f_t\}$ in $z_1, \cdots, z_n \in \mathbb{C}$, and let d be the maximal multiple degree of the input polynomials, i.e. $d = \max(\text{multideg}(f_1), \cdots, \text{multideg}(f_t))$. Suppose that F generates a zero-dimensional ideal. Then, the complexity for computing the reduced Gröbner basis is given by $d^{O(n)}$ [86]. Therefore, for a larger system, the Gröbner basis takes a tremendously long time due to its complexity. Efficiency improvement of computing Gröbner basis is a timely problem. For example, recently, Gritzmann and Sturmfels proposed the idea of dynamic alternation of the the mono-

mial ordering while the algorithm progresses [57, 26].

2.4.2 Gröbner basis approach to Hamiltonian parameter identifiability

In this section, we introduce the application of Gröbner basis technique to introduce a working definition of Hamiltonian parameter identifiability in interacting many-qubit systems via the eigensystem realization algorithm [138]. Particularly, we restrict to identifying only the parameter magnitude $|\theta_j|$ [138].

Identifiability test

Let us first introduce our definition of Hamiltonian identifiability [138]:

Definition 4. *An Hamiltonian is identifiable when the system of polynomial equations derived from the transfer function equation $T(s) = T_{est}(s)$ provided by eigensystem realization algorithm has a finite set of solutions such that all θ_j^2 take only one positive real value.*

Let F be a polynomial set $F = \{f_1, \cdots, f_p\} \subseteq \mathbb{C}[\theta_1, \cdots, \theta_M]$. Based on this definition, the algorithm to test identifiability is as follows:

Step 1: We define new variables z_j such that $\{z_j\} = \{\theta_r^2, \theta_l | 1 \leq r, l \leq M)\}$, where θ_r's only appear in F as even powers (and θ_l's are all the remaining variables in F). Then, the polynomial ideal generated by F becomes $\mathcal{I} = \langle f_1, \cdots, f_p \rangle \subseteq \mathbb{C}[z_1, \cdots, z_M]$.

Step 2: From the Buchberger's algorithm and the definition of reduced Gröbner basis, we obtain $\mathscr{G}(\mathcal{I}) = \{g_1, \cdots, g_t\}$. If $t < M$, the Hamiltonian is non-identifiable.

Step 3: By elimination of variables, we can obtain M univariate polynomials $h_j(z_j)$, i.e. $h_j \in \mathcal{I} \cap \mathbb{C}[z_j]$.

Then, we can construct the radical ideal $\sqrt{\mathcal{I}} = \mathcal{I} + \langle \varphi_1, \cdots, \varphi_M \rangle$ [36, 37], where

$$\varphi_j = \frac{h_j}{\gcd\left(h_j, \frac{\partial h_j}{\partial z_j}\right)},$$

and we can construct a new polynomial set

$$F' = \{g_1, \cdots, g_t, \varphi_1, \cdots, \varphi_M\} \subseteq \mathbb{C}[z_1, \cdots, z_M].$$

Step 4: Since $\sqrt{\mathcal{I}}$ is a radical zero-dimensional ideal, the Shape Lemma can be applied. From Buchberger's algorithm and the definition of reduced Gröbner basis, we obtain:

$$\mathscr{G}_{\text{red}}(\sqrt{\mathcal{I}}) = \{z_1^\alpha + q_1(z_1), z_2 + q_2(z_1), \cdots, z_M + q_M(z_1)\},$$

where $\alpha > \deg(q_j)$.

Step 5: Finally, we employ Sturm theorem to calculate the distinct number of real zeros of the polynomial $\theta_1^\alpha + q_1(z_1)$, so that we can obtain the number of real zeros of each polynomial in $\mathscr{G}_{\text{red}}(\sqrt{\mathcal{I}})$. If there is only one set of solutions such that all the values of z_j's are real, the Hamiltonian is identifiable. Otherwise, the Hamiltonian is nonidentifiable.

2.4.3 Required experimental resources

The number of sampling points and total evolution time required to fully characterize the system are important experimental resources. Here, we use the eigensystem realization algorithm to provide the lower bound in required sampling points and the upper bound in total evolution time for the Hamiltonian parameter identification [138].

The bound is found from the minimum realization of the system, which is discussed in Sec. 2.2.4. Recall that in order to obtain the new realization $[\tilde{\mathbf{A}}_e, \mathbf{C}_e, \mathbf{x}_{0,e}]$, the system is required to be both controllable and observable, namely minimal, so that

we need the controllability and observability matrix to be full rank:

$$\text{rank}(M_O(r)) = \text{rank}(M_C(s)) = \text{rank}(\mathbf{A}) = n,$$

where n is the model order. Since the Hankel matrix $\mathbf{H}_{r,s}$ can be decomposed into $\mathbf{H}_{r,s} = M_O(r)M_C(s)$, from Sylvester inequality [68], we find that

$$\text{rank}(\mathbf{H}_{r,s}) = n.$$

Therefore, the minimum dimension of the Hankel matrix is $n \times n$, which means we just need $(2n-1)$ sampling points: $\{y(0), y(1), y(2), \cdots, y(2n-1)\}$. Taking into account the need of constructing the shifted Hankel matrix $\bar{\mathbf{H}}_{r,s}$ in Eq. (2.19) to obtain $\mathbf{A}_e$, we have to add one more sampling point $y(2n)$; therefore, the minimum number of sampling points $\mathcal{Q}_{\min}$ is $\mathcal{Q}_{\min} = 2n$. Therefore, the lower bound in required number of sampling points is given by

$$\mathcal{Q} \geq 2n.$$

Since the number of different polynomial equations obtained from Eq. (2.21) is $\leq n-1$, we can also obtain the inequality between the minimum number of sampling points $\mathcal{Q}$ and the number of elements of the reduced Gröbner basis $\mathcal{B}[\mathscr{G}_{\text{red}}]$ as

$$\frac{\mathcal{Q}_{\min}}{2} \leq \mathcal{B}[\mathscr{G}_{\text{red}}] + 1.$$

From the number of sampling points, we can further obtain the total evolution time T_{tot} to identify the Hamiltonian parameters. The upper bound of the sampling time Δt, which is regarded as an optimal choice of sampling time, is given by the sampling theorem [135] as

$$\Delta t \leq \frac{\pi}{\Omega_{\max}},$$

where $\Omega_{\max}/(2\pi)$ is the maximum frequency that would appear in the measured sig-

nal. Therefore, the required maximum evolution time with the minimum number of sampling points satisfies

$$T_{\text{tot}} \leq \frac{(2n-1)\pi}{\Omega_{\max}}.$$

In reality, the maximum frequency of the signal depends on the values of the parameters θ_m, which are unknown. Thus, for a time-optimal estimation procedure we would need prior information about the range of values that the parameters can take. For example, we could then assume that all the parameters take the largest value and obtain the smallest time steps Δt that still satisfies the sampling theorem.

2.4.4 Examples of Hamiltonian parameter identifiability

While we have shown the example for 3-qubit exchange Hamiltonian accordingly in different sections in order to make the discussion more concrete, here, focusing on the one-dimensional N-qubit chain system with nearest-neighboring interaction, we classify the Hamiltonians based on their identifiability [138]. To provide analytical results, we focus on the qubit-chain system with nearest-neighboring couplings, which is useful for quantum information transport between distant qubits [13, 46, 29]. Here, two different Hamiltonians, the Ising and exchange interaction, are considered and their Hamiltonian identifiability by assuming that the spin chain is coupled to a single quantum probe is analyzed. More precisely, the following assumptions are made (see also Fig. 2-5) [138].

The quantum probe is a well-characterized system, which can be initialized, controlled, and read out. The quantum probe is coupled to the qubit-chain system as a first spin with a coupling which follows the chain Hamiltonian model. The qubit-chain system cannot be initialized nor measured because the parameters characterizing the systems are unknown. For simplicity, it is assumed that the target qubit-chain system is initially in the maximally mixed state $\frac{\mathbb{1}}{2}$, and only collective control on the total system is possible. The only unknown information is only the parameters, but the interaction model $\mathcal{M}$ and the dimension of the Hilbert space $\dim(\mathcal{H})$ of the total system

is knwon. Let N be the number of qubits in the total system with nearest-neighbor interactions and possibly an interaction to an external fields. The parameters θ_m are thus given by the coupling strengths between the k-th and $(k+1)$-th spins, denoted by $J_k/2$, and the Zeeman energy $\omega_k/2$ of the k-th spin due to external fields. These assumptions are realistic in many practical scenarios for qubit-chain system applications to quantum engineering tasks at room temperature. In addition, they could also approximate some scenarios in quantum metrology, such as recently proposed schemes for protein structure reconstructions via the interaction of their nuclear spins with a quantum probe [2].

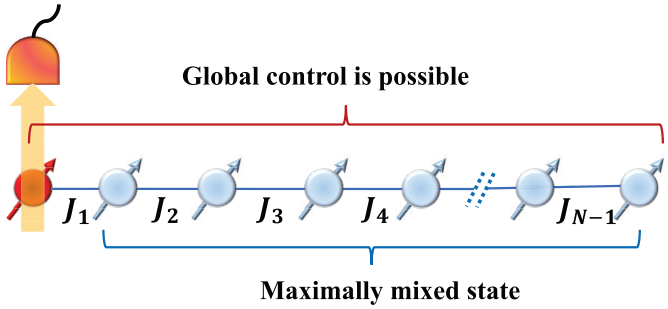

Figure 2-5: Hamiltonian identification model. A quantum probe is coupled to one end of the spin chain. A part from the quantum sensor (red spin), the rest of the spins (blue spins) are initially in the maximally mixed state. We further assume that we only have selective control on the quantum probe and global control on the spin chain.

Ising model without transverse field

Let us consider the following Hamiltonian:

$$H = \sum_{k=1}^{N-1} \frac{J_k}{2} X_k X_{k+1}.$$

Let us choose the observable set as $G_0 = \{Z_1\}$ without loss of generality. The accessible set becomes

$$G = \{Z_1, Y_1 X_2\}.$$

Then, only the spin directly interacting with the quantum probe becomes correlated with it during the evolution and its parameter can be identified. As a consequence, $\text{rank}(\mathbf{A}) = 2$ and full Hamiltonian identification is only possible for $N = 2$. Physically, this can be understood by a lack of information propagation in the Ising spin chain, which prevents the quantum probe at its end to gain information about the rest of the system. Indeed, the group velocity for information propagation in the Ising chain is 0.

Let the initial coherent vector be $\mathbf{x}(0) = (1, 0)^T$ and the output matrix $\mathbf{C} = \begin{pmatrix} 1 & 0 \end{pmatrix}$. Then, the transfer function is:

$$\Xi(s) = \frac{s}{s^2 + J_1^2},$$

where we can identify $z_1 = J_1^2$. Through eigensystem realization algorithm, we can obtain a new transfer function from the experimental data, which can be written in the most generality as:

$$\Xi_e(s) = \frac{s + b_0}{s^2 + b_1^2 s + a_1^2}.$$

Here we fixed the transfer function order to 2, as expected from the Ising model evolution. However, the form of $T_{\text{est}}(s)$ might differ from the ideal $T(s)$: in particular we might have additional terms, with coefficients b_j arising from experimental errors or numerical approximations. Since a_1^2 reflects the contribution of J_1^2, we still expect $b_j^2 \ll a_1^2$, and b_j's are negligible. Therefore, the reduced Gröbner basis is simply given by: $\mathscr{G}_{\text{red}} = \{z_1 - a_1^2\} = \{J_1^2 - a_1^2\}$ and the $N = 2$ Ising chain can be identified with $\mathcal{Q}_{\min} = 4$ sampling points.

Note that an alternative way of estimating J_1 is to measure the quantum probe (in particular Z_1) at known times. However, due to the periodicity of the signal, J_1 cannot be identified uniquely, even if measuring more than one time point. Then, we can generally state the following result.

Ising model with transverse field

Adding a transverse field to the Ising model drastically changes the system dynamics and consequently its identifiability.

The Hamiltonian is now

$$H = \sum_{k=1}^{N} \frac{\omega_k}{2} Z_k + \sum_{k=1}^{N-1} \frac{J_k}{2} X_k X_{k+1}.$$

$G_0 = \{X_1\}$ or $\{Y_1\}$ is the best choice, as $G_0 = \{Z_1\}$ would result in a larger-size $\tilde{\mathbf{A}}$. Either $G_0 = \{X_1\}$ or $\{Y_1\}$ yields the accessible set:

$$G = \{X_1, Y_1, Z_1X_2, Z_1Y_2, \cdots, Z_1 \cdots Z_{N-1}X_N, Z_1 \cdots Z_{N-1}Y_N\},$$

so that

$$|G| = 2N.$$

All the qubits are thus correlated with the quantum probe and we can hope to identify all the parameters. Then, $\tilde{\mathbf{A}}$ is a $2N \times 2N$ skew-symmetric matrix with the only non-zero elements $\tilde{\mathbf{A}}_{2k,2k-1} = \omega_k$ and $\tilde{\mathbf{A}}_{2k+1,2k} = J_k$. Since $|G| = \text{rank}(\mathbf{A})$, we have: $\text{rank}(\mathbf{A}) = 2N$. Choosing the initial state of the quantum probe to be an eigenstate of X_1, we have:

$$\mathbf{x}(0) = (1, 0 \cdots, 0)^T \in \mathbb{R}^{2N}$$

If we measure X_1, the output matrix is $\mathbf{C} = \begin{pmatrix} 1 & 0 & \cdots & 0 \end{pmatrix} \in \mathbb{R}^{2N}$. From eigensystem realization algorithm and Eq. (2.21), we arrive at the following shape of the reduced Gröbner basis:

$$\mathscr{G}_{\text{red}} = \{z_1 - a_1^2, \cdots, z_N - a_N^2, z_{N+1} - b_1^2, \cdots, z_{2N-1} - b_{N-1}^2\},$$

where $z_k = \omega_k$ $(k = 1, 2, \cdots, N)$ and $z_{N+k} = J_k^2$ $(k = 1, 2, \cdots, N-1)$. In this case $\mathcal{I}$

generated from Eq. (2.21) is a maximal ideal of the form $\langle z_1 - a_1^2, \cdots, z_N - a_N^2, z_{N+1} - b_1^2, \cdots, z_{2N-1} - b_{N-1}^2 \rangle$ $(a_l, b_k \in \mathbb{R})$, and there is only one positive real solution for the magnitudes of all the parameters; therefore, the Hamiltonian is fully identifiable. Furthermore, the minimum number of sampling points is

$$\mathcal{Q}_{\min} = 2\text{rank}(\mathbf{A}) = 4N.$$

Physically, this result shows that identifiability is connected to information propagation along the whole chain. Indeed, since we assumed that we can extract information from the system only through the probe spin at one end of the chain, propagation of information through the whole chain is necessary to reveal the system's properties. Adding a transverse field to the Ising model enables this information propagation.

Exchange model without transverse field

The exchange (XY) model is another example where information propagation allows Hamiltonian identification via single-probe measurement.

The Hamiltonian can be written as:

$$H = \sum_{k=1}^{N-1} \frac{J_k}{2}(X_k X_{k+1} + Y_k Y_{k+1}). \tag{2.43}$$

For this case, $G_0 = \{X_1\}$ or $\{Y_1\}$ is the best choice because the corresponding accessible set has the smallest size. Choosing, e.g., $G_0 = \{X_1\}$, we can obtain the following accessible set

$$G = \{X_1, Z_1Y_2, Z_1Z_2X_3, Z_1Z_2Z_3Y_4, ..., Z_1 \cdots Z_{2m-2}X_{2m-1}, Z_1 \cdots Z_{2m-1}Y_{2m}\},$$

for an even-number of qubits in the chain, $N = 2m$ $(\forall m \in \mathbb{N})$, and

$$G = \{X_1, Z_1Y_2, Z_1Z_2X_3, Z_1Z_2Z_3Y_4, ..., Z_1 \cdots Z_{2m-3}Y_{2m-2}, Z_1 \cdots Z_{2m-2}X_{2m-1}\},$$

for an odd number, $N = 2m - 1$ ($\forall m \in \mathbb{N}$). The accessible set has

$$|G| = N.$$

If we had chosen $G_0 = \{Z_1\}$, the accessible set would have had $|G| = N^2$. Therefore, in the following discussion, we consider $G_0 = \{X_1\}$. As all the qubits are correlated with the quantum probe, we can expect the Hamiltonian to be fully identifiable. For this model, $\tilde{\mathbf{A}}$ becomes an $N \times N$ skew-symmetric matrix with the only non-zero elements $(\tilde{\mathbf{A}})_{k,k+1} = (-1)^k J_k$, which has the same form as the system matrix of the Ising model with the transverse field. Since $|G| = \text{rank}(\mathbf{A})$, we have $\text{rank}(\mathbf{A}) = N$. Choosing the initial state of the quantum probe to be the eigenstate of X_1, we have:

$$\mathbf{x}(0) = (1, 0, \cdots, 0)^T \in \mathbb{R}^N.$$

Since we can only measure the quantum probe, the output matrix is $\mathbf{C} = \begin{pmatrix} 1 & 0 & \cdots & 0 \end{pmatrix} \in \mathbb{R}^N$. From eigensystem realization algorithm and Eq. (2.21), we arrive at the following shape of the reduced Gröbner basis:

$$\mathscr{G}_{\text{red}} = \{z_1 - a_1^2, \cdots, z_{N-1} - a_{N-1}^2\},$$

where $z_k = J_k^2$ and $a_k \in \mathbb{R}$. Therefore, the Hamiltonian is fully identifiable since we have only one positive real solution for the magnitudes of all the parameters, and the minimum number of sampling points for N qubits is

$$\mathcal{Q}_{\text{min}} = 2\text{rank}(\mathbf{A}) = 2N.$$

Exchange model with transverse field

The Hamiltonian is now given by:

$$H = \sum_{k=1}^{N} \frac{\omega_k}{2} Z_k + \sum_{k=1}^{N-1} \frac{J_k}{2} (X_k X_{k+1} + Y_k Y_{k+1}).$$

The best choice is $G_0 = \{Y_1\}$ or $\{X_1\}$ which both yield the following accessible set [138]:

$$G = \{X_1, Y_1, Z_1X_2, Z_1Y_2, Z_1Z_2X_3, Z_1Z_2Y_3, \cdots, \\ Z_1 \cdots Z_{N-1}X_N, Z_1 \cdots Z_{N-1}Y_N\},$$

with $|G| = 2N$. $\tilde{\mathbf{A}}$ is a $2N \times 2N$ skew-symmetric matrix with the only non-zero elements $(\tilde{\mathbf{A}})_{2k-1,2k} = \omega_k$ and $(\tilde{\mathbf{A}})_{2k+2,2k-1} = (\tilde{\mathbf{A}})_{2k,2k+1} = J_k$. Choosing the initial state of the quantum probe to be an eigenstate of X_1, we have:

$$\mathbf{x}(0) = (0, 1, \cdots, 0)^T \in \mathbb{R}^{2N}.$$

If we measure X_1, then we have $\mathbf{C} = \begin{pmatrix} 1 & 0 & \cdots & 0 \end{pmatrix} \in \mathbb{R}^{2N}$. From eigensystem realization algorithm and Eq. (2.21), we can obtain the following reduced Gröbner basis

$$\mathscr{G}_{\text{red}} = \{z_1^\alpha + q_1(z_1), z_2 + q_2(z_1), \cdots, z_{2N-1} + q_{2N-1}(z_1)\},$$

where $z_l = \omega_l^2$ $(l = 1, \cdots, N)$ and $z_{N+k} = J_k^2$ $(k = 1, \cdots, N-1)$. Note that $\alpha > \deg(q_j)$ and $\alpha \geq 2$. Here, $q_j(z_1)$ is the univariate polynomial in z_1. In general z_1 could have multiple values, so that we could have multiple sets of real solutions of the system of polynomial equations. Therefore, in general, this model is not identifiable.

If we measure Y_1 with the initial state of the quantum probe being the eigenstate of X_1 [161, 138], we can obtain

$$\mathscr{G}_{\text{red}} = \{z_1 - a_1, \cdots, z_N - a_N, z_{N+1} - b_1^2, \cdots, z_{2N-1} - b_{N-1}^2\},$$

where $z_k = \omega_k$ $(k = 1, 2, \cdots, N)$ and $z_{N+k} = J_k^2$ $(k = 1, 2, \cdots, N-1)$. In this case $\mathcal{I}$ generated from Eq. (2.21) is a maximal ideal of the form $\langle z_1 - a_1^2, \cdots, z_N - a_N^2, z_{N+1} - b_1^2, \cdots, z_{2N-1} - b_{N-1}^2 \rangle$ $(a_l, b_k \in \mathbb{R})$, and there is only one positive real solution for the magnitudes of all the parameters; therefore, Hamiltonian is now fully identifiable

since we have only one positive real solution for the magnitudes of all the parameters, and in addition we can find the sign of ω_k. Furthermore, the minimum number of sampling points is

$$\mathcal{Q}_{\min} = 2\text{rank}(\mathbf{A}) = 4N.$$

Derivation of shape of reduced Gröbner basis for identifiable Hamiltonians

Here, we show how to derive the shape of reduced Gröbner basis for the identifiable Hamiltonians discussed above by employing the Elimination Theorem [138]. For example, let us consider the exchange model without transverse field. Let us take $\mathbf{x}(0) = (1, 0, \cdots, 0)^T \in \mathbb{R}^N$, and $\mathbf{C} = \begin{pmatrix} 1 & 0 & \cdots & 0 \end{pmatrix} \in \mathbb{R}^N$. The system matrix $\tilde{\mathbf{A}}$ is an $N \times N$ skew-symmetric matrix with the only non-zero elements $\theta_k = (\tilde{\mathbf{A}})_{k+1,k} = -(\tilde{\mathbf{A}})_{k,k+1}$, where $k = 1, 2, \cdots, N-1$. Then, from Eq. (2.21), we can obtain the following system of polynomial equations:

$$\begin{aligned} f_1(z_1, \cdots, z_{N-1}) &= 0 \\ f_2(z_1, \cdots, z_{N-1}) &= 0 \\ &\vdots \\ f_{N-1}(z_1, \cdots, z_{N-1}) &= 0, \end{aligned}$$

where $z_k = \theta_l^2$ $(k, l = 1, 2, \cdots, N-1)$. We can construct a polynomial ideal

$$\mathcal{I} = \langle f_1, \cdots, f_n \rangle \in \mathbb{C}[z_1, \cdots, z_{N-1}].$$

Note that for convenience we consider the polynomial ideal over the polynomial ring $\mathbb{C}[z_1, \cdots, z_{N-1}]$. In this case, we have found that there exists a proper choice for the pair (k, l) such that the corresponding elimination ideal $\mathcal{I}_{l-1}$ has the basis $z_k - c_k^2$ for $\exists c_k \in \mathbb{R}$, meaning that:

$$z_k - c_k^2 \in \mathscr{G}_{l-1}.$$

From the Elimination Theorem, we have:

$$\begin{aligned}\mathscr{G}_{l-1} &= \mathscr{G} \cap \mathbb{C}[z_l, \cdots, z_{N-1}] \\ &= \mathscr{G} \cap (\mathbb{C}[z_l] \cup \mathbb{C}[z_{l+1}, \cdots, z_{N-1}]) \\ &= (\mathscr{G} \cap \mathbb{C}[z_l]) \cup (\mathscr{G} \cap \mathbb{C}[z_{l+1}, \cdots, z_{N-1}]) \\ &= (\mathscr{G} \cap \mathbb{C}[z_l]) \cup \mathscr{G}_l,\end{aligned}$$

which yields:

$$\mathscr{G}_l \subset \mathscr{G}_{l-1}.$$

Therefore, we can inductively obtain:

$$\mathscr{G}_{N-2} \subset \mathscr{G}_{N-3} \subset \cdots \subset \mathscr{G}_2 \subset \mathscr{G}_1 \subset \mathscr{G}.$$

By the definition of the reduced Gröbner basis, $\mathscr{G}(\mathcal{I})$ has the shape:

$$\mathscr{G}(\mathcal{I}) = \langle z_1 - a_1, \cdots, z_{N-1} - a_{N-1} \rangle,$$

where $a_k = c_l^2$. This tells us the fact that $\mathcal{I}$ is the maximal ideal of $\mathbb{C}[z_1, \cdots, z_{N-1}]$, so that $\mathcal{I} = \sqrt{\mathcal{I}}$ and $\mathscr{G}(\mathcal{I})$ is equivalent to the reduced Gröbner basis $\mathscr{G}_{\text{red}}(\sqrt{\mathcal{I}})$:

$$\mathscr{G}(\mathcal{I}) = \mathscr{G}_{\text{red}}(\sqrt{\mathcal{I}}) = \langle z_1 - a_1, \cdots, z_{N-1} - a_{N-1} \rangle,$$

2.4.5 Global correlation propagation as necessary condition for identifiability

We further check that the analyses on the required experimental resources are consistent with our intuitive physical picture that connects Hamiltonian identification to the propagation of information through the whole spin chain. Consider for example the exchange Hamiltonian, Eq. (2.43), with all equal couplings. We can assume that the spins are equally spaced, with a the lattice constant, and $L = (N-1)a$ the length

of the chain. The eigenvalues of the Hamiltonian in the first excitation manifold are then

$$\Omega_n = 2J\cos\left(\frac{n\pi}{N+1}\right) = 2J\cos(k_n a), \quad k_n = n\pi\frac{N-1}{L(N+1)},$$

with $n = 1, 2, \ldots, N$. Then, the maximum angular frequency is

$$\Omega_{\max} = 2J\cos\left(\frac{\pi}{N+1}\right).$$

Since we need at least $2N$ sampling points, the longest evolution time is

$$T_{\text{tot}} = (2N-1)\pi/\Omega_{\max}.$$

For large $N \gg 1$, we can simplify this to

$$T_{\text{tot}} \simeq \pi\frac{N}{J}.$$

In order for the quantum probe to extract information on the whole spin chain, information needs to propagate to the other end and back. We can compute the group velocity for the propagation of the initial excitation on the first (probe) spin from the Hamiltonian eigenvalues $\Omega(k)$ [127],

$$v_g = \left|\frac{d\Omega(k)}{dk}\right|_{\max} = 2Ja = \frac{2JL}{N-1}.$$

Then, the time required for the information to come back to the probe spin is approximately given by

$$\tau \simeq \frac{2L}{v_g} = \frac{N-1}{J}$$

Thus, for large $N \gg 1$, we have

$$\tau \simeq \frac{N}{J},$$

in agreement with the result obtained from the mathematical requirements for system identification.

2.4.6 Identifiability assisted by external control

Until now, we have analyzed identifiability under the assumption that only the quantum probe can be initialized, measured and controlled. Also, we have discussed that some Hamiltonians cannot be identified, since they do not generate enough correlations among the target spins, or equivalently they do not transport information about the probe spin excitation through the whole chain. If we relax these assumptions and allow for a minimum level of control on the target spins, the picture changes. For example, if the target spins can be controlled via collective rotations, it is possible to turn a nonidentifiable Hamiltonian into an identifiable one. Here, we demonstrate an example which can point out this possibility by engineering the Hamiltonian [138].

Consider for example the Ising Hamiltonian,

$$H_{\text{is}} = \sum_{k=1}^{N} \frac{J_k}{2} S_k^{\alpha} S_{k+1}^{\alpha},$$

where $iS_k^{\alpha} \in \mathfrak{su}(2)$ acting on k-th qubit. Again, $\{iS_k^{\alpha}, iS_k^{\alpha}, iS_k^{\gamma}\}$ are the bases of $\mathfrak{su}(2)$, and they satisfy the commutation relation in Eq. (2.24)

$$[S_k^{\alpha}, S_k^{\beta}] = 2iS_k^{\gamma},\ [S_k^{\beta}, S_k^{\gamma}] = 2iS_k^{\alpha},\ [S_k^{\gamma}, S_k^{\alpha}] = 2iS_k^{\beta}.$$

From Sec. 3.5, this Hamiltonian is nonidentifiable. Using a simple control sequence in Fig. 2-6, we can generate an effective Hamiltonian of the exchange model,

$$H_{\text{ex}} = \sum_{k=1}^{N} \frac{J_k}{2} (S_k^{\alpha} S_{k+1}^{\alpha} + S_k^{\beta} S_{k+1}^{\beta}),$$

which is identifiable.

More precisely, periodic pulse-sequences such as in Fig. 2-6 make the system evolve as if under an effective time-independent Hamiltonian averaged over the cy-

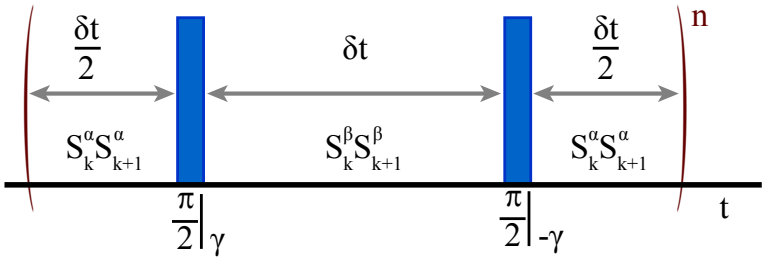

Figure 2-6: Identifiability with external control: By applying a periodic control pulse sequence n times in the limit of a very small $J_k\delta t \ll 1$, we can transfer $H_{\rm is} = \sum_{k=1}^{N-1} \frac{J_k}{2} S_k^\alpha S_{k+1}^\alpha$ to $H_{\rm ex} = \sum_{k=1}^{N-1} \frac{J_k}{2}(S_k^\alpha S_{k+1}^\alpha + S_k^\beta S_{k+1}^\beta)$ so that we can use $2N$ sampling points to identify the parameters J_k.

cle time. The effective Hamiltonian can be approximated by a first order Magnus expansion [101] (average Hamiltonian theory [61]). In this limit, to analyze the identifiability it is sufficient to consider the average Hamiltonian. The exact effective Hamiltonian will be identifiable as long as we can identify its approximation, however its expression might be too complex and analytical results only available in the limit of small enough time interval $\delta t \ll 1$ between the pulses where the approximation holds.

Let us write

$$\hat{A} = \sum_{k=1}^{N-1} \frac{J_k}{2} S_k^\alpha S_{k+1}^\alpha, \ \ \hat{B} = \sum_{k=1}^{N-1} \frac{J_k}{2} S_k^\beta S_{k+1}^\beta.$$

Let T_0 be the evolution time of interest. From the Suzuki-Trotter expansion of the second order, the time evolution $\mathcal{U}(T_0, 0)$ can be written by:

$$\mathcal{U}(T_0, 0) = e^{-i(\hat{A}+\hat{B})T_0} = \left[e^{-i\frac{\hat{A}}{2n}} e^{-i\frac{\hat{B}}{n}} e^{-i\frac{\hat{A}}{2n}}\right]^n + \mathcal{O}(1/n^2),$$

where m is defined by $n = T_0/\delta t$, which is called Trotter number. If we have small enough time intervals $\delta t \ll 1$, the correction can be negligible. Particularly, δt must be much smaller than the decoherence time. Note that

$$S_k^\beta = U_k^\gamma\left(\frac{\pi}{2}\right) S_k^\alpha U_k^{\gamma\dagger}\left(\frac{\pi}{2}\right),$$

where

$$U_k^\gamma\Big(\frac{\pi}{2}\Big) = \exp\Big(-i\frac{\pi}{4}\hat{S}_k^\gamma\Big).$$

Let $U_{\frac{\pi}{2}}^\gamma$ be

$$U_{\frac{\pi}{2}}^\gamma = U_1^\gamma\Big(\frac{\pi}{2}\Big) \otimes U_2^\gamma\Big(\frac{\pi}{2}\Big) \otimes \cdots \otimes U_N^\gamma\Big(\frac{\pi}{2}\Big).$$

In the limit $\delta t \ll 1$, Fig. 2-6 corresponds to

$$\mathcal{U}(T_0,0) = e^{-i(\hat{A}+\hat{B})T_0} \simeq \Big[e^{-i\frac{\hat{A}}{2n}}e^{-i\frac{\hat{B}}{n}}e^{-i\frac{\hat{A}}{2n}}\Big]^n = \Big[U_{\frac{\pi}{2}}^{\gamma\dagger}\Big(U_{\frac{\pi}{2}}^\gamma e^{-i\frac{\hat{A}}{n}}U_{\frac{\pi}{2}}^{\gamma\dagger}\Big)U_{\frac{\pi}{2}}^\gamma\Big(U_{\frac{\pi}{2}}^\gamma e^{-i\frac{\hat{A}}{n}}U_{\frac{\pi}{2}}^{\gamma\dagger}\Big)e^{-i\frac{\hat{A}}{2n}}\Big]^n,$$

which can help one achieve identifiability.

2.4.7 Robustness of eigensystem realization algorithm approach

While previous works have already analyzed the robustness of the eigensystem realization algorithm approach to experimental errors [69], here we evaluate the accuracy of the identification algorithm when it is implemented using only the minimum number of measurement points found above.

To compare with previous results, we consider the Ising model (with transverse field) for a chain of $N = 3$ spins and the exchange model (without field) for a chain of $N = 6$ spins. We consider the average error in 500 random Hamiltonian realizations and implement the ERA method, with the minimum number of measurement points ($\mathcal{Q}_{\min} = 4N = 12$ for the Ising model and $\mathcal{Q}_{\min} = 2N = 12$ points for the exchange Hamiltonian). We find that the relative error averaged over all the realization is still small ($10^{-10} - 10^{-2}$ [%]) and comparable to previous results, where many more points were measured.

Since the addition of experimental noise could change this result, we study the algorithm robustness in the presence of noise, as a function of the resources employed during the overall measurement process. To that end, we statistically compare the estimation robustness achieved by using Hankel matrices with different size but keeping

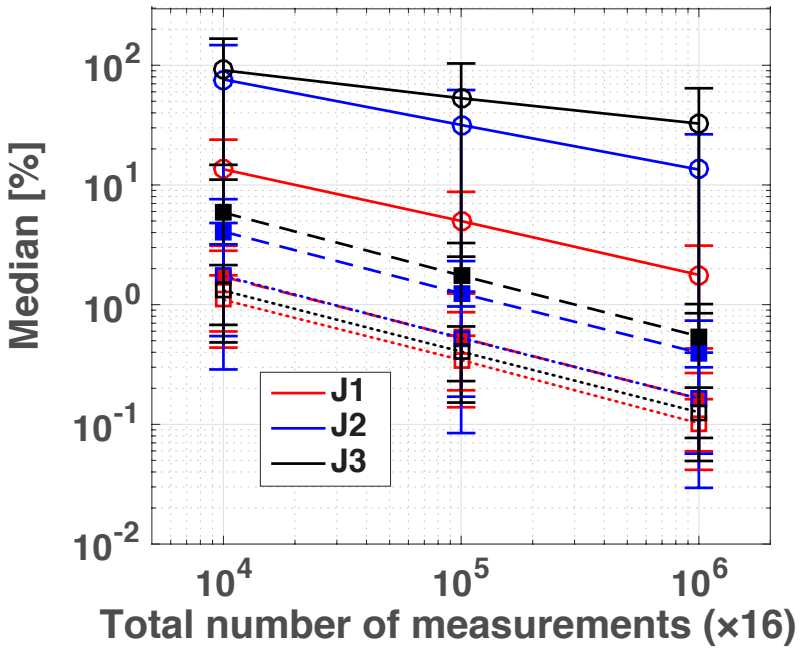

Figure 2-7: Estimation error with fixed time step Δt: Median of the estimation error $\{\langle\epsilon(J_i)\rangle\}$ over 500 random Hamiltonian realizations as a function of the total number of measurements. For each Hamiltonian, we repeated the ERA estimation 100 times, to evaluate the average error $\langle\epsilon(J_i)\rangle$. Solid lines with circles: 4×4 Hankel matrix; Dashed lines with solid square: 8×8 and dotted lines with squares: 40×40. The error bars are the absolute median deviation.

fixed the experimental resources.

We assume that each sampling point is measured M times, yielding a random outcome with a Gaussian distribution $\mathcal{N}(y(k), \sigma/\sqrt{M})$, that is, we assume that the mean is centered around the "true outcome" value $y(k)$ at each time $k\Delta t$ and for simplicity consider a gaussian noise (with $\sigma = 1$). By acquiring $2j$ sampling points (with $2jM$ total measurements) we can construct the (noisy) $j \times j$ Hankel matrices $\tilde{\mathbf{H}}_{j,j}$ and $\tilde{\mathbf{H}}_{j,j}$. Using the eigensystem realization algorithm, we can extract a set of parameters $\{\theta_m + \delta\theta_m\}_{m=1}^{M}$ that differ from the true parameters $\{\theta_m\}_{m=1}^{M}$. Since we are interested in the magnitude of the parameters, the estimation error can be written as:

$$\epsilon(\theta_m) = \left| \frac{|\theta_m + \delta\theta_m| - |\theta_m|}{|\theta_m|} \right| \times 100 \ [\%].$$

In the simulations, we repeat r times this procedure in order to obtain the mean

estimation error, $\langle\epsilon(\theta_m)\rangle$ and we further take the median over many realizations of the input model parameters.

In my simulation, we compare the estimation errors for Hankel matrices of different sizes j, keeping however fixed the total number of measurements, $2jM$. The smallest matrix has dimension $n\times n$, where n is the model order. Larger matrices, of dimension $Ln \times Ln$, will thus have an increased error rate by a factor $\sqrt{L}$. Since the presence of the noise forces $\tilde{\mathbf{H}}_{Ln,Ln}$ to be full-rank, we employ low-rank approximation via singular value decomposition [104] to generate an approximated $Ln \times Ln$ Hankel matrix with rank n.

We further consider two scenarios: either the time step Δt is fixed (thus larger matrices require longer total times) or the total evolution time T_{tot} is fixed (reflecting, e.g., constraints imposed by decoherence or experimental drifts). In the first case, Δt is chosen by assuming all the parameters take the possible maximal values so that the sampling theorem still holds. In the second case, we fix the total time evolution time to $T_{\text{tot}} = (2n-1)\Delta t$ as required for the smallest Hankel matrix, and we use smaller sampling time in the other cases.

As an example, we focus on the $N = 4$ exchange model without transverse field, which is shown in Eq. (2.43). The model order is given by $n = 4$. Since we assume that the maximal possible value taken by coupling strengths is 100, we have $\Delta t = \frac{\pi}{25\sqrt{5}}$. In Fig. 2-7 we plot the estimation errors $\{\langle\epsilon(J_i)\rangle\}$ as a function of the total number of measurement for different Hankel matrix dimensions.

Note that the smallest Hankel matrix leads to larger errors, but already slightly larger matrices, possibly thanks to the low-rank approximation, give more accurate estimation. Indeed, thanks to the low-rank approximation, we can generate a 4-rank approximation of $\tilde{\mathbf{H}}_{4L,4L}$ by neglecting the smallest singular values, which corresponds to an effective strategy for noise reduction. A second reason for the larger error is related to the shorter total time for the smallest Hankel matrix realization, that might in some cases not allow to fully capture the smallest frequencies in the signal. While this is not typically an issue in the ideal case, in the presence of experimental noise this leads to higher estimation errors.

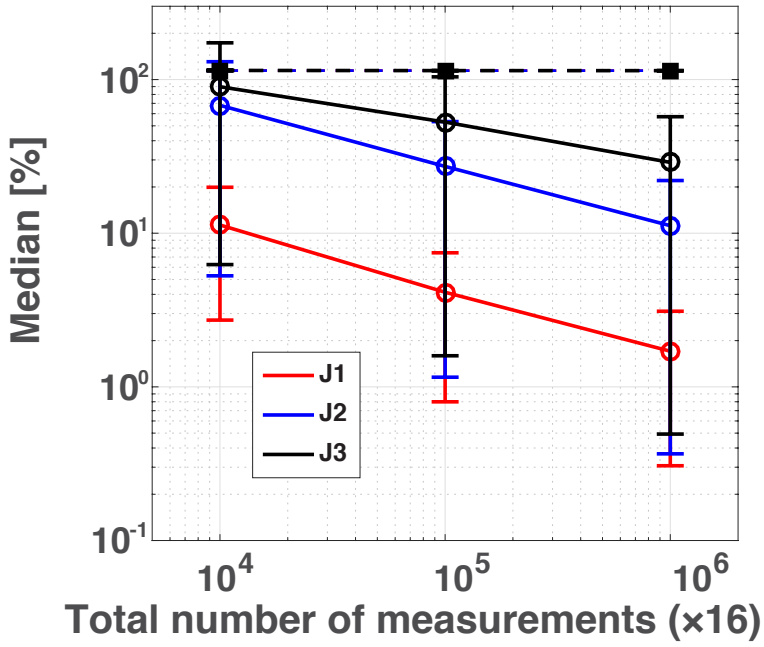

Figure 2-8: Estimation error with fixed total time T: Median of the estimation error $\{\langle\epsilon(J_i)\rangle\}$ over 500 random realizations of the Hamiltonian as a function of the total number of measurements. For each Hamiltonian, we repeated the ERA estimation 100 times, to evaluate the averaged error. Solid lines with circles: 4×4 Hankel matrix; Dashed lines with solid square: 8×8. The error bars are the absolute median deviation.

The role of the total time T_{tot} is highlighted when we consider the second scenario where T_{tot} is fixed: we fix the total time evolution time T_{tot} used for constructing $\tilde{\mathbf{H}}_{4,4}$, and compare the estimation performance between $\tilde{\mathbf{H}}_{4,4}$ and $\bar{\mathbf{H}}_{8,8}$. Then, the time step for $\tilde{\mathbf{H}}_8$ is chosen to be $\Delta t' = \frac{7}{15}\Delta t$. The result in Fig. 2-8 show that in this case the larger Hankel matrix leads to larger errors although the time step $\Delta t'$ satisfies the sampling theorem. In the presence of noise, the additional sampling points acquired mostly contribute to increasing the noise, but do not convey much more information. In addition, a very small time step might lead to larger errors, since it appears in the denominator of estimation equations in Eq. (2.20).

2.5 Examples of Gröbner basis for identifiable Hamiltonians

While we have shown the Gröbner basis for 3-qubit exchange Hamiltonian, in this section, we show the explicit polynomials for more particular identifiable models.

2.5.1 $N = 3$ Ising model with transverse field

For the Ising model with transverse field with $N = 3$ spins, the Hamiltonian can be written as:

$$H = \sum_{k=1}^{3} \frac{\omega_k}{2} Z_k + \sum_{k=1}^{2} \frac{J_k}{2} X_k X_{k+1}.$$

Let us choose $G_0 = \{X_1\}$ and let the initial state of the probe be the eigenstate of X_1 and the rest of spins in the chain be the maximally mixed state. The system matrix $\tilde{\mathbf{A}}$ is:

$$\tilde{\mathbf{A}} = \begin{pmatrix} 0 & -\omega_1 & 0 & 0 & 0 & 0 \\ \omega_1 & 0 & -J_1 & 0 & 0 & 0 \\ 0 & J_1 & 0 & -\omega_2 & 0 & 0 \\ 0 & 0 & \omega_2 & 0 & -J_2 & 0 \\ 0 & 0 & 0 & J_2 & 0 & -\omega_3 \\ 0 & 0 & 0 & 0 & \omega_3 & 0 \end{pmatrix}$$

and output matrix $\mathbf{C}$ is given as:

$$\mathbf{C} = \begin{pmatrix} 1 & 0 & 0 & 0 & 0 & 0 \end{pmatrix},$$

and the initial coherent vector is:

$$\mathbf{x}(0) = (1, 0, 0, 0, 0, 0)^T.$$

Let us define $(z_1, z_2, z_3, z_4, z_5) = (\omega_1^2, \omega_2^2, \omega_3^2, J_1^2, J_2^2)$. Then, we can obtain the following form of system of polynomial equations:

$$\begin{aligned}
&z_1 z_2 z_3 = v_1 \\
&z_1 z_2 + z_1 z_3 + z_2 z_3 + z_3 z_4 + z_1 z_5 + z_4 z_5 = v_2 \\
&z_1 + z_2 + z_3 + z_4 + z_5 = v_3 \\
&z_2 z_3 + z_3 z_4 + z_4 z_5 = v_4 \\
&z_2 + z_3 + z_4 + z_5 = v_5,
\end{aligned}$$

where $v_k > 0$ $(k = 1, \cdots, 5)$. Then, the Gröbner basis takes the following form: $\mathscr{G} = \{z_1 - a_1^2, z_2 - a_2^2, z_3 - a_3^2, z_4 - a_4^2, z_5 - a_5^2\}$, where $\{a_1^2, a_2^2, a_3^2, a_4^2, a_5^2\}$ are given in Eq. (2.44):

$$\begin{aligned}
a_1^2 &= v_3 - v_5 \\
a_2^2 &= \frac{v_2 - v_4}{v_3 - v_5} + \frac{v_1 + v_4(v_5 - v_3)}{v_4 - v_2 + v_5(v_3 - v_5)} \\
a_3^2 &= \frac{v_1(v_4 - v_2 + v_5(v_5 - v_3))}{(v_2 - v_4)^2 + v_3^2 v_4 - v_3 v_5(v_2 + v_4) + v_2 v_5^2 + v_1(v_5 - v_3)} \\
a_4^2 &= \frac{v_4 - v_2}{v_3 - v_5} \\
a_5^2 &= -\frac{v_1}{v_2} + \frac{v_1 - v_4(v_3 - v_5)}{v_2 - v_4 - v_5(v_3 - v_5)} + \frac{v_1(v_1(v_5 - v_3) + v_4(-v_2 + v_4 + v_3(v_3 - v_5)))}{v_2((v_2 - v_4)^2 - v_1 v_3 + v_3^2 v_4 + v_5(v_1 - v_3(v_2 + v_4)) + v_2 v_5^2)},
\end{aligned} \tag{2.44}$$

2.5.2 $N = 4$ Exchange model without transverse field

Next, let us consider the exchange model without transverse field with $N = 4$ spins. The Hamiltonian can be written as:

$$H = \sum_{k=1}^{3} \frac{J_1}{2}(X_k X_{k+1} + Y_k Y_{k+1}).$$

Let us take same observable set and initial state of spin chain in Sec. 2.5.1. The system matrix $\tilde{\mathbf{A}}$ is:

$$\tilde{\mathbf{A}} = \begin{pmatrix} 0 & -J_1 & 0 & 0 \\ J_1 & 0 & J_2 & 0 \\ 0 & -J_2 & 0 & -J_3 \\ 0 & 0 & J_3 & 0 \end{pmatrix}$$

and output matrix $\mathbf{C}$ is given as:

$$\mathbf{C} = \begin{pmatrix} 1 & 0 & 0 & 0 \end{pmatrix},$$

and the initial coherent vector is:

$$\mathbf{x}(0) = (1, 0, 0, 0)^T.$$

Let us define $(z_1, z_2, z_3) = (J_1^2, J_2^2, J_3^2)$. Then, we can obtain the following form of system of polynomial equations:

$$z_2 + z_3 = v_1$$

$$z_1 z_3 = v_2$$

$$z_1 + z_2 + z_3 = v_3$$

where $v_k > 0$ $(k = 1, \cdots, 5)$. Then, the Gröbner basis takes the following form: $\mathscr{G} = \{z_1 - a_1^2, z_2 - a_2^2, z_3 - a_3^2\}$, where $\{a_1^2, a_2^2, a_3^2\}$ are given in Eq. (2.45):

$$\begin{aligned} a_1^2 &= v_3 - v_1 \\ a_2^2 &= \frac{v_1 v_3 - v_2 - v_1^2}{v_3 - v1} \\ a_3^3 &= \frac{v_2}{v_3 - v1} \end{aligned} \tag{2.45}$$

where $v_3 > v_1$, $v_1(v_3 - v_1) > v_2 > 0$.

2.5.3 $N = 2$ Exchange model with transverse field

Finally, let us consider the exchange model with $N = 3$ spins with transverse field. The Hamiltonian can be written as:

$$H = \frac{\omega_1}{2} Z_1 + \frac{\omega_2}{2} Z_2 + \frac{J_1}{2}(X_1 X_2 + Y_1 Y_2).$$

In Sec. 2.4.4, we have discussed that the Hamiltonian becomes fully identifiable if we measure X_1 and Y_1 separately. Let us always prepare the initial state of the spin probe to be the eigenstate of $\{X_1\}$ and rest of all spins to be the maximally mixed state. The system matrix is:

$$\tilde{\mathbf{A}} = \begin{pmatrix} 0 & \omega_1 & 0 & -J_1 \\ -\omega_1 & 0 & -J_1 & 0 \\ 0 & J_1 & 0 & \omega_2 \\ J_1 & 0 & -\omega_2 & 0 \end{pmatrix}$$

Here, the output matrix becomes

$$\mathbf{C} = \begin{pmatrix} 0 & 1 & 0 & 0 \end{pmatrix}$$

and the initial coherent vector is

$$\mathbf{x}(0) = (1, 0, 0, 0)^T.$$

Let us define $(z_1, z_2, z_3) = (\omega_1, \omega_2, J_1^2)$. Then, we can obtain the following form of system of polynomial equations:

$$\begin{aligned}
-z_1 z_2^2 - z_2 z_3 &= v_1 \\
z_2^2 + z_3 &= v_2 \\
z_1 &= v_3 \\
(z_1 z_2 + z_3)^2 &= v_4 \\
z_1^2 + z_2^2 + 2z_3 &= v_5
\end{aligned}$$

Then, the Gröbner takes the following form: $\mathscr{G} = \{z_1 - a_1, z_2 - a_3, z_3 - a_3^2\}$, where $\{a_1, a_2, a_3^2\}$ are given in Eq. (2.46):

$$\begin{aligned}
a_1 &= v_3 \\
a_2 &= \frac{v_1 + 2v_2v_3 + v_3^3 - v_3v_5}{v_2 + v_3^2 - v_5} \\
&= \frac{v_2^2 - v_2v_3^2 - v_3^4 + v_4 - v_2v_5 + v_3^2v_5}{v_1 - v_3^3 + v_3v_5} \\
&= \frac{2v_1(v_2 - v_5) + v_3(-v_2^2 + 2v_2v_3^2 + 2v_3^4 - 3v_4 - 3v_3^2v_5 + v_5^2)}{2(v_3^4 + v_4 - v_3^2v_5)} \\
a_3^2 &= v_5 - v_2 - v_3^2
\end{aligned} \tag{2.46}$$

where $v_2 + v_3^2 - v_5 \neq 0$, $v_1 - v_3^2 + v_3v_5 \neq 0$, $v_3^4 + v_4 - v_3^2v_5 \neq 0$ and $v_5 - v_2 - v_3^2 > 0$. Here a_1 and a_2 are the nonzero real numbers.

2.6 Conclusion and open problems

We have studied the concept of quantum system identifiability by focusing on the dimension estimation and Hamiltonian parameter estimation in closed quantum many-

qubit systems through the local measurement of a well-characterized quantum probe coupled to the target system.

In the dimension estimation problem, we assumed that the target system model is given as prior information, but that the system can be accessed only indirectly via a quantum probe. These assumptions considerably relax the required experimental resources, as well as other implicit assumptions about the controllability and observability of the target system. Provided the coupling model allows the generation of non-local correlations with the quantum probe during the system dynamics, the dimension of the system can be exactly estimated from sampling the quantum probe evolution at discrete time steps. The estimation is based on measuring the rank of the Hankel matrix constructed from the experimental data, a step in the recently proposed procedure for the similar problem of Hamiltonian identification [161, 162, 138].

This study provides a useful application of local quantum probes, which can serve as a quantum sensor to determine the exact dimension of the system. Our method can also be employed more broadly to determine the dimension of a general interacting $N-$body qudit system, i.e. a system with dimension $\dim(\mathcal{H}) = d^N$: as long as d and the interaction model $\mathcal{M}$ are given, conservation of the operator algebraic structure ensures that a similar procedure than described here can be applied.

In the presence of noise, which changes the rank of the experimentally obtained Hankel matrix, we numerically show that the dimension of the system can still be estimated by finding the final peak in the sequence of ratios of the Hankel matrix singular values. We conclude that the methodology has an acceptable performance for weak noise and small number of qubits. Also, the method is model-sensitive because we must employ the modified function for the suspected model to find the dimension if we allow some noise on the model itself.

For the Hamiltonian parameter estimation scenario, we re-analyzed Hamiltonian identification via the eigensystem realization algorithm (ERA) approach and provided a systematic algorithm to test identifiability by employing the Gröbner basis. Even more importantly from a practical point of view, we showed that analyzing these techniques yields bounds on the experimental resources required to estimate

the Hamiltonian parameters, both in terms of the minimum coherence time required for Hamiltonian identification and for the overall total experimental time for the multi-parameter estimate. These bounds can guide experimentalists in implementing the most efficient Hamiltonian identification protocol. We further numerically studied the estimation performance of ERA in the presence of noise. We found that the low-rank approximation for larger numbers of sampling points leads to more accurate estimation, even when the total number of measurements is kept fixed. This effects is however already at play for small number of points above the minimum one, thus allowing to keep the total evolution time short enough. When instead we fix the total evolution time as required to construct the smallest size Hankel matrix, there is no longer an advantage in using a larger number of sampling points, as the smaller time step leads to larger estimation errors. These analyses quantitatively provide helpful insights for a practical experimental approach to Hamiltonian identification based on ERA.

In order to obtain exemplary analytical results for our Hamiltonian identification protocol, we considered simple models of spin chains coupled by one end to the quantum probe. While these models are less complex than what would be found in practical experimental scenarios, they allowed us to clarify an interesting relation between Hamiltonian identifiability by a quantum probe and quantum information propagation in a chain. Indeed, as Hamiltonian identification relies on building a complete accessible set, the transport of information along the spin chain, in the form of spin-spin correlation, is a necessary condition. This result further imposes conditions on the time required for Hamiltonian identification: while in the cases we considered here these time bounds were consistent with the bounds directly imposed by ERA, it will be interesting to analyze in the future whether this result changes in the presence of disorder, when localization (either single particle or many-body) appear.

We finally showed that by relaxing some of the assumptions on control constraints, by allowing for example collective control of the target system, can turn a previously non-identifiable system into an identifiable one. These results can contribute to make

Hamiltonian identification more experimentally practical in many real-system scenarios.

Chapter 3

Quantum system identification in equilibrium regime

This chapter discusses the role of nonclassical correlations in estimating parameters characterizing a thermal equilibrium state, namely the Gibbs' state, by comparing the global measurement scheme and greedy local measurement scheme [140, 139]. We focus on the ultimate precision limit quantified by quantum Fisher information (QFI) [63, 67, 159, 74], which bounds the estimation variance over all possible sets of measurements. We study the relation between a measure of nonclassical correlations and the ultimate precision loss quantified by the difference in the QFI of global measurement scheme and the local QFI in greedy local measurement scheme.

In Sec. 3.2, by following [63, 67, 159, 74], we review the concept of ultimate precision limit, which can be quantified by the quantum Fisher information (QFI), and introduce the formalism of the QFI in the global measurement scheme and greedy local measurement scheme. Here, we call the QFI in greedy local measurement scheme the LOCC QFI [1] because this protocol belongs to the class of local operations and classical communication (LOCC) [115]. In Sec. 3.3, we will review the quantum discord proposed by Ollivier and Zurek in 2001 [118], which is a general quantity to measure of nonclassical correlations between two subsystems, introduce diagonal quantum dis-

[1] Note that the equivalent concept of the LOCC QFI has been originally proposed by [96] from information-theoretic perspective and by [111] from quantum metrology perspective.

cord by following [91]. Then, in order to explore the role of nonclassical correlations in quantum metrology, we introduce *discord for local metrology* [140], which quantifies the information contents of nonclassical correlations revealed by the optimal local measurements on the subsystems in the greedy local measurement scheme. In Sec. 3.4, we will discuss the relation between the discord for local metrology and difference in the QFI for global and greedy local measurement scheme [140] in the high-temperature limit, followed by the conclusion in Sec. 3.8.

3.1 Introduction

Hamiltonian parameter estimation at thermal equilibrium has been considered before by Mehboudi *et al.* [108], in which they considered a special Hamiltonian consisting of two commuting operators, to which temperature-independent parameters are linearly coupled. For this special case, they proved that the QFI for estimating either parameter can be characterized as a curvature of the Helmholtz free energy at an arbitrary temperature. However, for a general Hamiltonian H_λ parameterized by a temperature-independent parameter λ, this is not always the case, because of the noncommutativity of the Hamiltonian and the generator of parameter λ. Still, in the high-temperature limit, the QFI can be well approximated by the susceptibility and the relation provided in [108] can be applied.

For thermometry, temperature estimation also requires a fully quantum treatment [17, 18, 109, 33, 126, 76, 103, 155, 34, 122, 120, 66]. Correa *et al.* [33] showed that the optimal measurement strategy involves projective measurements of the energy eigenstates, since heat capacity corresponds to energy fluctuations. Unfortunately, performing projective measurements of (global) energy eigenstates is typically hard, as eigenstates usually contain nonclassical correlations among different parts of the system. Recent works [121, 119] considered measurements on a single subsystem, finding that the local QFI [2] bounds the ultimate achievable precision. We can however

[2] In Ref. [121, 119], they define the local quantum thermal susceptibility as the local QFI for estimating the inverse temperature.

expect that a more general measurement scheme with sequential local measurements on multiple subsystems and (classical) feed forward from previous measurements could improve the estimate precision. This scheme still remains practical and belongs to the class of local operations and classical communication (LOCC) [115].

For systems with classical Gibbs states, given by product states among subsystems, such local greedy schemes are optimal. However, for generic quantum systems, Gibbs states can be highly nonclassical. Thus, temperature as a global property requires global measurements to be optimally estimated, while local sequential schemes cannot achieve optimal precision due to the nonclassical correlations in the system. The local QFI has been recently shown to depend on the correlation length at low temperature [70]. In a related metrology task, channel parameter estimation, the correlation metric for pure quantum states based on the local QFI, was shown [84] to coincide with the geometric discord [38]. Also, the relation between the decreasing the QFI due to the measurements on the total system and the disturbance has been considered [133]. In order to explore the relation between ultimate precision loss and nonclassical correlation more broadly, we focus on temperature estimation and seek a relation between precision loss and quantum discord [118], which quantifies nonclassical correlations in a quantum system.

We focus on the high-temperature limit and analytically find that the precision loss can be exactly quantified by a quantum correlation metric in this regime, despite that entanglement or nonclassical correlations are expected to play lesser roles. In addition, temperature estimation at high temperature is a practically important task as the capability of performing coherent operations at room temperature is a desirable feature for quantum information processing devices. Also, quantum phenomena such as superconductivity [82, 45] survive at temperatures as high as 165 K.

3.2 Quantification of precision

In this section, we review the theory of classical Fisher information and quantum Fisher information by following. Refs. [63, 67, 159, 74].

3.2.1 Classical Fisher information

Before introducing the QFI , we review classical Fisher information first by following Ref. [74]. Suppose that we want to estimate a parameter ξ by performing a measurement M_x with a measurement result x. Then, this measurement is characterized by the conditional probability distribution $P_{M_x}(x|\xi)$. Let us define the estimate of ξ as $\tilde{\xi}_{M_x}(x)$, which indicates that we estimate ξ from our measurement outcome x obtained by performing the measurement M_x. Here, x is called estimator.

Let us define the estimator error $\delta\xi(x) = \tilde{\xi}_{M_x}(x) - \xi$. Here, ξ is the true value, and for unbiased estimator, we expect the expectation value of $\tilde{\xi}_{M_x}(x)$ to be equivalent to ξ, i.e.

$$\int dx\ \tilde{\xi}_{M_x}(x) P_{M_x}(x|\xi) dx = \xi$$

so that the error average over all the measurement outcomes is 0, i.e.

$$\langle \delta\xi \rangle = \int dx\ \delta\xi(x) P_{M_x}(x|\xi) dx = \int dx (\tilde{\xi}_{M_x}(x) - \xi) P_{M_x}(x|\xi) = 0.$$

Taking the derivative of $\langle \delta\xi \rangle = 0$ with respect to ξ, we obtain

$$\begin{aligned} 0 &= \int dx \Big(\tilde{\xi}_{M_x}(x) \frac{\partial P_{M_x}(x|\xi)}{\partial \xi} - P_{M_x}(x|\xi) - \xi \frac{\partial P_{M_x}(x|\xi)}{\partial \xi} \Big) \\ &= \int dx \Big(\tilde{\xi}_{M_x}(x) - \xi \Big) \frac{\partial P_{M_x}(x|\xi)}{\partial \xi} - 1 \\ &= \int dx (\tilde{\xi}_{M_x}(x) - \xi) P_{M_x}(x|\xi) \Big(\frac{\partial}{\partial \xi} \ln P_{M_x}(x|\xi) \Big) - 1. \end{aligned}$$

Then, we can write

$$\int\ dx (\tilde{\xi}_{M_x}(x) - \xi) P^{1/2}_{M_x}(x|\xi) \cdot P^{1/2}_{M_x}(x|\xi) \Big(\frac{\partial}{\partial \xi} \ln P_{M_x}(x|\xi) \Big) = 1.$$

From Cauchy-Schwartz inequality,

$$\Big(\int_{\mathbb{R}} dx |f(x)|^2 \Big) \Big(\int_{\mathbb{R}} dx |g(x)|^2 \Big) \geq \Big| \int_{\mathbb{R}} dx f^*(x) g(x) \Big|^2,$$

by defining $f(x) = \tilde{\xi}_{M_x}(x) - \xi)P^{1/2}_{M_x}(x|\xi)$ and $g(x) = P^{1/2}_{M_x}(x|\xi)\big(\frac{\partial}{\partial\xi}\ln P_{M_x}(x|\xi)\big)$, we have

$$\Big(\int dx(\tilde{\xi}_{M_x}(x) - \xi)^2 P_{M_x}(x|\xi)\Big)\Big(\int dx P_{M_x}(x|\xi)\Big(\frac{\partial}{\partial\xi}\ln P_{M_x}(x|\xi)\Big)^2\Big) \geq 1,$$

Since the variance of the estimation can be written as

$$\delta\xi^2 = \int dx(\tilde{\xi}_{M_x}(x) - \xi)^2 P_{M_x}(x|\xi)dx,$$

if we define the Fisher information $I_{M_x}(\xi)$ as

$$I_{M_x}(\xi) = \int \Big(\frac{\partial}{\partial\xi}\ln P_{M_x}(x|\xi)\Big)^2 P_{M_x}(x|\xi)dx,$$

we can obtain

$$\delta\xi^2 \geq \frac{1}{I_{M_x}(\xi)}. \tag{3.1}$$

3.2.2 Quantum Fisher information (QFI)

For quantum parameter estimation, we introduce the quantum Fisher information (QFI) $\mathcal{F}(\xi;\rho(\xi))$, which is defined as

$$\mathcal{F}(\xi;\rho(\xi)) = \mathrm{Tr}[\rho(\xi)L^2_\xi], \tag{3.2}$$

where $L_\xi = L^\dagger_\xi$ is called symmetric logarithmic derivative, which satisfies

$$\frac{\partial\rho(\xi)}{\partial\xi} = \frac{L_\xi\rho(\xi) + \rho(\xi)L_\xi}{2},$$

and

$$\langle L_\xi\rangle = \mathrm{Tr}[\rho(\xi)L_\xi] = 0.$$

For a single parameter estimation, we have the following theorem [33, 110, 121]:

Theorem 4. *The QFI $\mathcal{F}(\xi, \rho(\xi))$ of a quantum state $\rho(\xi)$ characterized by a single parameter ξ to be estimated can be written as*

$$\mathcal{F}(\xi; \rho(\xi)) = -2 \lim_{\epsilon \to 0} \frac{\partial^2}{\partial \epsilon^2} \mathbb{F}[\rho(\xi), \rho(\xi + \epsilon)], \tag{3.3}$$

where $\mathbb{F}[\rho(\xi), \rho(\xi + \epsilon)]$ is the fidelity between two quantum states $\rho(\xi)$ and $\rho(\xi + \epsilon)$ defined as

$$\mathbb{F}[\rho(\xi), \rho(\xi + \epsilon)] = \Big(Tr[\sqrt{\rho^{1/2}(\xi)\rho(\xi + \epsilon)\rho^{1/2}(\xi)}] \Big).$$

Proof. A distance measure between two different quantum state ρ and σ is the Bures distance, which is defined as

$$(d_B[\rho, \sigma])^2 = 2(1 - \sqrt{\mathbb{F}[\rho, \sigma]})$$

where $\mathbb{F}[\rho, \sigma]$ is the fidelity between states ρ, σ defined as [77]:

$$\mathbb{F}\left[\rho, \sigma\right] = \left(\mathrm{Tr}\Big[\sqrt{\sqrt{\rho}\sigma\sqrt{\rho}} \Big] \right)^2.$$

For the states ρ and $\rho + \delta\rho$, the Bures distance is defined as

$$(d_B[\rho, \rho + \delta\rho])^2 = \frac{1}{2} \mathrm{Tr}[\Lambda \delta\rho],$$

where the operator Λ satisfies

$$\Lambda\rho + \rho\Lambda = \delta\rho.$$

If we define

$$\delta\rho = \frac{\partial \rho(\xi)}{\partial \xi} \epsilon,$$

where ϵ is the error of the estimation. We have

$$\delta\rho = \frac{L_\xi \rho(\xi) + \rho(\xi) L_\xi}{2}\epsilon,$$

so that

$$G = \frac{1}{2} L_\xi \epsilon.$$

Therefore,

$$(d_B[\rho, \rho + \delta\rho])^2 = \frac{1}{2}\mathrm{Tr}\Big[\frac{1}{2}(L_\xi\rho(\xi) + \rho(\xi)L_\xi)\epsilon \cdot \frac{1}{2}L_\xi\epsilon\Big] = \frac{1}{4}\mathrm{Tr}[\rho(\xi)L_\xi^2]\epsilon^2,$$

which yields

$$(d_B[\rho, \rho + \delta\rho])^2 = (d_B[\rho(\xi), \rho(\xi + \epsilon))^2 = \frac{1}{4}\mathcal{F}(\xi; \rho(\xi))\epsilon^2.$$

Since

$$(d_B[\rho(\xi), \rho(\xi + \epsilon)])^2 = 2\Big(1 - \sqrt{\mathbb{F}[\rho(\xi), \rho(\xi + \epsilon)]}\Big),$$

we have

$$\mathcal{F}(\xi; \rho(\xi)) = 8\frac{1 - \sqrt{\mathbb{F}[\rho(\xi), \rho(\xi + \epsilon)]}}{\epsilon^2}.$$

Here, let us define

$$\mathbb{F}(\epsilon) \equiv \mathbb{F}[\rho(\xi), \rho(\xi + \epsilon)].$$

For small $\epsilon \ll 1$, we have

$$\mathcal{F}(\xi;\rho(\xi)) = 8\frac{1-\sqrt{\mathbb{F}(0)}}{\epsilon^2} + \frac{4}{\epsilon\sqrt{\mathbb{F}(0)}}\frac{\partial\mathbb{F}(\epsilon)}{\partial\epsilon}\Big|_{\epsilon=0} + \frac{1}{\mathbb{F}^{3/2}(0)}\Big(\frac{\partial\mathbb{F}(\epsilon)}{\partial\epsilon}\Big|_{\epsilon=0}\Big)^2 - 2\frac{1}{\sqrt{\mathbb{F}(0)}}\frac{\partial^2}{\partial\epsilon^2}\mathbb{F}(\epsilon)\Big|_{\epsilon=0} + O(\epsilon).$$

Since

$$\mathbb{F}(0) = 1$$

and $\mathbb{F}(\epsilon)$ takes the maximum value at $\epsilon = 0$, i.e.

$$\frac{\partial\mathbb{F}(\epsilon)}{\partial\epsilon}\Big|_{\epsilon=0} = 0,$$

we have

$$\mathcal{F}(\xi,\rho(\xi)) = -2\lim_{\epsilon\to 0}\frac{\partial^2}{\partial\epsilon^2}\mathbb{F}[\rho(\xi),\rho(\xi+\epsilon)].$$

□

This shows that the QFI captures the response of the quantum state to a small change in its parameter, and if the true state and error state becomes more distinguishable, then the response to the small error is larger so that it is easier to extract the parameter.

Actually, $\mathcal{F}(\xi,\rho(\xi))$ is the upper bound of the classical Fisher information $I_{M_x}(\xi)$. Let us write a quantum state $\rho(\xi)$ in its diagonal form:

$$\rho(\xi) = \int P_{M_x}(x|\xi)|x\rangle\langle x|dx = \int P_{M_x}(x|\xi)E_x dx,$$

where $E_x = |x\rangle\langle x|$ are projectors so that $E_x = E_x^\dagger$, and satisfying the following completeness equation:

$$\int dx E_x = \int dx|x\rangle\langle x| = \mathbb{1}. \tag{3.4}$$

Therefore, the probability $P_{M_x}(x|\xi)$ is given by

$$P_{M_x}(x|\xi) = \mathrm{Tr}[\rho(\xi)E_x].$$

Thus, the classical Fisher information can be written as

$$\begin{aligned}
I(\xi) &= \int dx \Big(\frac{\partial}{\partial \xi} \ln P_{M_x}(x|\xi)\Big)^2 P_{M_x}(x|\xi) = \int dx \Big(\frac{\partial}{\partial \xi} P_{M_x}(x|\xi)\Big)^2 \frac{1}{P_{M_x}(x|\xi)} \\
&= \int dx \Big(\mathrm{Tr}\Big[E_x \frac{\partial \rho(\xi)}{\partial \xi}\Big]\Big)^2 \frac{1}{\mathrm{Tr}[\rho(\xi)E_x]} = \int dx \Big(\mathrm{Tr}\Big[E_x \frac{L_\xi \rho(\xi) + \rho(\xi) L_\xi}{2}\Big]\Big)^2 \frac{1}{\mathrm{Tr}[\rho(\xi)E_x]} \\
&= \int dx \Big(\mathrm{Tr}\Big[\frac{E_x L_\xi + L_\xi E_x}{2}\rho(\xi)\Big]\Big)^2 \frac{1}{\mathrm{Tr}[\rho(\xi)E_x]} \\
&= \int dx \Big(\mathrm{Tr}\Big[\frac{(L_\xi E_x)^\dagger + L_\xi E_x}{2}\rho(\xi)\Big]\Big)^2 \frac{1}{\mathrm{Tr}[\rho(\xi)E_x]} \\
&= \int dx \frac{\mathrm{Re}[\mathrm{Tr}[L_\xi E_x \rho(\xi)]]^2}{\mathrm{Tr}[\rho(\xi)E_x]} = \int dx \frac{\mathrm{Re}[\mathrm{Tr}[E_x \rho(\xi) L_\xi]]^2}{\mathrm{Tr}[\rho(\xi)E_x]},
\end{aligned}$$

where we used the cyclic property of trace operation, $L_\xi = L_\xi^\dagger$ and $E_x = E_x^\dagger$. Since

$$\frac{\mathrm{Re}[\mathrm{Tr}[E_x \rho(\xi) L_\xi]]^2}{\mathrm{Tr}[\rho(\xi)E_x]} \leq \Big|\frac{\mathrm{Tr}[E_x \rho(\xi) L_\xi]}{\mathrm{Tr}[\rho(\xi)E_x]}\Big|^2 = \Big|\mathrm{Tr}\Big[\Big(\frac{\sqrt{E_x}\sqrt{\rho(\xi)}}{\sqrt{\mathrm{Tr}[\rho(\xi)E_x]}}\Big)\Big(\sqrt{\rho(\xi)} L_\xi \sqrt{E_x}\Big)\Big]\Big|^2$$

From the Caushy-Schwartz inequality, since

$$|\mathrm{Tr}[A^\dagger B]|^2 \leq \mathrm{Tr}[A^\dagger A]\mathrm{Tr}[B^\dagger B],$$

by defining A and B as [74]

$$A = \frac{\sqrt{E_x}\sqrt{\rho(\xi)}}{\sqrt{\mathrm{Tr}[\rho(\xi)E_x]}}, \; B = \sqrt{\rho(\xi)} L_\xi \sqrt{E_x},$$

we have

$$\begin{aligned}
&\mathrm{Tr}[A^\dagger A] = \frac{\mathrm{Tr}[\sqrt{E_x}\sqrt{\rho(\xi)}\sqrt{\rho(\xi)}\sqrt{E_x}]}{\mathrm{Tr}[\rho(\xi)E_x]} = \frac{\mathrm{Tr}[\rho(\xi)E_x]}{\mathrm{Tr}[\rho(\xi)E_x]} = 1 \\
&\mathrm{Tr}[B^\dagger B] = \mathrm{Tr}[\sqrt{E_x} L_\xi \sqrt{\rho(\xi)}\sqrt{\rho(\xi)} L_\xi \sqrt{E_x}] = \mathrm{Tr}[\sqrt{E_x} L_\xi \rho(\xi) L_\xi \sqrt{E_x}] = \mathrm{Tr}[E_x L_\xi \rho(\xi) L_\xi].
\end{aligned}$$

Therefore, we can obtain

$$\left|\frac{\mathrm{Tr}[E_x\rho(\xi)L_\xi]}{\mathrm{Tr}[\rho(\xi)E_x]}\right|^2 \leq \mathrm{Tr}[E_x L_\xi \rho(\xi) L_\xi]$$

so that

$$I_{M_x}(\xi) \leq \int dx \mathrm{Tr}[E_x L_\xi \rho(\xi) L_\xi] = \mathrm{Tr}[\rho(\xi) L_\xi^2].$$

where we used Eq. (3.4) and Eq. (3.2). Therefore, we have

$$I_{M_x}(\xi) \leq \mathcal{F}(\xi; \rho(\xi)), \tag{3.5}$$

which means that the QFI is the optimization of classical Fisher information over all the possible measurements $\{M_x\}$.

$$\mathcal{F}(\xi; \rho(\xi)) = \max_{\{M_x\}} I_{M_x}(\xi)$$

From Eq. (3.5) and Eq. (3.1), we can obtain the quantum Cramer-Rao bound [63, 67, 159, 74], which states that the QFI $\mathcal{F}(\xi, \rho(\xi))$ bounds the estimation variance as

$$\delta\xi^2 \geq \frac{1}{\mathcal{F}(\xi, \rho(\xi))}, \tag{3.6}$$

and $\mathcal{F}(\xi; \rho(\xi))$ can be also interpreted as the *ultimate* precision limit.

3.2.3 LOCC QFI

Global measurements on a composite system are generally required to achieve the optimal QFI, but are usually difficult to implement. If only local measurements are available, even the best measurement protocol might not reach optimality. Here, we consider a local measurement scheme with sequential local optimal measurements on subsystems that we call "greedy" local measurement scheme [139, 140]. This scheme belongs to the class of LOCC, thus we call the constrained QFI of this scheme the

LOCC QFI.

Consider an arbitrary bipartite system in the state $\rho_{AB}(\xi)$. In the greedy local measurement scheme, we first perform a local optimal projection measurement $\tilde{\Pi}_j^A$ on the first subsystem, where we use the notation $\tilde{\Pi}$ in order to emphasize that the measurement is optimal. After the measurement, the state of subsystem B is a conditional state based on the measurement result of $\tilde{\Pi}_j^A$, $\rho_{B|\tilde{\Pi}_j^A}(\xi) = \mathrm{Tr}_A[(\tilde{\Pi}_j^A \otimes \mathbb{1}^B)\rho_{AB}(\xi)(\tilde{\Pi}_j^{A\dagger} \otimes \mathbb{1}^B)]/p_j(\xi)$, with $p_j(\xi) = \mathrm{Tr}[(\tilde{\Pi}_j^A \otimes \mathbb{1}^B)\rho_{AB}(\xi)(\tilde{\Pi}_j^{A\dagger} \otimes \mathbb{1}^B)]$ the measurement probability. Given the conditional QFI for outcome j, $\mathcal{F}_{B|\tilde{\Pi}_j^A}(\xi) = \mathcal{F}(\xi, \rho_{B|\tilde{\Pi}_j^A}(\xi))$, the unconditional local QFI for subsystem B is given by

$$\mathcal{F}_{B|A}(\xi) = \sum_j p_j(\xi)\mathcal{F}_{B|\tilde{\Pi}_j^A}(\xi),$$

Note that feed forward is required as the optimal measurement on B depends on the outcome of $\tilde{\Pi}_j^A$. From the additivity of the Fisher information, the LOCC QFI $\mathcal{F}_{A\to B}(\xi)$ is given by

$$\mathcal{F}_{A\to B}(\xi) = \mathcal{F}_A(\xi) + \mathcal{F}_{B|A}(\xi),$$

where $\mathcal{F}_A(\xi) = \mathcal{F}(\xi, \rho_A(\xi))$ is the local QFI for subsystem A [96, 111, 139]. This can be derived from the additivity of Fisher information [96, 111]. Since the QFI is simply the classical Fisher information over the optimal quantum measurement. Let us consider an arbitrary consecutive measurement result (X, Y) on A and B. Despite the quantum nature of the measurement, a classical derivation suffices. The joint distribution is a Markovian chain $X \to Y$ and thus the joint distribution is

$$P(x, y; \xi) = P(x; \xi)P(y|x; \xi).$$

Let us consider the most general scenario where the measurement result is continuous. The greedy local measurement scheme is characterized by the constrained Fisher

information

$$\begin{aligned}\mathcal{F}_{A\to B}(\xi) &= \int dxdyP(x,y;\xi)\Big(\frac{\partial}{\partial\xi}\ln P(x,y;\xi)\Big)^2 \\ &= \int dxdyP(x;\xi)P(y|x;\xi)\Big(\frac{\partial}{\partial\xi}\ln P(x;\xi)+\frac{\partial}{\partial\xi}\ln P(y:x;\xi)\Big)^2 \\ &= \int dxdyP(x;\xi)P(y|x;\xi)\Big[\Big(\frac{\partial}{\partial\xi}\ln P(x:\xi)\Big)^2+\Big(\frac{\partial}{\partial\xi}\ln P(y|x;\xi)\Big)^2\Big] \\ &= \int dxP(x;\xi)\Big(\frac{\partial}{\partial\xi}P(x;\xi)\Big)^2+\int dxP(x;\xi)\int dyP(y|x;\xi)\Big(\frac{\partial}{\partial\xi}\ln P(y|x;\xi)\Big)^2 \\ &= \mathcal{F}_A(\xi)+\mathcal{F}_{B|A}(\xi).\end{aligned}$$

Note the cross term

$$\int dxdyP(x;\xi)P(y|x;\xi)\frac{\partial}{\partial\xi}\ln P(x;\xi)\frac{\partial}{\partial\xi}\ln P(y|x;\xi)=\Big(\int dx\frac{\partial P(x;\xi)}{\partial\xi}\Big)\Big(\int dy\frac{\partial P(y|x;\xi)}{\partial\xi}\Big)=0.$$

integrates to zero in the second step. To obtain the last line, we use the fact that the greedy local measurement scheme saturates the local QFI on A.

By definition, $\mathcal{F}_{A\to B}(\xi)\leq\mathcal{F}_{AB}(\xi)$, with equality satisfied for ρ_{AB} in a product state. Then, the precision loss $\Delta\mathcal{F}(\xi)\equiv\mathcal{F}_{AB}(\xi)-\mathcal{F}_{A\to B}(\xi)$ is generally related to bipartite nonclassical correlations that can be quantified by a proper measure.

By definition, the global QFI $\mathcal{F}_{AB}(\xi)$ always satisfies $\mathcal{F}_{AB}(\xi)\geq\mathcal{F}_{A\to B}(\xi)$ [111, 139, 140]. Here we are interested in relating the precision loss $\Delta\mathcal{F}(\xi)=\mathcal{F}_{AB}(\xi)-\mathcal{F}_{A\to B}(\xi)$ due to local measurements to the presence of nonclassical correlations in $\rho_{AB}(\xi)$.

3.3 Quantum discord for quantifying nonclassical correlations

In this section, we review the theory of quantum discord, which is a measure of nonclassical correlations between two subsystems [118], and diagonal quantum discord, which is a special class of quantum discord which is revealed by the projection measurements on the diagonal bases of the reduced density matrix of the subsystem [91]. In order to explore the role of nonclassical correlations in quantum metrology, we

introduce *discord for local metrology* [140], which quantifies the information contents of nonclassical correlations revealed by the optimal local measurements on the subsystems in the greedy local measurement scheme.

3.3.1 Quantum discord as a measure of nonclassical correlations

Let us consider a quantum system (AB) composed of two subsystems (A) and (B), i.e.

$$\mathcal{H}_{AB} = \mathcal{H}_A \otimes \mathcal{H}_B,$$

where $\mathcal{H}_{AB}$, $\mathcal{H}_A$ and $\mathcal{H}_B$ are the Hilbert space of the total system (AB), subsystem (A) and subsystem (B), respectively. Suppose that subsystem (A) and subsystem (B) are interacting with each other via an interaction Hamiltonian H_{AB} so that the total Hamiltonian can be written as

$$H = H_A + H_B + H_{AB},$$

where H_A and H_B are the system Hamiltonians for subsystem (A) and subsystem (B), respectively. If we write ρ_{AB} as the state of the total system, i.e. $\rho_{AB} \in \mathcal{H}_{AB}$, then the reduced state of the subsystem is given by the partial trace over the other subsystems, i.e.

$$\rho_A = \mathrm{Tr}_B[\rho_{AB}]$$
$$\rho_B = \mathrm{Tr}_A[\rho_{AB}].$$

We introduce S_j, the von-Neumann entropy defined as

$$S_j = -\mathrm{Tr}[\rho_j \ln \rho_j],$$

where $j \in \{AB, A, B\}$.

Nonclassical correlations associated with the loss of quantum certainty in local measurements have been quantified by quantum discord [118, 55, 64]. For a bipartite system (AB), the quantum discord [118] upon measuring subsystem A is defined as

$$D_{A\to B} = -S_{AB} + S_A + \min_{\{\Pi_j^A\}} S_{B|\{\Pi_j^A\}},$$

where $\{\Pi_j^A\}$ are the set of projection measurements on subsystem A. Here, $S_{B|\{\Pi_j^A\}}$ is defined as

$$S_{B|\{\Pi_j^A\}} = \sum_j p_j S_{B|\Pi_j^A},$$

with $p_j = \mathrm{Tr}[(\Pi_j^A \otimes \mathbb{1}_B)\rho_{AB}(\Pi_j^{A\dagger} \otimes \mathbb{1}_B))]$ the probability associated with the projection measurement Π_j^A. The minimization over all sets of projection measurements on subsystem A is required in order for quantum discord to be basis-independent, and to extract the maximum information about subsystem B. Unfortunately, computing quantum discord is a computationally demanding task because it requires the optimization over all possible measurements, and it has been proved to be NP-complete [71].

In order to tackle this problem, Liu, Takagi, and Lloyd in 2017 proposed a new class of quantum discord, called diagonal quantum discord, which is a measure of nonclassical correlations revealed by the measurements corresponding to the diagonal bases of the reduced density matrix of the subsystem [91, 90]:

$$\mathcal{D}_{A\to B} = -S_{AB} + S_A + S_{B|\{\Pi_j^A\}},$$

where $\{\Pi_j^A\}$ are the set of projection measurements corresponding to the eigenbases of the reduced matrix of subsystem A:

$$\rho_A = \sum_j r_j |j\rangle\langle j| = \sum_j r_j \Pi_j^A, \quad (\forall r_j \in \mathbb{R}).$$

Recently it has been verified that the diagonal quantum discord plays an important

role in energy transfer in the thermodynamical systems [94] and parameter estimation [139, 140].

3.3.2 Discord for local metrology

In order to connect nonclassical correlations to the precision loss in metrology, we define a related metric, that we call *discord for local metrology*, where the minimization is restricted to projectors achieving optimal estimate of ξ [140]:

Definition 5. *Let $\{\tilde{\Pi}_j^A\}$ be a set of optimal projection measurements on subsystem A so that there exists an observable $\tilde{\Gamma}^A = \sum_j c_j \tilde{\Pi}_j^A$ ($c_j \in \mathbb{C}$), which can achieve the ultimate precision of estimating ξ, i.e.,*

$$(\delta\xi)^2 = \frac{(\delta\tilde{\Gamma}^A)^2}{\left(\partial_\xi \langle\tilde{\Gamma}^A\rangle\right)^2} = \frac{1}{\mathcal{F}_A(\xi)},$$

where $\mathcal{F}_A(\xi)$ is the local QFI for estimating ξ from $\rho_A(\xi)$. Then, discord for local metrology $\tilde{D}_{A\to B}(\xi)$ is defined as

$$\tilde{D}_{A\to B}(\xi) = -S_{AB}(\xi) + S_A(\xi) + \min_{\{\tilde{\Pi}_j^A\}} S_{B|\{\tilde{\Pi}_j^A\}}(\xi),$$

which is minimized over all the possible sets of projection measurements that are optimal for estimating the parameter ξ.

The minimization indicates that discord for local metrology is independent of the choice of the optimum basis for estimating ξ. Because the measurement basis is chosen according to the optimal parameter estimation, discord for local metrology is an upper bound of the discord, i.e., $\tilde{D}_{A\to B}(\xi) \geq D_{A\to B}$. Also, the minimization is required to avoid the ambiguity when multiple projection bases are optimal. Note that the discord for local metrology is a function of a state and a parameter; therefore, it is not a typical correlation measure for the state. Discord for local metrology has the following properties:

1. $\tilde{D}_{A\to B} \geq 0$ (nonnegative);

2. $\tilde{D}_{A\to B} \neq \tilde{D}_{B\to A}$ (asymmetric);

3. If the total system is in the product state, i.e., $\rho_{AB} = \rho_A \otimes \rho_B$, then $\tilde{D}_{A\to B} = 0$; If $\tilde{D}_{A\to B} = 0$, then the total system is in a classical-quantum state, i.e., $\rho_{AB} = \sum_j p_j |j\rangle\langle j| \otimes \rho_B^{(j)}$, for some set of orthonormal basis vectors $\{|j\rangle\}$, probability distribution $\{p_j\}$ and states $\{\rho_B^{(j)}\}$.

4. $\tilde{D}_{A\to B}$ is invariant under local unitary operations.

Properties 1 and 2 are trivial. The first half of Property 3 is straightforward, and the second part follows from the fact that $\tilde{D}_{A\to B}(\xi) \geq D_{A\to B}$; thus $\tilde{D}_{A\to B}(\xi) = 0$ leads to zero discord, and the state must be classical-quantum. Property 4 is due to the state dependence of the local measurement basis, which makes the quantity only a function of the state and parameter choice. Local unitary operations change the state, but the optimal basis also changes accordingly, thus leaving invariant the discord for local metrology. Note that one does not expect invariance under more general local operations, since discord can increase under local noise [142]. Property 4 distinguishes our metric from the family of basis-dependent discord [156, 164, 98], with which it otherwise shares many commonalities.

Since discord for local metrology satisfies the conditions of nonnegativity and the invariance under local unitary operations, we can regard it as a *good* measure of quantum correlations [90]. While it can be non-zero for some specific classical-quantum state, an unpleasant property for a discord metric, it is a practical quantity to measure correlations in terms of local optimal measurement for metrology.

3.4 Role of nonclassical correlations in general quantum parameter estimation

In this section, we discuss the role of nonclassical correlations in general quantum parameter estimation in thermal equilibrium, and study the role of nonclassical correlations more general than entanglement in the parameter estimation. To better

focus on this question, we consider a different metrology scenario, where the parameter is not encoded during the evolution but in the equilibrium state. We show that for a local detection protocol, nonclassical correlations in the state can be detrimental, in contrast to the dynamic scenario where they help in the estimation. In particular, we consider a greedy local measurement scheme [139, 140], in which each subsystem is measured sequentially with a local optimal measurement for estimating a general parameter (See Fig. 3-1). In addition, we focus on systems at thermal equilibrium in

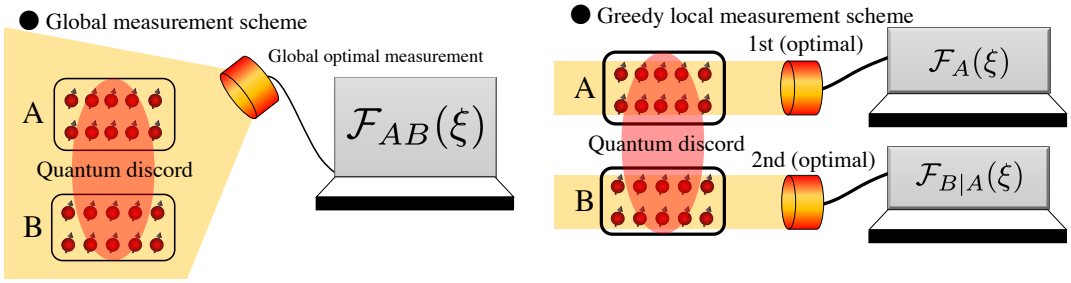

Figure 3-1: Global measurement and greedy local measurement scheme: One first measures a subsystem A with local optimal measurement in the sense of the local QFI and then measure the other subsystem B in order to estimate an unknown parameter ξ. The constrained QFI is given as $\mathcal{F}_{A\to B}(\xi) = \mathcal{F}_A(\xi) + \mathcal{F}_{B|A}(\xi)$. We explore the relation between the quantum discord $D_{A\to B}(\xi)$ and the precision loss $\Delta\mathcal{F}(\xi) = \mathcal{F}_{AB}(\xi) - \mathcal{F}_{A\to B}(\xi)$.

the Gibbs state and consider the high-temperature limit, which is a practical scenario in various systems, such as room-temperature NMR system or biological system, and where only nonclassical correlations beyond entanglement are typically found. Even in this regime, we find a precision loss when considering only local measurements, and we bound it by considering the discord present in the system.

In the following, let us consider a finite-dimensional system described by a Hamiltonian H_λ parameterized by a single temperature-independent parameter λ at temperature T. We assume the state to be in a Gibbs state,

$$\rho(\xi) = \frac{e^{-H_\lambda/T}}{\mathcal{Z}}, \quad \xi \in \{\lambda, T\},$$

where we set the Boltzmann constant to be unit, $k_B = 1$, and

$$\mathcal{Z} = \mathrm{Tr}[e^{-H_\lambda/T}]$$

is the partition function.

3.4.1 Hamiltonian parameter estimation in the high-temperature limit

Let us consider the case for Hamiltonian parameter estimation. The global QFI $\mathcal{F}(\xi, \rho_\xi)$ and the entropy of the global system $S(\rho_\xi)$ in the high-temperature limit satisfies the following Lemma. 1 [140]:

Lemma 1. *Consider a finite-dimensional system in Gibbs state at temperature T, with its Hamiltonian parameterized by a temperature-independent parameter λ to be estimated. Then, the global quantum Fisher information for estimating λ and the total system entropy, $S(\lambda; T)$ are related as*

$$\frac{\partial}{\partial T}\big(T\mathcal{F}(\lambda; T)\big) = \frac{\partial^2}{\partial \lambda^2} S(\lambda; T) + O(T^{-3}). \tag{3.7}$$

Proof. Let ϵ be an error in our estimation. Then, the Hamiltonian with the error becomes

$$H_{\lambda+\epsilon} = H_\lambda + \epsilon G_\lambda + O(\epsilon^2),$$

where

$$G_\lambda = \frac{\partial H_\lambda}{\partial \lambda}.$$

The fidelity between ρ_λ and $\rho_{\lambda+\epsilon}$ is defined as

$$\mathbb{F}[\rho(\lambda), \rho(\lambda+\epsilon)] = \Big(\mathrm{Tr}\Big[\sqrt{\rho^{1/2}(\lambda)\rho(\lambda+\epsilon)\rho^{1/2}(\lambda)}\ \Big]\Big)^2.$$

Since

$$e^{-\frac{H_\lambda}{2T}}e^{-\frac{1}{T}(H_\lambda+\epsilon G_\lambda)}e^{-\frac{H_\lambda}{2T}} = e^{-\frac{1}{T}(2H_\lambda+\epsilon G_\lambda)+O(T^{-3})}$$

we can write

$$\begin{aligned}\mathbb{F}[\rho(\lambda),\rho(\lambda+\epsilon)] &= \frac{1}{\mathcal{Z}_\lambda\mathcal{Z}_{\lambda+\epsilon}}\Big(\mathrm{Tr}[e^{-\frac{1}{T}(H_\lambda+\frac{\epsilon}{2}G_\lambda)+O(T^{-3})}]\Big)^2 \\ &= \frac{1}{\mathcal{Z}_\lambda\mathcal{Z}_{\lambda+\epsilon}}\Big(\mathrm{Tr}[e^{-\frac{1}{T}(H_\lambda+\frac{\epsilon}{2}G_\lambda)}]\Big)^2 + O(T^{-3}).\end{aligned}$$

In the high-temperature limit, the fidelity between ρ_λ and $\rho_{\lambda+\epsilon}$ becomes

$$\mathbb{F}[\rho_\lambda,\rho_{\lambda+\epsilon}] = \frac{\mathcal{Z}^2_{\lambda+\frac{\epsilon}{2}}}{\mathcal{Z}_\lambda\mathcal{Z}_{\lambda+\epsilon}} + O(T^{-3}),$$

where $\mathcal{Z}_{\lambda+\frac{\epsilon}{2}} = \mathrm{Tr}[e^{-H_{\lambda+\frac{\epsilon}{2}}/T}]$, and from the definition of the QFI , we can obtain

$$\mathcal{F}(\lambda;T) = \frac{1}{\mathcal{Z}_\lambda}\frac{\partial^2\mathcal{Z}_\lambda}{\partial\lambda^2} - \Big(\frac{1}{\mathcal{Z}_\lambda}\frac{\partial\mathcal{Z}_\lambda}{\partial\lambda}\Big)^2 + O(T^{-3})$$

Here, for Gibbs state, $\langle G_\lambda\rangle = \mathrm{Tr}[G_\lambda\rho_\lambda]$ is always

$$\langle G_\lambda\rangle = -T\frac{\partial}{\partial\lambda}\ln\mathcal{Z}_\lambda.$$

Then, the susceptibility with respect to a temperature-independent parameter λ can be defined as

$$\chi(\lambda;T) = -\frac{\partial\langle G_\lambda\rangle}{\partial\lambda}.$$

so that we have

$$\mathcal{F}(\lambda;T) = \frac{\chi(\lambda;T)}{T} + O(T^{-3}). \tag{3.8}$$

Since the entropy of the bipartite system, $S(\lambda;T) = -\mathrm{Tr}[\rho_\lambda\ln\rho_\lambda]$, satisfies the following relation

$$\frac{\partial}{\partial T}\langle G_\lambda\rangle = -\frac{\partial}{\partial\lambda}S(\lambda;T), \tag{3.9}$$

from Eq. (3.8) and Eq. (3.9), we can obtain

$$\frac{\partial}{\partial T}\big(T\mathcal{F}(\lambda;T)\big) = \frac{\partial^2}{\partial \lambda^2} S(\lambda;T) + O(T^{-3}).$$

□

In the high-temperature limit, the QFI for estimating λ can be quantified by the susceptibility $\chi(\lambda;T)$ to leading order: $\mathcal{F}(\lambda;T) = \chi(\lambda;T)/T + O(T^{-3})$. In the classical case, Eq. (3.7) becomes exact, as it can also be derived from properties of the classical Fisher information in the linear exponential family [99, 35, 6]. From the relation between the general susceptibility and entropy, $\frac{\partial}{\partial T}\chi(\lambda;T) = \frac{\partial^2}{\partial \lambda^2} S(\lambda;T)$, we can obtain Eq. (3.7). Furthermore, let $A(\lambda;T)$ be the Helmholtz free energy. Then, from the relation between the Helmholtz free energy and entropy, $\frac{\partial}{\partial T} A(\lambda;T) = -S(\lambda;T)$, we can obtain:

$$\mathcal{F}(\lambda;T) = -\frac{1}{T}\frac{\partial^2}{\partial \lambda^2} A(\lambda;T) + O(T^{-3}).$$

This recovers the result of [108] to leading order, which demonstrates that, in the high-temperature limit, the QFI can be characterized as the curvature of the Helmholtz free energy.

Next, for the thermometry case, $\xi = T$, the global QFI and is related to the heat capacity as $\mathcal{F}(T) = C(T)/T^2$ [33] for finite temperature, and it satisfies the following Lemma. 2 [33, 139, 140]:

Lemma 2. *Consider a general quantum system in Gibbs state at temperature T, whose Hilbert space could have both finite or infinite dimensions. Then, the global QFI for estimating T and the total system entropy, $S(T)$ are related as For the thermometry case,*

$$\frac{\partial^2}{\partial T^2} S(T) = \frac{\partial}{\partial T}\big(T\mathcal{F}(T)\big),$$

which is exact.

Proof. Let H be the Hamiltonian of a system thermalized at temperature T. Let β be the inverse temperature, i.e., $\beta = 1/T$, where we have set the Boltzmann constant as $k_B = 1$. Then, the Gibbs state is given by

$$\rho(\beta) = \frac{1}{\mathcal{Z}_\beta} e^{-\beta H},$$

where $\mathcal{Z}$ is the partition function:

$$\mathcal{Z}_\beta = \mathrm{Tr}(e^{-\beta H}).$$

Suppose that we have an error ϵ when estimating β. Then, the state with this error is given by:

$$\rho(\beta+\epsilon) = \frac{1}{\mathcal{Z}_{\beta+\epsilon}} e^{-(\beta+\epsilon)H}.$$

The QFI $\mathcal{F}(\beta)$ to estimate β is defined by

$$\mathcal{F}(\beta) = -2 \lim_{\epsilon \to 0} \frac{\partial^2}{\partial \epsilon^2} \mathbb{F}[\rho(\beta),\ \rho(\beta+\epsilon)],$$

where $\mathbb{F}[\rho(\beta),\ \rho(\beta+\epsilon)]$ is the fidelity between $\rho(\beta)$ and $\rho(\beta+\epsilon)$

$$\mathbb{F}[\rho(\beta), \rho(\beta+\epsilon)] = \left(\mathrm{Tr} \sqrt{\rho^{1/2}(\beta) \rho(\beta+\epsilon) \rho^{1/2}(\beta)} \right)^2.$$

First, let us calculate the fidelity. The fidelity is given by

$$\begin{aligned}
\mathbb{F}[\rho(\beta), \rho(\beta+\epsilon)] &= \left(\mathrm{Tr} \sqrt{\rho^{1/2}(\beta) \rho(\beta+\epsilon) \rho^{1/2}(\beta)} \right)^2 \\
&= \frac{1}{\mathcal{Z}_\beta \mathcal{Z}_{\beta+\epsilon}} \left(\mathrm{Tr} \sqrt{e^{-\frac{1}{2}\beta H} e^{-(\beta+\epsilon)H} e^{-\frac{1}{2}\beta H}} \right)^2 \\
&= \frac{1}{\mathcal{Z}_\beta \mathcal{Z}_{\beta+\epsilon}} \left(\mathrm{Tr} \sqrt{e^{-(2\beta+\epsilon)H}} \right)^2 \\
&= \frac{1}{\mathcal{Z}_\beta \mathcal{Z}_{\beta+\epsilon}} \left(\mathrm{Tr}[e^{-(\beta+\frac{\epsilon}{2})H}] \right)^2 \\
&= \frac{\mathcal{Z}^2_{\beta+\frac{\epsilon}{2}}}{\mathcal{Z}_\beta \mathcal{Z}_{\beta+\epsilon}},
\end{aligned}$$

which yields

$$\mathcal{F}(\beta) = \frac{1}{\mathcal{Z}_\beta}\frac{\partial^2 \mathcal{Z}_\beta}{\partial \beta^2} - \Big(\frac{1}{\mathcal{Z}_\beta}\frac{\partial \mathcal{Z}_\beta}{\partial \beta}\Big) = \delta H^2,$$

This can also be calculated as the following. Before calculating the QFI, let us show the following fact:

$$\begin{aligned}
\lim_{\epsilon\to 0}\frac{\partial}{\partial \epsilon}\mathcal{Z}_{\beta+\epsilon} &= -\lim_{\epsilon\to 0}\mathrm{Tr}[e^{-(\beta+\epsilon)H}H] = -\mathrm{Tr}[e^{-\beta H}H] \\
\lim_{\epsilon\to 0}\frac{\partial^2}{\partial \epsilon^2}\mathcal{Z}_{\beta+\epsilon} &= \lim_{\epsilon\to 0}\mathrm{Tr}[e^{-(\beta+\epsilon)H}H^2] = \mathrm{Tr}[e^{-\beta H}H^2] \\
\lim_{\epsilon\to 0}\frac{\partial}{\partial \epsilon}\mathcal{Z}_{\beta+\frac{\epsilon}{2}} &= -\lim_{\epsilon\to 0}\mathrm{Tr}\Big[e^{-(\beta+\frac{\epsilon}{2})H}\frac{H}{2}\Big] = -\frac{1}{2}\mathrm{Tr}[e^{-\beta H}H] \\
\lim_{\epsilon\to 0}\frac{\partial^2}{\partial \epsilon^2}\mathcal{Z}_{\beta+\frac{\epsilon}{2}} &= \lim_{\epsilon\to 0}\mathrm{Tr}\Big[e^{-(\beta+\frac{\epsilon}{2})H}\frac{H^2}{4}\Big] = \frac{1}{4}\mathrm{Tr}[e^{-\beta H}H^2]
\end{aligned}$$

For two functions $f(x)$ and $g(x)$, where $g(x) \neq 0$, we have:

$$\begin{aligned}
\frac{\partial^2}{\partial x^2}\frac{f^2}{g} =& 2\frac{\partial^2 f}{\partial x^2}\frac{f}{g} + \frac{2}{g}\Big(\frac{\partial f}{\partial x}\Big)^2 \\
&- \frac{4f}{g^2}\Big(\frac{\partial f}{\partial x}\Big)\Big(\frac{\partial g}{\partial x}\Big) - \frac{\partial^2 g}{\partial x^2}\cdot\frac{f^2}{g^2} + \frac{2f^2}{g^3}\Big(\frac{\partial g}{\partial x}\Big)^2.
\end{aligned}$$

Therefore, if we define $x = \epsilon$, $f = \mathcal{Z}_{\beta+\frac{\epsilon}{2}}$, and $g = \mathcal{Z}_{\beta+\epsilon}$, we can obtain

$$\begin{aligned}
\lim_{\epsilon\to 0}\frac{\partial^2}{\partial \epsilon^2}\mathbb{F} &= \lim_{\epsilon\to 0}\frac{\partial^2}{\partial \epsilon^2}\frac{\mathcal{Z}^2_{\beta+\frac{\epsilon}{2}}}{\mathcal{Z}_\beta \mathcal{Z}_{\beta+\epsilon}} = \lim_{\epsilon\to 0}\frac{1}{\mathcal{Z}_\beta}\frac{\partial^2}{\partial \epsilon^2}\frac{\mathcal{Z}^2_{\beta+\frac{\epsilon}{2}}}{\mathcal{Z}_{\beta+\epsilon}} \\
&= -\frac{1}{2}\mathrm{Tr}\Big[\frac{e^{-\beta H}}{\mathcal{Z}_\beta}H^2\Big] + \frac{1}{2}\Big(\mathrm{Tr}\Big[\frac{e^{-\beta H}}{\mathcal{Z}_\beta}H\Big]\Big)^2 \\
&= -\frac{1}{2}\Big(\mathrm{Tr}[\rho_\beta H^2] - (\mathrm{Tr}[\rho_\beta H])^2\Big) \\
&= -\frac{1}{2}\Big(\langle H^2\rangle - \langle H\rangle^2\Big) = -\frac{1}{2}\delta H^2.
\end{aligned}$$

Therefore, the QFI becomes

$$\mathcal{F}(\beta) = -2\lim_{\epsilon\to 0}\frac{\partial^2}{\partial \epsilon^2}\mathbb{F} = \delta H^2,$$

which is the variance of the Hamiltonian. Therefore, the variance of β satisfies the following Cramer-Rao bound:

$$\epsilon^2 \geq \frac{1}{\mathcal{F}(\beta)} = \frac{1}{\delta H^2}$$

Since $\beta = 1/T$, we have

$$\frac{\epsilon}{\delta T} = \frac{\delta \beta}{\delta T} = -\frac{1}{T^2},$$

therefore, we can obtain

$$\delta T^2 \geq \frac{T^4}{\delta H^2}$$

Therefore, we can find that the QFI to estimate the temperature T can be written as

$$\mathcal{F}(T) = \frac{\delta H^2}{T^4} = \frac{\mathcal{F}(\beta)}{T^4}.$$

By definition, heat capacity $C(T)$ is given by

$$C(T) = \frac{1}{T^2}\delta H^2.$$

The QFI to estimate temperature T for the Gibbs state becomes:

$$\mathcal{F}(T) = \frac{C(T)}{T^2}.$$

Since

$$C(T) = T\frac{\partial S(T)}{\partial T},$$

we can obtain

$$\frac{\partial}{\partial T}\Big(T\mathcal{F}(T)\Big) = \frac{\partial^2 S(T)}{\partial T^2}.$$

□

Let us define the optimal measurement in the high-temperature limit as the measurement which achieves the ultimate precision up to order $O(T^{-2})$ of the QFI (for thermometry, $O(T^{-4})$ of the QFI [139]). Different from thermometry case ($\xi = T$), While to estimate a generic parameter λ the optimal measurement is generally not projection measurement onto energy eigenstates, this is instead the case for thermometry or if λ is linearly coupled to the Hamiltonian. Formally, we can have the following lemma:

Lemma 3. *Consider a finite-dimensional system in Gibbs state at temperature T with its Hamiltonian parameterized by a temperature-independent parameter λ to be estimated. If the Hamiltonian depends only linearly on λ, i.e., $\frac{\partial^2 H_\lambda}{\partial \lambda^2} = 0$, projection measurements on the energy eigenstates are optimal to estimate λ.*

Proof. First, let us prove the case of $\xi = \lambda$. When $\frac{\partial G_\lambda}{\partial \lambda} = 0$, the QFI becomes

$$\mathcal{F}(\lambda, T) = \frac{(\delta G_\lambda)^2}{T^2} + O(T^{-3}). \tag{3.10}$$

Let $E_k(\lambda)$ be the eigenvalues of the Hamiltonian H_λ. Then, H_λ can be diagonalized as $H_\lambda = P_\lambda K_\lambda P_\lambda^\dagger$, where P_λ is an unitary operator, $P_\lambda^\dagger P_\lambda = P_\lambda P_\lambda^\dagger = \mathbb{1}$ and $K_\lambda = \mathrm{diag}(E_1(\lambda), E_2(\lambda), \cdots, E_d(\lambda)) = \sum_{k=1}^d E_k(\lambda)|k\rangle\langle k|$ and $|k\rangle$'s form a complete basis independent of λ, and d is the dimension of the system. Thus,

$$\frac{\partial K_\lambda}{\partial \lambda} = \sum_{k=1}^d \frac{\partial E_k(\lambda)}{\partial \lambda} |k\rangle\langle k|.$$

Then, Gibbs state becomes

$$\rho(\lambda) = \frac{1}{\mathcal{Z}_\lambda} P_\lambda e^{-K_\lambda/T} P_\lambda^\dagger = \frac{1}{\mathcal{Z}_\lambda} \sum_{k=1}^d e^{-E_k(\lambda)/T} P_\lambda |k\rangle\langle k| P_\lambda^\dagger.$$

Let us calculate the expectation value of $G_\lambda = \frac{\partial H_\lambda}{\partial \lambda}$. Since

$$G_\lambda = \frac{\partial P_\lambda}{\partial \lambda} K_\lambda P_\lambda^\dagger + P_\lambda \frac{\partial K_\lambda}{\partial \lambda} P_\lambda^\dagger + P_\lambda K_\lambda \frac{\partial P_\lambda^\dagger}{\partial \lambda},$$

we have

$$\begin{aligned}
\langle G_\lambda \rangle =& \mathrm{Tr}[\rho_\lambda G_\lambda] = \frac{1}{\mathcal{Z}_\lambda} \mathrm{Tr}\Big[\Big(P_\lambda e^{-K_\lambda/T} P_\lambda^\dagger \Big) \Big(\frac{\partial P_\lambda}{\partial \lambda} K_\lambda P_\lambda^\dagger + P_\lambda \frac{\partial K_\lambda}{\partial \lambda} P_\lambda^\dagger + P_\lambda K_\lambda \frac{\partial P_\lambda^\dagger}{\partial \lambda} \Big) \Big] \\
=& \mathrm{Tr}\Big[\frac{e^{-K_\lambda/T}}{\mathcal{Z}_\lambda} \frac{\partial K_\lambda}{\partial \lambda} \Big] + \frac{1}{\mathcal{Z}_\lambda} \mathrm{Tr}\Big[K_\lambda e^{-K_\lambda/T} P_\lambda^\dagger \frac{\partial P_\lambda}{\partial \lambda} + \frac{P_\lambda^\dagger}{\partial \lambda} P_\lambda e^{-K_\lambda/T} K_\lambda \Big] \\
=& \mathrm{Tr}\Big[\frac{e^{-K_\lambda/T}}{\mathcal{Z}_\lambda} \frac{\partial K_\lambda}{\partial \lambda} \Big] + \frac{1}{\mathcal{Z}_\lambda} \mathrm{Tr}\Big[e^{-K_\lambda/T} K_\lambda \frac{\partial}{\partial \lambda} (P_\lambda^\dagger P_\lambda) \Big] \\
=& \mathrm{Tr}\Big[\frac{e^{-K_\lambda/T}}{\mathcal{Z}_\lambda} \frac{\partial K_\lambda}{\partial \lambda} \Big] = \mathrm{Tr}\Big[\rho_\lambda P_\lambda \frac{\partial K_\lambda}{\partial \lambda} P_\lambda^\dagger \Big],
\end{aligned}$$

where we used the cyclic property of trace operation, and the fact of $[e^{-K_\lambda/T}, K_\lambda] = 0$. Therefore,

$$\langle G_\lambda \rangle = \Big\langle P_\lambda \frac{\partial K_\lambda}{\partial \lambda} P_\lambda^\dagger \Big\rangle,$$

and $P_\lambda \frac{\partial K_\lambda}{\partial \lambda} P_\lambda^\dagger$ has same diagonal basis of ρ_λ, which are $\{P_\lambda |k\rangle\langle k| P_\lambda^\dagger\}_{k=1}^d$. This means that the optimal measurement for estimating the linear coupling parameter is the projection measurement to the diagonal basis of ρ_λ.

Here we note that for a generic Hamiltonian, H_λ, the susceptibility with respect to λ is given by

$$\begin{aligned}
\chi(\lambda; T) &= \frac{\langle G_\lambda^2 \rangle - \langle G_\lambda \rangle^2}{T} - \Big\langle \frac{\partial G_\lambda}{\partial \lambda} \Big\rangle \\
&= \frac{(\delta G_\lambda)^2}{T} - \Big\langle \frac{\partial G_\lambda}{\partial \lambda} \Big\rangle,
\end{aligned}$$

where $G_\lambda = \frac{\partial H_\lambda}{\partial \lambda}$. From Eq. (3.8), the QFI becomes:

$$\mathcal{F}(\lambda; T) = \frac{(\delta G_\lambda)^2}{T^2} - \frac{1}{T} \Big\langle \frac{\partial G_\lambda}{\partial \lambda} \Big\rangle + O(T^{-3}). \tag{3.11}$$

If λ is linearly coupled to the Hamiltonian, i.e.,

$$\frac{\partial G_\lambda}{\partial \lambda} = \frac{\partial^2 H_\lambda}{\partial \lambda^2} = 0,$$

the projection measurements on the energy eigenstate are optimal since measuring G_λ corresponds to projection measurements on the energy eigenstates and the sensitivity of measuring G_λ saturates the Fisher information as follows

$$(\delta\lambda)^2 = \frac{(\delta G_\lambda)^2}{(\frac{\partial \langle G_\lambda \rangle}{\partial \lambda})^2} = \frac{(\delta G_\lambda)^2}{\chi(\lambda;T)^2} = \frac{T^2}{(\delta G_\lambda)^2} \approx \frac{1}{\mathcal{F}(\lambda;T)}. \tag{3.12}$$

Second, for the case of $\xi = T$, the QFI is given as

$$\mathcal{F}(T) = \frac{C(T)}{T^2} = \frac{1}{T}\frac{\partial S(T)}{\partial T}, \tag{3.13}$$

where $C(T)$ is the heat capacity [33] and $S(T)$ is the entropy. Because of $C(T) = \frac{\partial}{\partial T}\langle H_\lambda \rangle = (\delta H_\lambda)^2/T^2$, the temperature variance, $(\delta T)^2$, becomes

$$(\delta T)^2 = \frac{(\delta H_\lambda)^2}{(\frac{\partial \langle H_\lambda \rangle}{\partial T})^2} = \frac{T^2}{C(T)} = \frac{1}{\mathcal{F}(T)}.$$

Therefore, for thermometry, the projection measurements on diagonal basis are also optimal. □

For a general parameter λ, we usually have $\langle \frac{\partial}{\partial \lambda} G_\lambda \rangle \neq 0$ and from Eq. (3.11), the projection measurements on the energy eigenstate are not optimal. However, there still exits a set of observables that achieves the optimal measurement.

3.4.2 Diagonal quantum discord for quantifying ultimate precision for thermometry

Here, let us first demonstrate that diagonal quantum discord and precision loss quantified by the difference between the global QFI and the LOCC QFI.

In the high-temperature limit, for the finite-dimensional bipartite systems in the

Gibbs state at temperature T, we find that the precision loss is given by

$$\Delta\mathcal{F}(T) = -\frac{1}{T}\frac{\partial}{\partial T}\mathcal{D}_{A\to B}(T) + O(T^{-5}). \tag{3.14}$$

This relation can be proved by realizing that in the high-temperature limit, the partial states are still well approximated by the Gibbs states. Then Eq. (3.13) is still approximately valid and one can relate the local QFI to the entropy of the subsystem and thus to diagonal discord. Let us write the total Hamiltonian as

$$H = H_A + H_B + H_{AB},$$

where H_A and H_B are the system Hamiltonians of A and B, respectively, and H_{AB} is the interaction Hamiltonian between A and B. The Gibbs state of the total system is then $\rho_{AB}(T) = \mathcal{Z}_{AB}^{-1} e^{-\frac{1}{T}(H_A+H_B+H_{AB})}$. Since the heat capacity is given by $C_{AB}(T) = T\frac{\partial S_{AB}(T)}{\partial T}$, we can write

$$\mathcal{F}_{AB}(T) = \frac{C_{AB}(T)}{T^2} = \frac{1}{T}\frac{\partial S_{AB}(T)}{\partial T}. \tag{3.15}$$

For a general finite-dimensional system, in the high-temperature limit $\beta \ll 1$, ρ_{AB} can be written as

$$\rho_{AB} = \frac{1}{d_{AB}}\Big(\mathbb{1}_{AB} - \beta\Big(H - \frac{\mathrm{Tr}[H]}{d_{AB}}\Big)\Big) + O(\beta^2). \tag{3.16}$$

Within the same approximation, the reduced state $\rho_A = \mathrm{Tr}_B[\rho_{AB}]$ is $\rho_A \propto (\mathbb{1}_A - \beta H_A - \beta\Omega_A) + O(\beta^2)$, where $\Omega_A = \mathrm{const} + \frac{1}{d_B}\sum_k \langle E_k^{(B)}|H_{AB}|E_k^{(B)}\rangle$, which is *independent* of the temperature T (here $E_k^{(B)}, |E_k^{(B)}\rangle$ are B's energy eigenvalues and eigenstates). Note that when the interaction between A and B is absent, i.e. $H_{AB} = 0$, due to $[H_A,\ H_B] = 0$, the Gibbs' state of the total system can be written as the product Gibbs' state of the subsystems, which are only relevant to their system Hamiltonians. Therefore, in this case, we have $\Omega_A = 0$ for any temperature T. In the high-temperature limit, in general, $H_A^{\mathrm{eff}} = H_A + \Omega_A$ behaves as an effective Hamil-

tonian for subsystem A. Therefore, at high temperature, ρ_A is approximated by a Gibbs state, $\rho_A \simeq \mathcal{Z}_A^{-1} \exp\big(-\beta H_A^{\text{eff}}\big)$, with $\mathcal{Z}_A \equiv \text{Tr}[\exp\big(-\beta H_A^{\text{eff}}\big)]$. Then, the local QFI still follows Eq. (3.13) and can be written, within this approximation, as

$$\mathcal{F}_A(T) \simeq \frac{1}{T}\frac{\partial S_A(T)}{\partial T}. \tag{3.17}$$

The measurements that saturate this local QFI are the projectors Π_j^A onto local eigenstates of ρ_A, since they are also eigenstates of the effective Hamiltonian $H_A + \Omega_A$.

Similar to ρ_A, the conditional state $\rho_{B|\Pi_j^A}$ after measuring A can be also approximated by a Gibbs state, $\rho_{B|\Pi_j^A} \simeq \mathcal{Z}_{B|\Pi_j^A}^{-1} \exp\big(-\beta H_{B|\Pi_j^A}^{\text{eff}}\big)$, with effective Hamiltonian $H_{B|\Pi_j^A}^{\text{eff}} = H_B + \Omega_{B|\Pi_j^A}$, where $\Omega_{B|\Pi_j^A} = \text{const} + \langle j|H_{AB}|j\rangle$. This allows us to relate the corresponding local QFI to entropy

$$\mathcal{F}_{B|\Pi_j^A}(T) \simeq \frac{1}{T}\frac{\partial}{\partial T} S_{B|\Pi_j^A}(T), \tag{3.18}$$

where $S_{B|\Pi_j^A}(T)$ is the entropy of subsystem B after the measurement Π_j^A. By selecting a set of projection measurements that minimize B's entropy, we can relate the entropies to diagonal discord. More precisely, let $\{\Pi_{j*}^A\}$ be the set of projection measurements on subsystem A such that $\sum_{j*} p_{j*}(T) S_{B|\Pi_{j*}^A}(T) = \min_{\{\Pi_j^A\}} \sum_j p_j(T) S_{B|\Pi_j^A}(T)$.

From Eqs. (3.15-3.18), we have

$$-\frac{\partial}{\partial T}\mathcal{D}_{A\to B}(T) \simeq T\Delta\mathcal{F}(T) - \sum_k \frac{\partial p_{k*}(T)}{\partial T} S_{B|\Pi_{k*}^A}(T). \tag{3.19}$$

Here, let us consider $p_{j*}(T)$. Let d_A and d_B be the dimensions of the subsystems A and B, respectively, and the dimension of the total system d_{AB} is written as $d_{AB} = d_A d_B$. By definition, from Eq. (3.16), in the high-temperature limit, we can obtain

$$p_{j*}(T) = \text{Tr}\Big[(\Pi_{j*}^A \otimes \mathbb{1}_B)\rho_{AB}(\Pi_{j*}^A \otimes \mathbb{1}_B)\Big] = \frac{1}{d_A} + O(T^{-1}),$$

where we use the fact that $\mathrm{Tr}[\mathbb{1}_B] = d_B$. Therefore, we have

$$\frac{\partial p_{j*}(T)}{\partial T} = O(T^{-2}).$$

Also, because $\sum_{j*} p_{j*}(T) = 1$, we have

$$\sum_{j*} \frac{\partial p_{j*}(T)}{\partial T} = 0$$

and also the order of magnitude of the entropy is given by

$$S_{B|\Pi_j^A}(T) = \ln(d_B) + O(T^{-2}).$$

Therefore, we can obtain

$$\frac{1}{T}\sum_{j*} \frac{\partial p_{j*}(T)}{\partial T} S_{B|\Pi_{j*}^A}(T) = \frac{1}{T}\sum_{j*} \frac{\partial p_{j*}(T)}{\partial T} \ln(d_B) + O(T^{-5}) = O(T^{-5}).$$

Therefore, we have:

$$\frac{1}{T}\sum_{j*} \frac{\partial p_{j*}(T)}{\partial T} S_{B|\Pi_{j*}^A}(T) = O(T^{-5}). \tag{3.20}$$

Then we have two cases. A trivial case is when the greedy local method is asymptotically optimal at high temperature, i.e., $\lim_{T\to\infty} \Delta\mathcal{F}(T)/\mathcal{F}(T) = 0$, as the deviation $\Delta\mathcal{F}$ is no longer important.

The magnitude of order of $\mathcal{F}(T)$ is

$$\mathcal{F}(T) \simeq O(T^{-4}). \tag{3.21}$$

This can be shown as the following. Let H be the Hamiltonian for the finite-dimensional system. Then, the partition function can be written as

$$\mathcal{Z} = \mathrm{Tr}[e^{-\beta H}] = \sum_{k=1}^{d} e^{-\beta h_k}.$$

where d is the dimension of the Hamiltonian (i.e., the number of eigenvalues of H),

and $\{h_k\}_{k=1}^d$ are the eigenvalues of the Hamiltonian H. Then, the heat capacity $C(\beta)$ at high temperature ($\beta \ll 1$) can be written as:

$$\begin{aligned} C(\beta) &= \Big[\frac{1}{d}\sum_{k=1}^{d} h_k^2 - \Big(\frac{1}{d}\sum_{k=1}^{d} h_k\Big)^2 \Big]\beta^2 + O(\beta^3) \\ &= \delta h^2 \beta^2 + O(\beta^3), \end{aligned}$$

where

$$\delta h^2 = \frac{1}{d}\sum_{k=1}^{d} h_k^2 - \Big(\frac{1}{d}\sum_{k=1}^{d} h_k\Big)^2$$

is the variance of the eigenvalues. Since $\beta = 1/T$, we have

$$C(T) = \frac{\delta h^2}{T^2} + O(T^{-3}).$$

For the Gibbs state, the QFI of estimating temperature is

$$\mathcal{F}(T) = \frac{C(T)}{T^2}.$$

Therefore, the order of magnitude of $\mathcal{F}(T)$ is

$$\mathcal{F}(T) = O(T^{-4}).$$

In our approach, in the high-temperature limit, the subsystem can be regarded as the Gibbs state; $\mathcal{F}_A(T)$, $\mathcal{F}_{B|A}(T)$, and $\mathcal{F}_{AB}(T)$ all have the order of magnitude $O(T^{-4})$. Therefore, if the greedy local method is not asymptotically optimal at high temperature, i.e.,

$$\lim_{T\to\infty} \frac{\Delta\mathcal{F}(T)}{\mathcal{F}(T)} > 0,$$

then we have

$$\Delta\mathcal{F}(T) = O(T^{-4}),$$

which shows that $\Delta\mathcal{F}(T)$ is more dominant in the high-temperature limit, i. e.

$$\Delta\mathcal{F}(T) \gg \frac{1}{T}\sum_{j*}\frac{\partial p_{j*}(T)}{\partial T}S_{B|\Pi^A_{j*}}(T).$$

If instead $\Delta\mathcal{F}(T)/\mathcal{F}(T)$ remains finite at high temperature, due to $\mathcal{F}(T) = O(T^{-4})$, we must also have $\Delta\mathcal{F}(T) = O(T^{-4})$, which is then the dominant term in the right-hand-side of Eq. (3.19) and we recover Eq. (3.14).

3.4.3 Discord for local metrology for quantifying ultimate precision

In this section, we prove our main result, Theorem 5, stating the relation between the discord for local metrology and the precision loss quantified by the difference between the global QFI and the LOCC QFI.

Theorem 5. *Consider a finite-dimensional system in Gibbs state with its Hamiltonian H_λ parameterized by a temperature-independent parameter λ at temperature T. Let $\xi \in \{\lambda, T\}$ denote an unknown parameter to be estimated. If $\mathcal{F}_{AB}(\xi;T)$ is the global QFI, and $\mathcal{F}_{A\to B}(\xi;T)$ is the LOCC QFI for estimating ξ, in the high-temperature limit, we have*

$$-\frac{\partial^2}{\partial\xi^2}\tilde{D}_{A\to B}(\xi;T) = \frac{\partial}{\partial T}\Big(T\Delta\mathcal{F}(\xi;T)\Big) + O(T^{-\alpha_\xi}), \tag{3.22}$$

where $\alpha_\lambda = 3$ and $\alpha_T = 5$. Particularly, for thermometry ($\xi = T$), $\tilde{D}_{A\to B}(T)$ becomes the diagonal quantum discord $\mathcal{D}_{A\to B}(T)$, which obeys

$$-\frac{\partial^2}{\partial T^2}\mathcal{D}_{A\to B}(T) = \frac{\partial}{\partial T}\Big(T\Delta\mathcal{F}(T)\Big) + O(T^{-5}), \tag{3.23}$$

Proof. First, let us prove the case for $\xi = \lambda$. For a general finite-dimensional system, in the high-temperature limit, the state of the total system $\rho_{AB,\lambda}$ can be written as

$$\rho_{AB,\lambda} = \frac{1}{d_{AB}}\Big(\mathbb{1}_{AB} - \frac{1}{T}\Big(H_\lambda - \frac{\mathrm{Tr}[H_\lambda]}{d_{AB}}\Big)\Big) + O(T^{-2}),$$

where d_{AB} is the dimension of the system. The reduced state of subsystem A is given by $\rho_A(\lambda;T) = \mathrm{Tr}_B[\rho_{AB}(\lambda;T)]$, and within the same approximation we have $\rho_A(\lambda;T) \propto \mathbb{1}_A - \frac{1}{T}\big(H_{A,\lambda} + \Omega_{A,\lambda}\big) + O(T^{-2})$, where $\Omega_{A,\lambda} = \text{const} + \frac{1}{d_B}\sum_k \langle E_k^{(B)}|H_{AB,\lambda}|E_k^{(B)}\rangle$, which is *independent* of temperature. In the high-temperature limit, $\rho_A(\lambda;T)$ can be approximated by a Gibbs state $\rho_{A,\lambda} \simeq \mathcal{Z}_{A,\lambda}^{-1} e^{-H_{A,\lambda}^{\mathrm{eff}}/T}$ with the effective Hamiltonian $H_{A,\lambda}^{\mathrm{eff}} = H_{A,\lambda} + \Omega_{A,\lambda}$ and the normalization factor $\mathcal{Z}_{A,\lambda} = \mathrm{Tr}[e^{-H_{A,\lambda}^{\mathrm{eff}}/T}]$. Then, the local QFI follows Eq. (3.7), i.e.,

$$\frac{\partial}{\partial T}\Big(T\mathcal{F}_A(\lambda;T)\Big) = \frac{\partial^2}{\partial\lambda^2} S_A(\lambda;T) + O(T^{-3}). \tag{3.24}$$

Suppose that projectors $\tilde{\Pi}_j^A$ are the local optimal projection measurements for estimating λ from state $\rho_A(\lambda;T)$. Then, the conditional state $\rho_{B|\tilde{\Pi}_j^A}(\lambda;T)$ after measuring subsystem A can also be approximated as Gibbs state in the high-temperature limit with the effective Hamiltonian $H_{B|\tilde{\Pi}_j^A,\lambda} = H_{B,\lambda} + \Omega_{B|\tilde{\Pi}_j^A,\lambda}$, where $\Omega_{B|\tilde{\Pi}_j^A,\lambda} = \text{const} + \mathrm{Tr}[H_{AB,\lambda}\tilde{\Pi}_j^A]$. Then, the local QFI obeys Lemma 1, i.e.,

$$\frac{\partial}{\partial T}\Big(T\mathcal{F}_{B|\tilde{\Pi}_j^A}(\lambda;T)\Big) = \frac{\partial^2}{\partial\lambda^2} S_{B|\tilde{\Pi}_j^A}(\lambda;T) + O(T^{-3}). \tag{3.25}$$

Let us select $\tilde{\Pi}_{j*}^A$ such that $\sum_{j*} p_{j*}(\lambda;T) S_{B|\tilde{\Pi}_{j*}^A}(\lambda;T) = \min_{\{\tilde{\Pi}_j^A\}} \sum_j p_j(\lambda;T) S_{B|\tilde{\Pi}_j^A}(\lambda;T)$. Then,

$$\frac{\partial^2}{\partial\lambda^2}\tilde{D}_{A\to B}(\lambda;T) = \Big(\frac{\partial^2 S_A}{\partial\lambda^2} + \sum_{j*} p_{j*}\frac{\partial^2}{\partial\lambda^2} S_{B|\tilde{\Pi}_{j*}^A} - S_{AB}\Big) + \sum_{j*}\Big(\frac{\partial^2 p_{j*}}{\partial\lambda^2} S_{B|\tilde{\Pi}_{j*}^A} + 2\frac{\partial p_{j*}}{\partial\lambda}\frac{\partial}{\partial\lambda} S_{B|\tilde{\Pi}_{j*}^A}\Big).$$

From Eq. (3.7), Eq. (3.24), and 3.25), we can obtain

$$-\frac{\partial^2}{\partial\lambda^2}\tilde{D}_{A\to B}(\lambda;T) = \frac{\partial}{\partial T}\Big(T\Delta\mathcal{F}(\lambda;T)\Big) - \sum_{j*}\Big(\frac{\partial^2 p_{j*}}{\partial\lambda^2}S_{B|\tilde{\Pi}^A_{j*}} + 2\frac{\partial p_{j*}}{\partial\lambda}\frac{\partial}{\partial\lambda}S_{B|\tilde{\Pi}^A_{j*}}\Big).$$

In the high-temperature limit, the entropy has the order of $S_{B|\tilde{\Pi}^A_{j*}}(\lambda;T) = \ln(d_B) + O(T^{-2})$ and the measurement probability is

$$p_{j*}(\lambda;T) = \mathrm{Tr}[(\tilde{\Pi}^A_{j*}\otimes\mathbb{1}_B)\rho_{AB}(\lambda;T)(\tilde{\Pi}^{A\dagger}_{j*}\otimes\mathbb{1}_B)] = \frac{1}{d_A} + O(T^{-1}). \tag{3.26}$$

In the high-temperature limit, we have

$$\frac{\partial^2}{\partial\lambda^2}S_{B|\tilde{\Pi}^A_{j*}}(\lambda;T) = O(T^{-2}).$$

By using the fact $\sum_{j*} p_{j*}(\lambda;T) = 1$, we can write

$$\sum_{j*}\frac{\partial^2 p_{j*}(\lambda;T)}{\partial\lambda^2}S_{B|\tilde{\Pi}^A_{j*}}(\lambda;T) = O(T^{-1})O(T^{-2}) = O(T^{-3})$$
$$\sum_{j*}\frac{\partial}{\partial\lambda}p_{j*}(\lambda;T)\frac{\partial}{\partial T}S_{B|\tilde{\Pi}^A_{j*}}(\lambda;T) = O(T^{-1})O(T^{-2}) = O(T^{-3}).$$

Therefore, we can write

$$-\frac{\partial^2}{\partial\lambda^2}\tilde{D}_{A\to B}(\lambda;T) = \frac{\partial}{\partial T}\Big(T\Delta\mathcal{F}(\lambda;T)\Big) + O(T^{-3}).$$

Second, for thermometry, from Eq. 3.14, we can have

$$-\frac{\partial^2}{\partial T^2}\mathcal{D}_{A\to B}(T) = \frac{\partial}{\partial T}\Big(T\Delta\mathcal{F}(T)\Big) + O(T^{-5}).$$

Therefore, we have

$$-\frac{\partial^2}{\partial\xi^2}\tilde{D}_{A\to B}(\xi;T) = \frac{\partial}{\partial T}\Big(T\Delta\mathcal{F}(\xi;T)\Big) + O(T^{-\alpha_\xi}),$$

where $\alpha_\lambda = 3$ and $\alpha_T = 5$, and for thermometry ($\xi = T$), $\tilde{D}_{A\to B}(T)$ becomes the

diagonal quantum discord $\mathcal{D}_{A\to B}(T)$, which obeys

$$-\frac{\partial^2}{\partial T^2}\mathcal{D}_{A\to B}(T)=\frac{\partial}{\partial T}\Big(T\Delta\mathcal{F}(T)\Big)+O(T^{-5}).$$

□

Therefore, for any parameter $\xi\in\{\lambda,T\}$, in the high-temperature limit, we can approximately write

$$\frac{\partial^2}{\partial\xi^2}\tilde{D}_{A\to B}(\xi;T)\simeq-\frac{\partial}{\partial T}\big(T\Delta\mathcal{F}(\xi;T)\big),\tag{3.27}$$

which demonstrates that $\frac{\partial}{\partial T}\big(T\Delta\mathcal{F}(\lambda;T)\big)$ is the curvature of $\tilde{D}_{A\to B}$. Even if the curvature of the discord for local metrology is not directly related to the amount of nonclassical correlations, Eq. (3.27) still describes the role of nonclassical correlations in the greedy local measurement scheme in the LOCC regime.

When the parameter λ is linearly coupled in the Hamiltonian, discord for local metrology becomes diagonal discord. From Theorem 5 and Lemma 3, we can obtain the following corollary:

Corollary 1. *Consider a finite-dimensional system in Gibbs state at temperature T, with its Hamiltonian parameterized by a temperature-independent parameter λ. When λ is linearly coupled to the Hamiltonian H_λ, i.e., $\frac{\partial^2 H_\lambda}{\partial\lambda^2}=0$, we have*

$$\frac{\partial^2}{\partial\lambda^2}\mathcal{D}_{A\to B}(\lambda;T)=-\frac{\partial}{\partial T}\big(T\Delta\mathcal{F}(\lambda;T)\big)+O(T^{-3}),\tag{3.28}$$

where $\mathcal{D}_{A\to B}(\lambda;T)$ is the diagonal discord.

In addition, let us note the case for estimating a parameter linearly coupled to the single-body term. For this case, we can obtain the following corollary:

Corollary 2. *For a finite-dimensional system in Gibbs state at temperature T, when λ is a parameter linearly coupled to the single-body term as*

$$H_\lambda=\lambda H_A+\lambda H_B+H_{AB},$$

where H_A and H_B are the system Hamiltonians and H_{AB} is the interaction Hamiltonian. Then we have

$$\begin{aligned} -\frac{\partial^2}{\partial\lambda^2}\mathcal{D}_{A\to B}(\lambda;T) &= O(T^{-3}) \\ \frac{\partial}{\partial T}\Big(T\Delta\mathcal{F}(\lambda;T)\Big) &= O(T^{-3}). \end{aligned} \tag{3.29}$$

Proof. Let us consider the following Hamiltonian:

$$H_\lambda = \lambda H_A + \lambda H_B + H_{AB},$$

where H_A and H_B are the system Hamiltonians, i.e., $[H_A, H_B] = 0$ and H_{AB} is the interaction Hamiltonian and generally $[H_A + H_B, H_{AB}] \neq 0$. Here, λ is the parameter to be estimated. In this case, $H_{\lambda+\epsilon} = H_\lambda + \epsilon G_\lambda + O(\epsilon^2)$, where $G_\lambda = H_A + H_B$, which is independent of $\xi = \{\lambda, T\}$. Here, we just simply write G_λ as G in order to emphasize its independence of λ.

We already know that for the Gibbs state, we have $\langle G\rangle = -T\frac{\partial}{\partial\lambda}\ln\mathcal{Z}_\lambda$. In this case, we can immediately obtain

$$\langle G\rangle = \langle H_A\rangle + \langle H_B\rangle = O(T^{-1})$$

because the entropy is $S_{AB}(\lambda;T) = \ln(d_{AB}) + O(T^{-2})$ and the relation between the entropy and $\langle G\rangle$ is

$$\frac{\partial}{\partial T}\langle G\rangle = -\frac{\partial}{\partial\lambda}S_{AB}(\lambda;T) = O(T^{-2}).$$

By defining a general susceptibility with respect to λ as

$$\chi(\lambda;T) = -\frac{\partial}{\partial\lambda}\langle G\rangle = O(T^{-1}),$$

the QFI can be given as

$$\mathcal{F}_{AB}(\lambda;T) = -\frac{1}{T}\frac{\partial\langle H_A\rangle}{\partial\lambda} - \frac{1}{T}\frac{\partial\langle H_B\rangle}{\partial\lambda} = O(T^{-2}). \tag{3.30}$$

Now, let us consider the subsystem A. The effective Hamiltonian $H^{\text{eff}}_{A,\lambda}$ can be written as $H^{\text{eff}}_{A,\lambda} = \lambda(H_A + \text{const}) + \Omega_A$. Therefore,

$$\mathcal{F}_A(\lambda; T) = -\frac{1}{T}\frac{\partial\langle H_A\rangle}{\partial\lambda} + O(T^{-3}).$$

Similarly, for $\rho_{B|\tilde{\Pi}^A_{j*}}(\xi)$, we have

$$\mathcal{F}_{B|\tilde{\Pi}^A_{j*}}(\lambda; T) = -\frac{1}{T}\frac{\partial\langle H_B\rangle}{\partial\lambda} + O(T^{-3}).$$

Therefore, by using Eq. (3.26), we have

$$\mathcal{F}_{A\to B}(\lambda; T) = -\frac{1}{T}\Big(\frac{\partial\langle H_A\rangle}{\partial\lambda} + \frac{\partial\langle H_B\rangle}{\partial\lambda}\Big) + O(T^{-3})$$

From Eq. (3.30) and Eq. (3.28), we can obtain

$$\begin{aligned} -\frac{\partial^2}{\partial\lambda^2}\mathcal{D}_{A\to B}(\lambda; T) &= O(T^{-3}) \\ \frac{\partial}{\partial T}\Big(T\Delta\mathcal{F}(\lambda; T)\Big) &= O(T^{-3}). \end{aligned}$$

□

To this order, the local measurements are optimal. Here, note that the leading term that Theorem 5 cares about is $O(T^{-2})$, and this is 0 in this case.

3.5 Examples

In this section, we verify the relation in Eq. (3.22), Eq. (3.28) and Eq. (3.23) by providing several examples of two-qubit Heisenberg interaction, whose Hamiltonian can be written as

$$H = \frac{B_1}{2}Z_A + \frac{B_2}{2}Z_B + \frac{J_x}{2}X_AX_B + \frac{J_y}{2}Y_AY_B + \frac{J_z}{2}Z_AZ_B,$$

where X_j, Y_j, and Z_j ($j = A,\ B$) are the Pauli matrices acting on jth spin. This model is an example given by a two-qubit X state [5, 30, 160].

Coupling strength

Next, let us consider the case of estimating the coupling strength J when $J_x = J_y = J$. Then, we have

$$\Delta\mathcal{F}(J;T) = \frac{1}{2T^2} + O(T^{-3})$$
$$\mathcal{D}_{A\to B}(J;T) = \frac{J^2}{4T^2} + O(T^{-3}),$$

which directly yields

$$\frac{\partial}{\partial T}\big(T\Delta\mathcal{F}(J;T)\big) = -\frac{1}{2T^2} + O(T^{-3})$$
$$-\partial_J^2\mathcal{D}_{A\to B}(J;T) = -\frac{1}{2T^2} + O(T^{-3}),$$

Therefore, Eq. (3.28) is valid.

Magnetometry

Finally, let us consider the magnetometry, which demonstrates Eq. (3.29). We consider the case $B_1 = B_2 = B$, where B is the parameter to be estimated. In this case, we can find that

$$\frac{\partial}{\partial T}\big(T\Delta\mathcal{F}(B;T)\big) = -\frac{(J_x - J_y)^2}{8T^4} + O(T^{-5})$$
$$-\partial_B^2\mathcal{D}_{A\to B}(B;T) = -\frac{J_x^2 + J_xJ_y + J_y^2}{24T^4} + O(T^{-5}).$$

From Eq. (3.29), the leading term should be $O(T^{-3})$; therefore, we can say that Eq. (3.29) is valid but the term to the corresponding order $O(T^{-3})$ is 0.

Thermometry

The Gibbs state of this system is the two-qubit X state. We can find an analytical expression for $\Delta\mathcal{F}(T)$ and $-(1/T)\frac{\partial}{\partial T}\mathcal{D}_{A\to B}$

$$\begin{aligned}\Delta\mathcal{F}(T) &= \left(J_x^2 + J_y^2\right)/(4T^4) + O(T^{-5}) \\ -\frac{1}{T}\frac{\partial}{\partial T}\mathcal{D}_{A\to B}(T) &= \frac{J_x^2 + J_y^2}{4T^4} + O(T^{-5}),\end{aligned} \tag{3.31}$$

which agrees with Eq. (3.14).

We note that $\Delta\mathcal{F}$ does not depend on B_1, B_2, and J_z. This can be intuitively understood since $J_x = J_y = 0$ yields a classical Ising model, where the Gibbs state is a classical state with zero quantum discord. In this case, Eq. (3.14) is exact for any temperature as trivially

$$\Delta\mathcal{F}(T) = -\frac{1}{T}\frac{\partial}{\partial T}\mathcal{D}_{A\to B}(T) = 0$$

at any temperature. The other case for $\Delta\mathcal{F}(T) = -(1/T)\frac{\partial}{\partial T}\mathcal{D}_{A\to B}(T)$ to be exact at any temperature is $B_1 = B_2 = 0$ and either $J_y = 0$ or $J_x = 0$. In this case, we can obtain

$$\Delta\mathcal{F}(T) = -\frac{1}{T}\frac{\partial}{\partial T}\mathcal{D}_{A\to B}(T) = \frac{J_k^2}{4T^4}\,\mathrm{sech}^2\left(\frac{J_k}{2T}\right),$$

where $k = x$ or y for $J_y = 0$ or $J_x = 0$.

We can further numerically evaluate these quantities for arbitrary temperature, with results given in Fig. 3-2 for representative parameters. To understand the non-trivial parameter region better, since our model is symmetric between J_x and J_y, without loss of generality, we fix J_x and vary J_y/J_x, B_1/J_x, and B_2/J_x. We find that for various parameters, at high temperature $\Delta\mathcal{F}(T)$ and $-(1/T)\frac{\partial}{\partial T}\mathcal{D}_{A\to B}(T)$ agree well. At intermediate and low temperature, however, we find that the behavior of the quantities depends strongly on the system parameters. The relationship between $\Delta\mathcal{F}(T)$ and nonclassical correlation at low temperature is still an open problem.

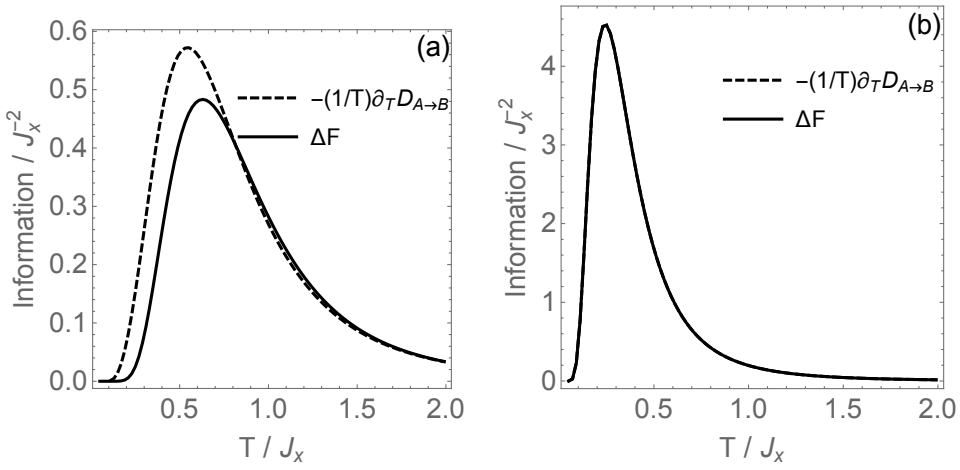

Figure 3-2: $\Delta\mathcal{F}$ and $-(1/T)\frac{\partial}{\partial T}\mathcal{D}_{A\to B}$, for a Heisenberg system with two qubits at (a) $B_1/J_x = 3, B_2/J_x = 1, J_z/J_x = 2, J_y/J_x = 1$ and (b) $B_1 = B_2 = 0, J_z/J_x = 2, J_y = 0$.

3.6 Generalization to multipartite case

Let us consider a finite-dimensional system composed of N subsystems indexed by an integers $1 \leq k \leq N$. In the multipartite case, each subsystem is measured with local optimal measurement sequentially, and we demonstrate that the difference in the global QFI and the LOCC QFI can be quantified via the curvature of the discord for local metrology in the high-temperature limit, in parallel to ref. [139].

We denote the order of measurement in a greedy local measurement scheme by $\sigma_{1:N} \equiv (\sigma_1, \sigma_2, \cdots, \sigma_N)$, where $\sigma_k = \{1, 2, \cdots, N\}$. Let us write $\mathcal{H}(\sigma_k)$ as the Hilbert space of the system on which we perform local optimal measurement $\tilde{\Pi}_{\sigma_k}$ and $\mathcal{H}(\sigma_{k+1:N})$ as the Hilbert space of the rest of system on which we perform the local optimal measurement $\tilde{\Pi}_{\sigma_{k+1:N}}$. Therefore, the total system can be decomposed sequentially into

$$\begin{aligned}
\mathcal{H}(\sigma_{1:N}) &= \mathcal{H}(\sigma_1) \otimes \mathcal{H}(\sigma_{2:N}) \\
&= \mathcal{H}(\sigma_1) \otimes \mathcal{H}(\sigma_2) \otimes \mathcal{H}(\sigma_{3:N}) \\
&\vdots \\
&= \mathcal{H}(\sigma_1) \otimes \mathcal{H}(\sigma_2) \otimes \cdots \otimes \mathcal{H}(\sigma_k) \otimes \mathcal{H}(\sigma_{k+1:N}),
\end{aligned}$$

where $2 \leq k \leq N-1$.

At the first step ($k = 1$), we first perform the local optimal measurement $\tilde{\Pi}_{\sigma_1}$. Then conditioned on the measurement result of $\tilde{\Pi}_{\sigma_1}$, we perform the other local optimal measurement $\tilde{\Pi}_{\sigma_{2:N}}$ on the rest of system. Let us write the global QFI as $\mathcal{F}_{\sigma_{1:N}}$ and the LOCC QFI as $\mathcal{F}_{\sigma_1 \to \sigma_{2:N}}$. Then, in the high-temperature limit, from Eq. (3.27), we have

$$\frac{\partial}{\partial T}\Big(T(\mathcal{F}_{\sigma_{1:N}} - \mathcal{F}_{\sigma_1 \to \sigma_{2:N}})\Big) \simeq -\frac{\partial^2}{\partial \xi^2}\tilde{D}_{\sigma_1 \to \sigma_{2:N}}.$$

For the $2 \leq k \leq N-1$ steps, the measurement $\tilde{\Pi}_{\sigma_k}$ is conditioned on the results of the previous sequence of local optimal measurements $\tilde{\Pi}_{1:k-1} \equiv (\tilde{\Pi}_{\sigma_1}, \tilde{\Pi}_{\sigma_2}, \cdots, \tilde{\Pi}_{\sigma_{k-1}})$. We treat the rest of system as bipartite system composed of $\mathcal{H}(\sigma_k)$ and $\mathcal{H}(\sigma_{k+1:N})$. Then, from Eq. (3.27), we have $\frac{\partial}{\partial T}\Big(T(\mathcal{F}_{\sigma_{k:N}|\tilde{\Pi}_{\sigma_{1:k-1}}} - \mathcal{F}_{\sigma_k \to \sigma_{k+1:N}|\tilde{\Pi}_{\sigma_{1:k-1}}})\Big) \simeq -\frac{\partial^2}{\partial \xi^2}\tilde{D}_{\sigma_k \to \sigma_{k+1:N}|\tilde{\Pi}_{\sigma_{1:k-1}}}$. Here, we have $\mathcal{F}_{\sigma_k \to \sigma_{k+1:N}|\tilde{\Pi}_{\sigma_{1:k-1}}} = \mathcal{F}_{\sigma_k|\tilde{\Pi}_{\sigma_{1:k-1}}} + \mathcal{F}_{\sigma_{k+1:N}|\tilde{\Pi}_{\sigma_{1:k}}}$.

The unconditional QFI is given by the average over measurement outcome distribution $p(\tilde{\Pi}_{\sigma_{1:k-1}})$ as

$$\mathcal{F}_{\sigma_k \to \sigma_{k+1:N}|\sigma_{1:k-1}} \equiv \sum_{\tilde{\Pi}_{\sigma_{1:k-1}}} p(\tilde{\Pi}_{\sigma_{1:k-1}})\mathcal{F}_{\sigma_k \to \sigma_{k+1:N}|\tilde{\Pi}_{\sigma_{1:k-1}}}.$$

Then one can define an unconditional version of discord

$$\tilde{D}_{\sigma_k \to \sigma_{k+1:N}|\sigma_{1:k-1}} = \sum_{\tilde{\Pi}_{\sigma_{1:k-1}}} p(\tilde{\Pi}_{\sigma_{1:k-1}})\tilde{D}_{\sigma_k \to \sigma_{k+1:N}|\tilde{\Pi}_{\sigma_{1:k-1}}},$$

which is related to the average measurement precision difference

$$\frac{\partial}{\partial T}\Big(T(\mathcal{F}_{\sigma_{k:N}|\sigma_{1:k-1}} - \mathcal{F}_{\sigma_k \to \sigma_{k+1}|\sigma_{1:k-1}})\Big) \simeq -\frac{\partial^2}{\partial \xi^2}\tilde{D}_{\sigma_k \to \sigma_{k+1:N}|\sigma_{1:k-1}},$$

where $\mathcal{F}_{\sigma_k \to \sigma_{k+1}|\sigma_{1:k-1}} = \mathcal{F}_{\sigma_k|\sigma_{1:k-1}} + \mathcal{F}_{\sigma_{k+1:N}|\sigma_{1:k}}$. Therefore, by adding the equation

above from $k = 1$ and $k = N$, the difference in the QFI can be written as

$$\Delta\mathcal{F}_{\sigma_{1:N}} = \mathcal{F}_{\sigma_{1:N}} - \sum_{k=1}^{N} \mathcal{F}_{\sigma_{\sigma_k}|\sigma_{1:k-1}}$$

so that we can obtain

$$\frac{\partial}{\partial T}(T\Delta\mathcal{F}_{\sigma_{1:N}}) \simeq -\frac{\partial^2}{\partial\xi^2}\tilde{D}_{\sigma_{1:N}}, \tag{3.32}$$

where

$$\tilde{D}_{\sigma_{1:N}} = \sum_{k=1}^{N} \tilde{D}_{\sigma_k\to\sigma_{k+1:N}|\sigma_{1:k-1}}.$$

Eq. (3.32) is the generalization of Eq. (3.27) for the multipartite case.

The following is the example for the thermometry with three-qubit Heisenberg system: $H = \frac{B}{2}\sum_{k=1}^{3} Z_k + \frac{J}{2}\sum_{k=1}^{2}(X_kX_{k+1} + Y_kY_{k+1} + \alpha Z_kZ_{k+1})$. We considered

$$\Delta\mathcal{F}_{\sigma_{1:N}}(T) \simeq -(1/T)\frac{\partial}{\partial T}\mathcal{D}_{\sigma_{1:N}}(T) + O(T^{-5}), \tag{3.33}$$

where

$$\mathcal{D}_{\sigma_{1:N}}(T) = \sum_{k=1}^{N-1} \mathcal{D}_{\sigma_k\to\sigma_{k+1:N}|\sigma_{1:k-1}}(T). \tag{3.34}$$

It has translational symmetry, and there are only three local measurement schemes to choose from: $1 \to 2 \to 3$, $1 \to 3 \to 2$, and $2 \to 3 \to 1$. However, we find that all three paths give the same $\Delta\mathcal{F}$ and diagonal discord. In the high-temperature limit we find $\Delta\mathcal{F} = -(1/T)\frac{\partial}{\partial T}\mathcal{D} = J^2/T^4 + O(T^{-5})$ (see Fig. 3-3). Compared with Eq. (3.31), we find that the loss is twice that of the two-qubit case, which is intuitive as there are two couplings. More generally, if the Gibbs state is symmetric under permutation, the measurement order does not matter. However, even if $\mathcal{D}_{\sigma_{1:N}}$ is identical for all sequences $\sigma_{1:N}$, each measurement may still depend on previous measurement results. Still, if N is large, we can show that feed forward is only required for the first few steps in a greedy local scheme. Indeed, according to the quantum de Finetti theorem [128], after a negligibly small number $K_1 \ll N$ of measurements,

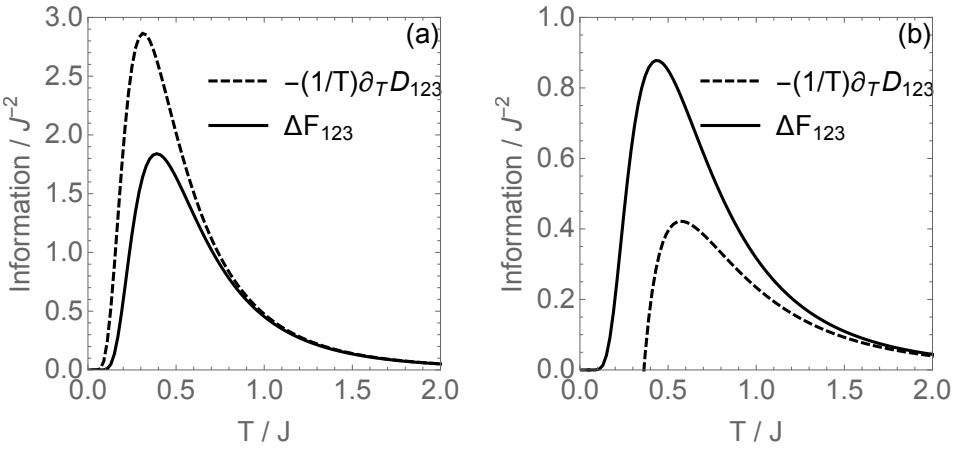

Figure 3-3: $\Delta\mathcal{F}_{123}$ and $-(1/T)\frac{\partial}{\partial T}\mathcal{D}_{123}$, for Heisenberg system with three qubits at (a) $B/J = 1, \alpha = 0.3$ and (b) $B/J = 2, \alpha = 0.3$. Note that the path denoted by subscript 132 and 213 have the same results.

the remaining $N - K_1$ subsystems becomes a mixture of independent and identically distributed states, i.e., $\rho_{1:N-K_1} \simeq \sum_x P_x \rho_x^{\otimes N-K_1}$. Because the QFI is convex, we have $\mathcal{F}\left(T, \rho_{1:N-K_1}\right) \leq \sum_x P_x \mathcal{F}\left(T, \rho_x^{\otimes N-K_1}\right) = (N - K_1) \sum_x P_x \mathcal{F}\left(T, \rho_x\right)$. This means that for the rest of the system, one can perform another $K_2 \ll N$ number of measurements to determine x and then perform the same local diagonal projection measurements on all $N - K_1 - K_2$ parts in state ρ_x.

3.7 More numerical results at low temperature

We also analyzed the thermometry case at low temperature [139]. We consider the two-qubit Heisenberg interaction Hamiltonian in the absence of external fields

$$H = \frac{1}{2}\Big((J + \lambda) X_A X_B + (J - \lambda) Y_A Y_B + J_z Z_A Z_B \Big)$$

To demonstrate the consistency between $\Delta\mathcal{F}(T)$ and $-(1/T)\frac{\partial}{\partial T}\mathcal{D}_{A\to B}(T)$, we plot the relative difference $\left|\left(\Delta\mathcal{F} + (1/T)\frac{\partial}{\partial T}\mathcal{D}_{A\to B}\right) / \left(\Delta\mathcal{F} - (1/T)\frac{\partial}{\partial T}\mathcal{D}_{A\to B}\right)\right|$ in Fig. 3-4. We see that except for a small region, the relative difference is small for both $T/J = 0.4$ and $T/J = 2$.

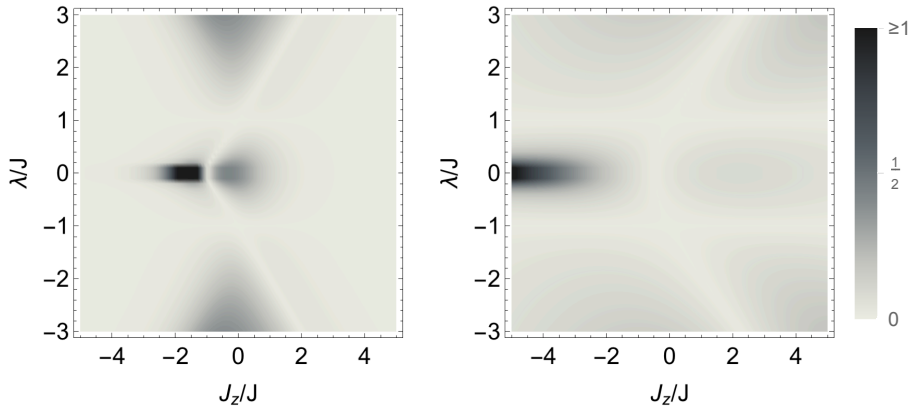

Figure 3-4: $\left|\left(\Delta\mathcal{F}+(1/T)\frac{\partial}{\partial T}\mathcal{D}_{A\to B}\right)/\left(\Delta\mathcal{F}-(1/T)\frac{\partial}{\partial T}\mathcal{D}_{A\to B}\right)\right|$. (a) $T/J=0.4$. Note that the increase of relative error at the edges is due to larger coupling amplitude making $T/|J\pm\lambda|$ smaller. (b) $T/J=2$.

3.8 Conclusion and outlook

In conclusion, we introduced a novel metric for nonclassical correlations, the discord for local metrology, which is defined as a quantum discord in the greedy local measurement scheme, and we derived a relation between discord for local metrology and the difference in the QFI of the global optimal scheme and the greedy local measurement scheme in the high-temperature limit. We demonstrated that the curvature of the discord for local metrology quantifies the precision loss in the estimation of a general parameter due to availability of local measurements only (Theorem 5).

This also indicates that variations in nonclassical correlations at thermal equilibrium, quantified by discord for local metrology, are related to the ability of the greedy local measurement scheme to achieve the ultimate estimation precision limit, quantified by the global QFI. We also showed that discord for local metrology coincides with diagonal discord when one estimates a linear coupling parameter (Corollary 1 and 2).

While we focused on finite-dimensional systems in the high-temperature limit, it would be interesting to extend the relation between the discord for local metrology and the QFI for more general Gibbs states, especially in the low-temperature limit where one could search for connections to phase transition phenomena, or for infinite-

dimensional systems, such as bosonic gases [105, 106].

The relation between the curvature of the discord for local metrology and the difference in the QFI explicitly demonstrates the role of nonclassical correlations in quantum metrology based on the original definition of quantum discord. This provides insights on the role of nonclassicality in quantum metrology and motivates further exploration in more general settings, which can potentially inspire experimentalists to design measurement and control protocols to utilize quantum discord as a resource to achieve precise sensing and imaging, e.g., in the context of room-temperature nuclear magnetic resonance or bioimaging with defect spins [41, 143, 72, 158].

The relationship between precision loss in estimating parameters and discord for local metrology could be potentially verified experimentally, exploiting nanoscale quantum devices. For example, recently, the local temperature of nanowires was measured [73] through the electron energy gain and loss spectroscopy from room temperature to 1600 K. In general, predicting the precision loss in local measurements could guide experimentalists to select measurement protocols with the desired performance.

Although we focused on the high-temperature limit, the exploration of the finite- and low-temperature cases is an interesting open direction. Indeed, as we showed in Sec. 3.7, for the two-qubit Heisenberg model, except for two analytical conditions for $-(1/T)\partial_T \mathcal{D}(T) = \Delta\mathcal{F}(T)$ $(\forall T)$ given in the main text, we also numerically observe that these two quantities are close to each other for various choices of the system parameters even at low temperature. We finally note that our derivation is only valid for finite-dimensional systems; the extension to infinite-dimensional systems is still open, due to the difficulty in the high-temperature expansion.

Chapter 4

Conclusion and prospectus

4.1 Conclusion

This thesis studied the problem of quantum system identification assisted by local measurements in two different regimes: dynamical regime and equilibrium regime, and demonstrated the conceptual understanding of quantum system identification problem by focusing on the roles played by correlations in the quantum system. In the dynamical regime, given prior information of the interaction model, we considered the identifiability of Hilbert space dimension and Hamiltonian parameters.

For the Hilbert space dimension estimation problem, we derived a practical strategy to estimate the dimension of many-qubit systems (Hilbert space dimensions), which relies on the indirect interaction with a single quantum probe under the experimenterâĂŹs control. We combined a graph-theoretical approach and linear system realization theory to demonstrate that the Hilbert space dimension can be *exactly* estimated by finding the minimum number of independent state variables required to fully describe the dynamics of the system, namely model order, which is a measurable quantity. We further proposed a practical algorithm to achieve the exact dimension estimation.

Focusing on identifying Hamiltonian parameters of interacting many-body systems assisted by a single quantum probe coupled to the system, we employed linear system realization theory and Gröbner bases to study the concept of identifiability,

and gave a practical algorithm to determine the identifiability, and derived a lower bound in the number of sampling points and lab time required to estimate all the parameters. Furthermore, the necessary condition for the system to be identifiable is the global generation of correlations between the system and probe. Focusing on the one-dimensional spin-chain model with nearest-neighboring interaction, we classified the systems based on their identifiability, and we also proposed a control protocol to transform a non-identifiable system into an identifiable system.

Finally, we considered the estimation of parameters characterizing thermal equilibrium state, which are the temperature and the Hamiltonian parameters. We considered a general local measurement scheme, where one performs a sequential optimal measurement on the multiple subsystems, and introduced a practical discord, called *discord for local metrology*, to measure the nonclassical correlations induced by local optimal measurements. By comparing the local and global measurement scheme, we explicitly demonstrated that in the high-temperature limit discord for local metrology quantifies the precision loss, and nonclassical correlations, other than entanglement, could contribute to the sensitivity enhancement in parameter estimation in thermal equilibrium.

4.2 Prospectus

Here, we address several possible future directions in the filed of quantum system identification, which are studying the relation between quantum information scrambling and controllability as well as observability, identification of decay dynamics, interaction model estimation, the relation between the quantum phase transition and quantum metrology, and mechanical properties by detecting quantized dislocation, namely dislon.

Focusing on an closed quantum system, in order to obtain physical intuitions of controllability and observability, it is interesting to rigorously study how quantum information scrambling influences the controllability and observability the system. Controllability and observability is well defined by controllability matrix and observ-

ability matrix in the linear system realization theory, and it might be interesting to explore the relation between these matrices and and out-of-time-ordered correlation function (OTOC), which is a measure of quantum information scrambling [87]. Especially, with disorders, in the interacting many-body quantum systems, the quantum correlations spread in time but the information will be localized, which is the many-body localization (MBL) phase [114, 152, 131]. This intuitively means that the localized phase prevents one from being able to extract the full information of the target system in the interested experiment time. With the limited information extractability due to the many-body localized phase, the controllability and observability of the system will vary. Therefore, it is an important task to explore how the properties of OTOC in localized and delocalized phase are associated with the behavior of controllability and observability matrices for these different phases.

For the near future quantum device, such as NISQ, the decoherence is an unavoidable effect due to the coupling of the target system to the environment. Therefore, in order to enable the robust gate operation against the noise, one needs to characterize the noisy dynamics. Therefore, taking into account the practicability, studying open quantum system identification assisted by a single quantum probe is an essential task. Focusing on Markovian open quantum dynamics, in which we neglect the memory of the environment, the dynamics of the quantum system can be described by quantum master equation in Lindblad form [49]:

$$\frac{\partial \rho}{\partial t} = i[\rho, H] + \sum_{k=1}^{N} \left(L_k \rho L^\dagger - \frac{1}{2}\{L_k^\dagger L_k, \rho\} \right)$$

in which the dynamics depends on both the Hamiltonian H and the Lindbladian term L_k [89] describing the decay of the system. Since the quantum master equation can be linearized by the vectorization of the density matrix [62], it might be worth to use the linear system realization theory to develop the method to estimate the operator attributed to the whole dynamics. Since we need to consider not only the Hamiltonian but also the Lindbladian term [89] describing the decay of the system due to its information flowing into environment, it is also important to explore a

method to identify the Hamiltonian and Lindbladian term separately.

Regarding to Hamiltonian estimation problem in open quantum system, the estimation of the interaction model is an important task. Kato and Yamamoto [81] employed quantum filtering theory [15, 148] to achieve the topology estimation of the spin network by finding the most probable graph with Bayesian update. Here, one could consider a same setup but to find the most probable coupling types given a set of possible physical interaction model.

For the equilibrium regime, by exploring the role of discord for local metrology in low-temperature limit for quantum metrology assisted by greedy local measurement scheme, one can expect to find the relation between the quantum phase transition in many-body system because quantum discord reveals the properties of the critical behaviors [163] and Fisher information is related to the second-order phase transition [125], through the theory to be established, one can also explore the role of phase transitions in quantum metrology.

Quantum system identification is not only the prerequisite of QIP, but also an important brach in quantum science to develop for more profound understanding to the quantum dynamics, characteristic properties of quantum matters and the precision sensing in the material and biological systems. For the era of quantum information science, it can be safely said that the active research activities in quantum system identification are fundamentally and practically important.

Bibliography

[1] Johan Ahrens, Piotr Badziąg, Marcin Pawlowski, Marek Żukowski, and Mohamed Bourennane. Experimental tests of classical and quantum dimensionality. *Phys. Rev. Lett.*, 112:140401, 2014.

[2] A. Ajoy, U. Bissbort, M. D. Lukin, R. L. Walsworth, and P. Cappellaro. Atomic-scale nuclear spin imaging using quantum-assisted sensors in diamond. *Phys. Rev. X*, 5:011001, 2015.

[3] A. Ajoy, Y. X. Liu, K. Saha, L. Marseglia, J.-C. Jaskula, U. Bissbort, and P. Cappellaro. Quantum interpolation for high resolution sensing. *Arxiv:1604.01677*, 2016.

[4] Tameem Albash, Victor Martin-Mayor, and Itay Hen. Temperature scaling law for quantum annealing optimizers. *Phys. Rev. Lett.*, 119:110502, 2017.

[5] Mazhar Ali, A. R. P. Rau, and Gernot Alber. Quantum discord for two-qubit x-states. *Phys. Rev. A*, 81:042105, 2010.

[6] Shun'ichi Amari and Hiroshi Nagaoka. *Methods of Information Geometry.* Translations of Mathematical Monographs, Vol. 191. Oxford University Press, Oxford,, 2000.

[7] Panos J. Antsaklis and Anthony N. Michel. *A Linear Systems Primer.* Birkhäuser, Boston, 2007.

[8] K. Arai, C. Belthangady, H. Zhang, N. Bar-Gill, S.J. DeVience, P. Cappellaro, A. Yacoby, and R.L. Walsworth. Fourier magnetic imaging with nanoscale

resolution and compressed sensing speed-up using electronic spins in diamond. *Nat. Nanotech.*, 10:859, 2015.

[9] Melanie Ast, Sebastian Steinlechner, and Roman Schnabel. Reduction of classical measurement noise via quantum-dense metrology. *Phys. Rev. Lett.*, 117(18):180801, 2016.

[10] J. F. Barry, M. J. Turner, J. M. Schloss, D. R. Glenn, Y. Song, M. D. Lukin, H. Park, and R. L. Walsworth. Optical magnetic detection of single-neuron action potentials using quantum defects in diamond. *Proc. Nat Acad. Sc.*, 113(49):14133–14138, 2016.

[11] Tillmann Baumgratz and Animesh Datta. Quantum enhanced estimation of a multidimensional field. *Phys. Rev. Lett.*, 116:030801, 2016.

[12] T. Becker and V. Weispfenning. *Gröbner basis: A Computational Approach to Commutative Algebra*. Springer, New York, 1998.

[13] Sougato Bose. Quantum communication through an unmodulated spin chain. *Phys. Rev. Lett.*, 91(20):207901, 2003.

[14] J. M. Boss, K. Chang, J. Armijo, K. Cujia, T. Rosskopf, J. R. Maze, and C. L. Degen. One- and two-dimensional nuclear magnetic resonance spectroscopy with a diamond quantum sensor. *Phys. Rev. Lett.*, 116:197601, 2016.

[15] Luc Bouten, Ramon Van Handel, and Matthew R. James. An introduction to quantum filtering. *SIAM J. Control Optim.*, 46:2199, 2007.

[16] Joseph Bowles, Nicolas Brunner, and Marcin Pawlowski. Testing dimension and nonclassicality in communication networks. *Phys. Rev. A*, 92:022351, 2015.

[17] Matteo Brunelli, Stefano Olivares, and Matteo G. A. Paris. Qubit thermometry for micromechanical resonators. *Phys. Rev. A*, 84(3):032105, 2011.

[18] Matteo Brunelli, Stefano Olivares, Mauro Paternostro, and Matteo G. A. Paris. Qubit-assisted thermometry of a quantum harmonic oscillator. *Phys. Rev. A*, 86(1):012125, 2012.

[19] Nicolas Brunner, Miguel Navascués, and Tamás Vértesi. Dimension witnesses and quantum state discrimination. *Phys. Rev. Lett.*, 110:150501, 2013.

[20] Nicolas Brunner, Stefano Pironio, Antonio Acin, Nicolas Gisin, André Allan Méthot, and Valeria Scarani. Testing the dimension of hilbert spaces. *Phys. Rev. Lett.*, 100:210503, 2008.

[21] Bruno Buchberger. Bruno buchberger's ph.d. thesis 1965: An algorithm for finding the basis elements of the residue class ring of a zero dimensional polynomial ideal. *J. Symb. Comput.*, 41:475–511, 2006.

[22] Daniel Burgarth and Koji Maruyama. Indirect hamiltonian identification through a small gateway. *New J. Phys.*, 11(10):103019, 2009.

[23] Daniel Burgarth, Koji Maruyama, and Franco Nori. Coupling strength estimation for spin chains despite restricted access. *Phys. Rev. A*, 79:020305(R), 2009.

[24] Daniel Burgarth and Kazuya Yuasa. Quantum system identification. *Phys. Rev. Lett.*, 108:080502, 2012.

[25] Daniel Burgarth and Kazuya Yuasa. Identifiability of open quantum systems. *Phys. Rev. A*, 89:030302(R), 2014.

[26] M. Caboara and J. Perry. Reducing the size and number of linear programs in a dynamic gröobner basis algorithm. *Appl. Algebra Eng. Comm. Comput.*, 25:99–117, 2014.

[27] Yu Cai, Jean-Daniel Bancal, Jacquiline Romero, and Valerio Scarani. A new device-independent dimension witness and its experimental implementation. *J. Phys. A: Math. Theor.*, 49:305301, 2016.

[28] Juan Martin Caicedo, Shirley J. Dyke, and Erik A. Johnson. Natural excitation technique and eigensystem realization algorithm for phase i of the iasc-asce benchmark problem: Simulated data. *J. Eng. Mech.*, 130(1):49, 2014.

[29] Paola Cappellaro, Lorenza Viola, and Chandrasekhar Ramanathan. Coherent-state transfer via highly mixed quantum spin chains. *Phys. Rev. A*, 83(3):032304, 2011.

[30] Qing Chen, Chengjie Zhang, Sixia Yu, X.X. Yi, and C.H. Oh. Quantum discord of two-qubit x-states. *Phys. Rev. A*, 84:042313, 2011.

[31] Matthias Christandl, Nilanjana Datta, Artur Ekert, and Andrew J. Landahl. Perfect state transfer in quantum spin networks. *Phys. Rev. Lett.*, 92:187902, 2004.

[32] A. Cooper, E. Magesan, H.N. Yum, and P. Cappellaro. Time-resolved magnetic sensing with electronic spins in diamond. *Nat. Commun.*, 5:3141, 2014.

[33] Luis A Correa, Mohammad Mehboudi, Gerardo Adesso, and Anna Sanpera. Individual quantum probes for optimal thermometry. *Phys. Rev. Lett.*, 114(22):220405, 2015.

[34] Luis A. Correa, MartÍ Perarnau-Llobet, Karen V. Hovhannisyan, Senaida Hernańdez-Santana, Mohammad Mehboudi, and Anna Sanpera. Low-temperature thermometry can be enhanced by strong coupling. *Phys. Rev. A*, 96:062103, 2017.

[35] T. M. Cover and J. A. Thomas. *Elements of Information Theory*. Wiley, 2nd Edition, 2006.

[36] D. A. Cox, J. Little, and D. O'Shea. *Using Algebraic Geometry, 2nd edition*. Springer, New York, 2005.

[37] D. A. Cox, J. Little, and D. O'Shea. *Ideals, Varieties, and Algorithms (An Introduction to Computational Algebraic Geometry and Commutative Algebra), 4th edition*. Springer, Cham, 2015.

[38] Borivoje Dakić, Vlatko Vedral, and Časlav Brukner. Necessary and sufficient condition for nonzero quantum discord. *Phys. Rev. Lett.*, 105(19):190502, 2010.

[39] Julio I. de Vicente. Shared randomness and device-independent dimension witnessing. *Phys. Rev. A*, 95:012340, 2017.

[40] C. L. Degen, F. Reinhard, and P. Cappellaro. Quantum sensing. *Rev. Mod. Phys.*, 89:035002, 2017.

[41] Stephen J. DeVience, Linh M. Pham, Igor Lovchinsky, Alexander O. Sushkov, Nir Bar-Gill, Chinmay Belthangady, Francesco Casola, Madeleine Corbett, Huiliang Zhang, Mikhail Lukin, Hongkun Park, Amir Yacoby, and Ronald L. Walsworth. Nanoscale nmr spectroscopy and imaging of multiple nuclear species. *Nat Nano*, 10(2):129–134, 2015.

[42] C. Di Franco, M. Paternostro, and M. S. Kim. Hamiltonian tomography in an access-limited setting without state initialization. *Phys. Rev. Lett.*, 102:187203, 2009.

[43] David P. Divincenzo. The physical implementation of quantum computation. *Fortschr. Phys.*, 48:771–783, 2000.

[44] A.B. Finnila, M.A. Gomez, C. Sebenik, C. Stenson, and J.D. Doll. Quantum annealing: A new method for minimizing multidimensional functions. *Chem. Phys. Lett.*, 219:343, 1994.

[45] Eduardo Fradkin, Steven A Kivelson, and John M Tranquada. Colloquium: Theory of intertwined orders in high temperature superconductors. *Rev. Mod. Phys.*, 87(2):457, 2015.

[46] C. Di Franco, M. Paternostro, and M. S. Kim. Perfect state transfer on a spin chain without state initialization. *Phys. Rev. Lett.*, 101:230502, 2008.

[47] R Fröberg. *An Introduction to Gröbner basis*. John Wiley & Sons, New York, 1997.

[48] Rodrigo Gallego, Nicolas Brunner, Christopher Hadley, and Antonio Acín. Device-independent tests of classical and quantum dimensions. *Phys. Rev. Lett.*, 105:230501, 2010.

[49] C. W. Gardiner and P. Zoller. *Quantum Noise: A Handbook of Markovian and Non-Markovian Quantum Stochastic Methods with Applications to Quantum Optics*. Springer-Verlag, 3rd edition, 2004.

[50] Wenchao Ge, Kurt Jacobs, Zachary Eldredge, Alexey V Gorshkov, and Michael Foss-Feig. Distributed quantum metrology and the entangling power of linear networks. *Phys. Rev. Lett.*, 121:043604, 2018.

[51] M. G. Genoni, M. G. A. Paris, G. Adesso, H. Nha, P. L. Knight, and M. S. Kim. Optimal estimation of joint parameters in phase space. *Phys. Rev. A*, 87:012107, 2013.

[52] Vittorio Giovannetti, Seth Lloyd, and Lorenzo Maccone. Quantum-enhanced positioning and clock synchronization. *Nature*, 412(6845):417–419, 2001.

[53] Vittorio Giovannetti, Seth Lloyd, and Lorenzo Maccone. Quantum metrology. *Phys. Rev. Lett.*, 96(1):010401, 2006.

[54] Vittorio Giovannetti, Seth Lloyd, and Lorenzo Maccone. Advances in quantum metrology. *Nat. Photon.*, 5:222, 2011.

[55] Davide Girolami, Tommaso Tufarelli, and Gerardo Adesso. Characterizing nonclassical correlations via local quantum uncertainty. *Phys. Rev. Lett.*, 110:240402, 2013.

[56] Christopher E Granade, Christopher Ferrie, Nathan Wiebe, and D G Cory. Robust online hamiltonian learning. *New J. Phys.*, 14:103013, 2012.

[57] Peter Gritzmann and Brend Sturmfels. Minkowski addition of polytopes: Computational complexity and applications to gröbner bases. *SIAM J. Discrete Math.*, 6:246–269, 1993.

[58] Jonathan L. Gross, Jay Yellen, and Ping Zhang. *Handbook of Graph Theory, 2nd edition.* Chapman & Hall/CRC, 2013.

[59] Mădălin Guţă and Naoki Yamamoto. Systems identification for passive linear quantum systems: the transfer function approach. *52nd IEEE Conference on Decision and Control.*, pages 1930–1937, 2013.

[60] Otfried Guhne, Costantino Budroni, Adán Cabello, Matthias Kleinmann, and Jan Ake Larsson. Bounding the quantum dimension with contextuality. *Phys. Rev. A*, 89:062107, 2014.

[61] U. Haeberlen. *High Resolution NMR in Solids: Selective Averaging.* Academic Press Inc., New York, 1976.

[62] T.F. Havel. Procedures for converting among lindblad, kraus and matrix representations of quantum dynamical semigroups. *J. Math. Phys.*, 44:534, 2018.

[63] C.W. Helstrom. *Quantum Detection and Estimation Theory.* Mathematics in Science and Engineering : A Series of Monographs and Textbooks, Vol. 123. Academic, New York, 1976.

[64] L. Henderson and V. Vedral. Classical, quantum and total correlations. *J. Phys. A*, 34:6899, 2001.

[65] Martin Hendrych, Rodrigo Gallego, Michal Micŭda, Nicolas Brunner, Antonio Acin, and Juan P. Torres. Experimental estimation of the dimension of classical and quantum systems. *Nat. Phys.*, 8:588, 2012.

[66] Patrick P. Hofer, Jonatan Bohr Brask, and Nicolas Brunner. Fundamental limits on low-temperature quantum thermometry. *arXiv:1711.09827.*

[67] A Holevo. *Probabilistic and Statistical Aspects of Quantum Theory.* North-Holland, Amsterdam, 1982.

[68] R. A Horn and C. R Johnson. *Matrix Analysis, 2nd edition.* Cambridge University Press, New York, 2013.

[69] Shi-Yao Hou, Hang Li, and Gui-Lu Long. Experimental quantum hamiltonian identification from measurement time traces. *arXiv:1410.3940v1*, 2014.

[70] Karen V. Hovhannisyan and Luis A. Correa. Probing the temperature of cold many-body quantum systems. *Phys. Rev. B*, 98:045101, 2018.

[71] Yichen Huang. Computing quantum discord is np-complete. *New J. Phys.*, 16:033027, 2014.

[72] Yuen Yung Hui, Chia-Liang Cheng, and Huan-Cheng Chang. Nanodiamonds for optical bioimaging. *J. Phys. D: Appl. Phys.*, 43(37):374021–, 2010.

[73] Juan Carlos Idrobo, Andrew R. Lupini, Tianli Feng, Raymond R. Unocic, Franklin S. Walden, Daniel S. Gardiner, Tracy C. Lovejoy, Niklas Dellby, Sokrates T. Pantelides, and Ondrej L. Krivanek. Temperature measurement by a nanoscale electron probe using energy gain and loss spectroscopy. *Phys. Rev. Lett*, 120:095901, 2018.

[74] Kurt Jacobs. *Quantum Measurement Theory and its Applications*. Cambridge University Press, 2014.

[75] Matthew R. James, Hendra I. Nurdin, and Ian R. Petersen. H-infinity control of linear quantum stochastic systems. *IEEE Trans Autom. Control.*, 53(8):1787, 2008.

[76] Sania Jevtic, David Newman, Terry Rudolph, and TM Stace. Single-qubit thermometry. *Phys. Rev. A*, 91(1):012331, 2015.

[77] Richard Jozsa. Fidelity for mixed quantum states. *J. Mod. Opt.*, 41:2315–2323, 1994.

[78] Tadashi Kadowaki and Hidetoshi Nishimori. Quantum annealing in the transverse ising model. *Phys. Rev. E*, 58:5355, 1998.

[79] T Kailath. *Linear Systems*. Prentice-Hall, 1980.

[80] T Katayama. *Subspace methods for system identification*. Springer Science and Business Media, London, 2006.

[81] Yuzuru Kato and Naoki Yamamoto. Structure identification and state initialization of spin networks with limited access. *New J. Phys.*, 16:023024, 2014.

[82] B. Keimer, S. A. Kivelson, M. R. Norman, S. Uchida, and J. Zaanen. From quantum matter to high-temperature superconductivity in copper oxides. *Nature*, 518(7538):179, 2015.

[83] Ronan Kerviche, Saikat Guha, and Amit Ashok. Fundamental limit of resolving two point sources limited by an arbitrary point spread function. *arXiv:1701.04913*.

[84] Sunho Kim, Longsuo Li, Asutosh Kumar, and Junde Wu. Characterizing nonclassical correlations via local quantum fisher information. *Phys. Rev. A*, 97:032326, 2018.

[85] G. Kucsko, P. C. Maurer, N. Y. Yao, M. Kubo, H. J. Noh, P. K. Lo, H. Park, and M. D. Lukin. Nanometre-scale thermometry in a living cell. *Nature*, 500(7460):54–58, 2013.

[86] Yagati N. Lakshman and Daniel Lazard. On the complexity of zero-dimensional algebraic systems. *In Effective methods in algebraic geometry, Progress in Mathematics (Birkhäuser, Boston)*, 94:217–225, 1991.

[87] Kevin A. Landsman, Caroline Figgatt, Thomas Schuster, Norbert M. Linke, Beni Yoshida, Norman Y. Yao, and Christopher Monroe. Verified quantum information scrambling. *Nature*, 567:61–65, 2010.

[88] Gao-Xiang Li, Sha-Sha Ke, and Zbigniew Ficek. Generation of pure continuous-variable entangled cluster states of four separate atomic ensembles in a ring cavity. *Phys. Rev. A*, 79:033827, 2009.

[89] G. Lindblad. On the generators of quantum dynamical semigroups. *Communications in Mathematical Physics*, 48(2):119–130, 1976.

[90] Zi-Wen Liu. Quantum correlations, quantum resource theories and exclusion game. Master's thesis, Massachusetts Institute of Technology, 2015.

[91] Zi-Wen Liu, Ryuji Takagi, and Seth Lloyd. Diagonal quantum discord. *J. Phys. A: Math. Theor.*, 52:135301, 2019.

[92] L Ljung. *System Identification: Theory for the User, 2nd edition*. Prentice-Hall, Upper Saddle River, NJ, 1999.

[93] Seth Lloyd. Enhanced sensitivity of photodetection via quantum illumination. *Science*, 321(5895):1463–1465, 2008.

[94] Seth Lloyd, Zi-Wen Liu, Stefano Pirandola, Vazrik Chiloyan, Yongjie Hu, Samuel Huberman, and Gang Chen. No energy transport without discord. *arXiv:1510.05035v2*.

[95] I. Lovchinsky, A. O. Sushkov, E. Urbach, N. P. de Leon, S. Choi, K. De Greve, R. Evans, R. Gertner, E. Bersin, C. Müller, L. McGuinness, F. Jelezko, R. L. Walsworth, H. Park, and M. D. Lukin. Nuclear magnetic resonance detection and spectroscopy of single proteins using quantum logic. *Science*, 351(6275):836–841, 2016.

[96] X.-M. Lu, S. Luo, and C. H. Oh. Hierarchy of measurement-induced fisher information for composite states. *Phys. Rev. A*, 86:022342, 2012.

[97] Cosmo Lupo and Stefano Pirandola. Ultimate precision bound of quantum and subwavelength imaging. *Phys. Rev. Lett.*, 117(19):190802, 2016.

[98] J. Ma, B. Yadin, D. Girolami, V. Vedral, and M. Gu. Unification of quantum resources in distributed scenarios. *Phys. Rev. Lett.*, 116:160407, 2016.

[99] D. J. C. MacKay. *Information Theory, Inference, and Learning Algorithms*. Cambridge. Univ. Press, 2003.

[100] Easwar Magesan, Alexandre Cooper, and Paola Cappellaro. Compressing measurements in quantum dynamic parameter estimation. *Phys. Rev. A*, 88:062109, 2013.

[101] Wilhelm Magnus. On the exponential solution of differential equations for a linear operator. *Communications on Pure and Applied Mathematics*, 7(4):649–673, 1954.

[102] P. Maletinsky, S. Hong, M. S. Grinolds, B. Hausmann, M. D. Lukin, R. L. Walsworth, M. Loncar, and A. Yacoby. A robust scanning diamond sensor for nanoscale imaging with single nitrogen-vacancy centres. *Nat. Nanotech.*, 7(5):320–324, 2012.

[103] Luca Mancino, Marco Sbroscia, Ilaria Gianani, Emanuele Roccia, and Marco Barbieri. Quantum simulation of single-qubit thermometry using linear optics. *Phys. Rev. Lett.*, 118(13):130502, 2017.

[104] Ivan Markovsky. *Low rank approximation: algorithms, implementation, applications*. Springer Communications and Control Engineering, London; New York, 2012.

[105] Ugo Marzolino and Daniel Braun. Precision measurements of temperature and chemical potential of quantum gases. *Phys. Rev. A*, 88:063609, 2013.

[106] Ugo Marzolino and Daniel Braun. Eratum: Precision measurements of temperature and chemical potential of quantum gases [phys. rev. a 88, 063609(2013)]. *Phys. Rev. A*, 91:039902(E), 2015.

[107] Yuichiro Matsuzaki, Shojun Nakayama, Akihito Soeda, Mio Murao, and Shiro Saito. Projective measurement of energy on an ensemble of qubits with unknown frequencies. *Phys. Rev. A*, 95:062106, 2017.

[108] Mohammad Mehboudi, Luis A. Correa, and Anna Sanpera. Achieving sub-shot-noise sensing at finite temperatures. *Phys. Rev. A*, 94:042121, 2016.

[109] Mohammad Mehboudi, Maria Moreno-Cardoner, Gabriele De Chiara, and Anna Sanpera. Thermometry precision in strongly correlated ultracold lattice gases. *New J. Phys.*, 17(5):055020, 2015.

[110] Mohammad Mehboudi, Anna Sanpera, and Luis A. Correa. Thermometry in the quantum regime: Recent theoretical progress. *arXiv: 1811.03988*, 2018.

[111] K. Micadei, D. A. Rowlands, F. A. Pollock, L. C. Céleri, R. M. Serra1, and K. Modi. Coherent measurements in quantum metrology. *New J. Phys*, 17:023057, 2015.

[112] Hever Moncayo, Johannio Marulanda, and Peter Thomson. Identification and monitoring of modal parameters in aircraft structures using the natural excitation technique (next) combined with the eigensystem realization algorithm (era). *J. Aerosp. Eng.*, 23(2):99–104, 2010.

[113] Ranjith Nair and Mankei Tsang. Far-field superresolution of thermal electromagnetic sources at the quantum limit. *Phys. Rev. Lett.*, 117(19):190801, 2016.

[114] Rahul Nandkishore and David A. Huse. Many-body localization and thermalization in quantum statistical mechanics. *Annu. Rev. Condens. Matter Phys.*, 6:15–38, 2015.

[115] Michael A Nielsen. Conditions for a class of entanglement transformations. *Phys. Rev. Lett.*, 83(2):436, 1999.

[116] Michael A. Nielsen and Isaac L. Chuang. *Quantum computation and quantum information*. Cambridge University Press, Cambridge; New York, 2000.

[117] Marc Noy and Ares Ribó. Recursively constructible families of graphs. *Adv.in Appl. Math.*, 32:350, 2004.

[118] Harold Ollivier and Wojciech H. Zurek. Quantum discord: A measure of the quantumness of correlations. *Phys. Rev. Lett*, 88:017901, 2001.

[119] Giacomo De Palma, Antonella De Pasquale, and Vittorio Giovannetti. Universal locality of quantum thermal susceptibility. *Phys. Rev. A*, 95:052115, 2017.

[120] Matteo G. A. Paris. Achieving the landau bound to precision of quantum thermometry in systems with vanishing gap. *J. Phys. A: Math. Theor.*, 49:03LT02, 2016.

[121] Antonella De Pasquale, Davide Rossini, Rosario Fazio, and Vittorio Giovannetti. Local quantum thermal susceptibility. *Nat. Comm*, 7:12782, 2016.

[122] Antonella De Pasquale, Kazuya Yuasa, and Vittorio Giovannetti. Estimating temperature via sequential measurements. *Phys. Rev. A*, 96:021316, 2017.

[123] John Preskill. Quantum computing in the nisq era and beyond. *Quantum*, 2:79, 2018.

[124] Timothy J Proctor, Paul A Knott, and Jacob A Dunningham. Multiparameter estimation in networked quantum sensors. *Phys. Rev. Lett.*, 120(8):080501, 2018.

[125] Mikhail Prokopenko, Joseph T. Lizier, Oliver Obst, and X. Rosalind Wang. Relating fisher information to order parameters. *Phys. Rev. E*, 84:041116, 2011.

[126] C Raitz, Alexandre M Souza, Ruben Auccaise, Roberto S Sarthour, and Ivan S Oliveira. Experimental implementation of a nonthermalizing quantum thermometer. *Quantum Inf. Process.*, 14(1):37–46, 2015.

[127] Chandrasekhar Ramanathan, Paola Cappellaro, Lorenza Viola, and David G Cory. Experimental characterization of coherent magnetization transport in a one-dimensional spin system. *New J. Phys.*, 13(10):103015, 2011.

[128] Renato Renner. Symmetry of large physical systems implies independence of subsystems. *Nat. Phys.*, 3(9):645, 2007.

[129] Sophie G. Schirmer and Frank C. Langbein. Ubiquitous problem of learning system parameters for dissipative two-level quantum systems: Fourier analysis versus bayesian estimation. *Phys. Rev. A*, 91:022125, 2015.

[130] B. De Schutter. Minimal state-space realization in linear system theory: an overview. *J. Comput. Appl. Math.*, 121:331–354, 2000.

[131] Maksym Serbyn and Dmitry A. Abanin. Loschmidt echo in many-body localized phases. *Phys. Rev. B*, 96:014202, 2017.

[132] Alexandr Sergeevich, Anushya Chandran, Joshua Combes, Stephen D. Bartlett, and Howard M. Wiseman. Characterization of a qubit hamiltonian using adaptive measurements in a fixed basis. *Phys. Rev. A*, 84:052315, 2011.

[133] Luigi Seveso and Matteo G. A. Paris. Trade-off between information and disturbance in qubit thermometry. *Phys. Rev. A*, 97:032129, 2018.

[134] A. Shabani, M. Mohseni, S. Lloyd, R. L. Kosut, and H. Rabitz. Estimation of many-body quantum hamiltonians via compressive sensing. *Phys. Rev. A*, 84:012107, 2011.

[135] Claude E. Shannon. Communication in the presenceof noise. *Proceedings of the IRE 37.1 (1949): 10-21.*, 37(1):10, 1949.

[136] Jamie Sikora, Antonios Varvitsiotis, and Zhaohui Wei. On the minimum dimension of a hilbert space needed to generate a quantum correlation. *Phys. Rev. Lett.*, 117:060401, 2016.

[137] Akira Sone and Paola Cappellaro. Exact dimension estimation of interacting qubit systems assisted by a single quantum probe. *Phys. Rev. A*, 96:062334, 2017.

[138] Akira Sone and Paola Cappellaro. Hamiltonian identifiability assisted by single-probe measurement. *Phys. Rev. A*, 95:022335, 2017.

[139] Akira Sone, Quntao Zhuang, and Paola Cappellaro. Quantifying precision loss in local quantum thermometry via diagonal discord. *Phys. Rev. A*, 98:012115, 2018.

[140] Akira Sone, Quntao Zhuang, Changhao Li, Y-X Liu, and Paola Cappellaro. Nonclassical correlations for quantum metrology in thermal equilibrium. *Phys. Rev. A*, 99:052318, 2019.

[141] Sebastian Steinlechner, Jöran Bauchrowitz, Melanie Meinders, Helge Müller-Ebhardt, Karsten Danzmann, and Roman Schnabel. Quantum-dense metrology. *Nat. Photonics*, 7(8):626–630, 2013.

[142] Alexander Streltsov, Hermann Kampermann, and Dagmar Bruß. Behavior of quantum correlations under local noise. *Phys. Rev. Lett.*, 107:170502, 2011.

[143] A. O. Sushkov, I. Lovchinsky, N. Chisholm, R. L. Walsworth, H. Park, and M. D. Lukin. Magnetic resonance detection of individual proton spins using quantum reporters. *Phys. Rev. Lett.*, 113:197601, 2014.

[144] Si-Hui Tan, Baris I. Erkmen, Vittorio Giovannetti, Saikat Guha, Seth Lloyd, Lorenzo Maccone, Stefano Pirandola, and Jeffrey H. Shapiro. Quantum illumination with gaussian states. *Phys. Rev. Lett.*, 101:253601, 2008.

[145] J. M. Taylor, P. Cappellaro, L. Childress, L. Jiang, D. Budker, P. R. Hemmer, A. Yacoby, R. Walsworth, and M. D. Lukin. High-sensitivity diamond magnetometer with nanoscale resolution. *Nat. Phys.*, 4(10):810–816, 2008.

[146] Mankei Tsang, Ranjith Nair, and Xiao-Ming Lu. Quantum theory of superresolution for two incoherent optical point sources. *Phys. Rev. X*, 6:031033, 2016.

[147] Toeno van der Sar, Francesco Casola, Ronald Walsworth, and Amir Yacoby. Nanometre-scale probing of spin waves using single electron spins. *Nat. Commun.*, 6:7886, 2014.

[148] Ramon van Handel, John K. Stockton, and Hideo Mabuchi. Feedback control of quantum state reduction. *IEEE Trans. Automat. Control*, 50 (6):768–780, 2005.

[149] Tamás Vértesi and Károly F. Pál. Bounding the dimension of bipartite quantum systems. *Phys. Rev. A*, 79:042106, 2009.

[150] Yuanlong Wang, Daoyi Dong, Bo Qi, Jun Zhang, Ian R. Petersen, and Hidehiro Yonezawa. A quantum hamiltonian identification algorithm: Computational complexity and error analysis. *arXiv:1610.08841*, 2016.

[151] Stephanie Wehner, Matthias Christandl, and Andrew C. Doherty. Lower bound on the dimension of a quantum system given measured data. *Phys. Rev. A*, 78:062112, 2008.

[152] Ken Xuan Wei, Chandrasekhar Ramanathan, and Paola Cappellaro. Exploring localization in nuclear spin chains. *Phys. Rev. Lett.*, 120:070501, 2018.

[153] Michael M. Wolf and David Perez-Garcia. Assessing quantum dimensionality from observable dynamics. *Phys. Rev. Lett.*, 102:190504, 2009.

[154] C. S. Wolfe, S. A. Manuilov, C. M. Purser, R. Teeling-Smith, C. Dubs, P. C. Hammel, and V. P. Bhallamudi. Spatially resolved detection of complex ferromagnetic dynamics using optically detected nitrogen-vacancy spins. *App. Phys. Lett*, 108:232409, 2016.

[155] Dong Xie, Chunling Xu, and An Ming Wang. Optimal quantum thermometry by dephasing. *Quantum Inf. Process.*, 16:155, 2017.

[156] Benjamin Yadin, Jiajun Ma, Davide Girolami, Mile Gu, , and Vlatko Vedral. Quantum processes which do not use coherence. *Phys. Rev. X*, 6:041028, 2016.

[157] Naoki Yamamoto. Coherent versus measurement feedback: Linear systems theory for quantum information. *Phys. Rev. X*, 4:041029, 2014.

[158] T. Yeung, D. Glenn, D. Le Sage, L. Pham, P. Stanwix, L. Yi, Y. Zhao, P. Cappellaro, P. Hemmer, M. Lukin, A. Yacoby, and R. Walsworth. Nv diamond magnetometers for bioimaging. In *APS Division of Atomic, Molecular and Optical Physics Meeting Abstracts*, page 1030, 2010.

[159] H Yuen and Melvin Lax. Multiple-parameter quantum estimation and measurement of nonselfadjoint observables. *IEEE Trans. Inf. Theory*, 19(6):740–750, 1973.

[160] Mikhail A. Yurishchev. Quantum discord in spin-cluster materials. *Phys. Rev. B*, 84:024418, 2011.

[161] Jun Zhang and Mohan Sarovar. Quantum hamiltonian identification from measurement time traces. *Phys. Rev. Lett.*, 113:080401, 2014.

[162] Jun Zhang and Mohan Sarovar. Identification of open quantum systems from observable time traces. *Phys. Rev. A*, 91:052121, 2015.

[163] Xi-Zheng Zhang and Jin-Liang Guo. Quantum correlation and quantum phase transition in the one-dimensional extended ising model. *Quantum Inf. Process.*, 16:223, 2017.

[164] Hongyi Zhou, Xiao Yuan, and Xiongfeng Ma. Unification of quantum resources in distributed scenarios. *Phys. Rev. A*, 99:022326, 2019.

[165] Quntao Zhuang, Zheshen Zhang, and Jeffrey H Shapiro. Entanglement-enhanced lidars for simultaneous range and velocity measurements. *Phys. Rev. A*, 96(4):040304, 2017.

[166] Quntao Zhuang, Zheshen Zhang, and Jeffrey H. Shapiro. Optimum mixed-state discrimination for noisy entanglement-enhanced sensing. *Phys. Rev. Lett.*, 118:040801, 2017.

[167] Quntao Zhuang, Zheshen Zhang, and Jeffrey H Shapiro. Distributed quantum sensing using continuous-variable multipartite entanglement. *Phys. Rev. A*, 97(3):032329, 2018.